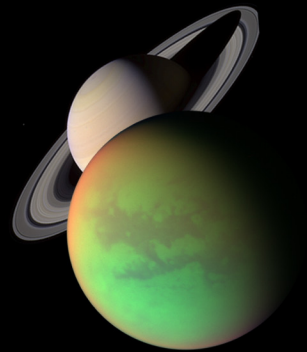
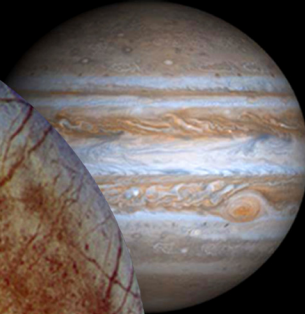
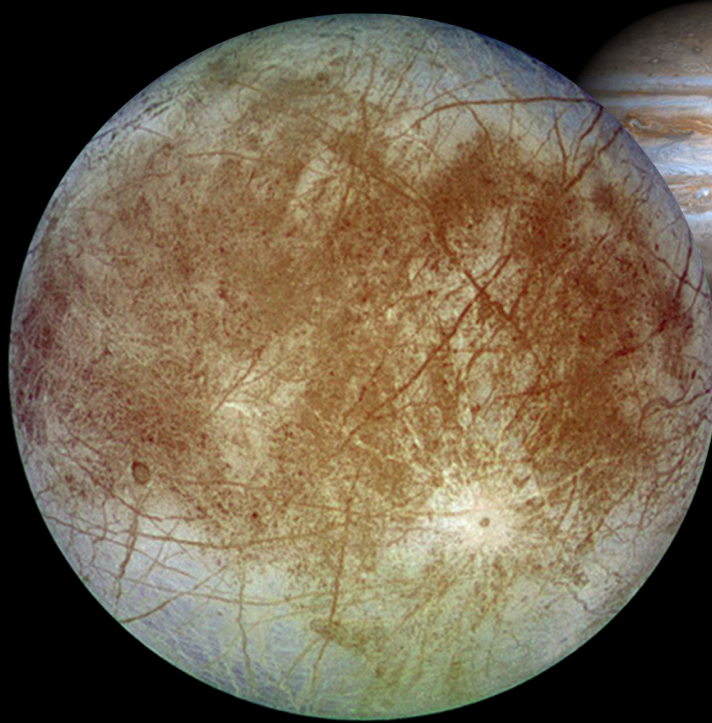
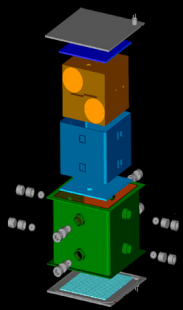
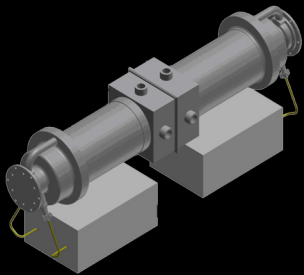
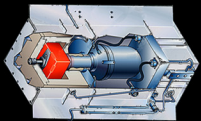
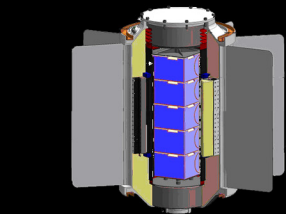


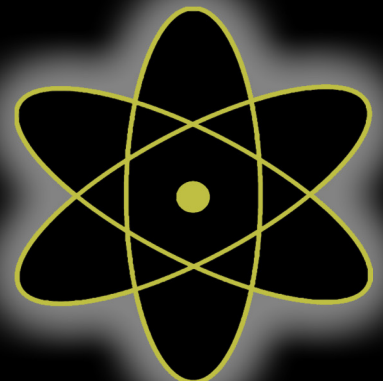
# Extending Exploration with Advanced Radioisotope Power Systems

---



---

**JPL**





JPL D-28903  
PP-266 0333

# Extending Exploration with Advanced Radioisotope Power Systems

**Prepared for**

Ajay Misra  
NASA Science Mission Directorate

**Written by**

Robert D. Abelson (Editor)  
Tibor S. Balint  
Michael Evans  
Timothy Schriener  
James H. Shirley  
Thomas R. Spilker

**November 2005**



Prepared by the Jet Propulsion Laboratory, California Institute of Technology through an agreement with the National Aeronautics and Space Administration.

Reference herein to any specific commercial product, process, or service by trade name, trademark, manufacturer, or otherwise, does not constitute or imply its endorsement by the United States Government, or the Jet Propulsion Laboratory, California Institute of Technology.

Cover Art: (Left Side, Top to Bottom): Conceptual Illustrations of an Advanced RTG, Advanced Stirling, Brayton, and TPV. (Right Side, Counterclockwise from Center): Europa with Jupiter in background, Venus, Moon with Earth in background, and Titan with Saturn in background.

---

**TABLE OF CONTENTS**

Table of Contents .....	v
List of Figures .....	vi
List of Tables .....	ix
1. Summary .....	1-1
1.1 Introduction .....	1-1
1.2 Purpose and Background .....	1-3
1.3 Results .....	1-5
1.4 Conclusions .....	1-16
2. Mission Concepts and Applications .....	2-1
2.1 Introduction .....	2-1
2.2 Background and Mission Categories .....	2-1
2.3 Satellite Missions .....	2-2
2.3.1 Titan Orbiter with Probe Mission .....	2-2
2.4 Lander Missions .....	2-26
2.4.1 Europa Lander Mission .....	2-26
2.5 Rover Missions .....	2-41
2.5.1 Titan Rover Mission .....	2-41
2.5.2 Venus Rover Mission .....	2-58
3. Power Technology for Advanced RPS systems .....	3-1
3.1 Introduction .....	3-1
3.2 Heat Sources .....	3-1
3.3 Advanced Radioisotope Thermoelectric Generator .....	3-2
3.4 Advanced Stirling Generator .....	3-4
3.5 Thermoacoustic Stirling Heat Engine and Cryocooler .....	3-7
3.6 Brayton Generator .....	3-9
3.7 Thermophotovoltaic Generator .....	3-11
3.8 Summary .....	3-15
4. Acknowledgements .....	4-1
5. References .....	5-1
6. Acronyms and Abbreviations .....	6-1

## LIST OF FIGURES

Figure 1-1. Conversion Efficiency versus Specific Power for Standard and Conceptual Advanced RPS Systems .....	1-4
Figure 1-2. Effective Specific Power versus Mission Power Requirement.....	1-9
Figure 1-3. RPS System Mass versus Mission Power Requirement .....	1-12
Figure 2.3.1-1. Image of Titan Taken from the Cassini Spacecraft in 2005. ....	2-2
Figure 2.3.1-2. Shifting Haze Layers on Titan Imaged by the Cassini Imaging Science System.....	2-4
Figure 2.3.1-3. Configuration of the Titan Orbiter, Aeroshell, and Probe within a Delta IV-Heavy Launch Vehicle Fairing.....	2-5
Figure 2.3.1-4. Titan Orbiter Spacecraft (shown within aeroshell) and Externally Mounted Probe.....	2-5
Figure 2.3.1-5. Aerocapture and Circularization Maneuver of the Conceptual Titan Orbiter .....	2-6
Figure 2.3.1-6. Top View of Titan Orbiter Illustrating Placement of Key Subsystems .....	2-7
Figure 2.3.1-7. Titan Orbiter Spacecraft with Aeroshell Opened During the Cruise Phase .....	2-7
Figure 2.3.1-8. Illustration of the Back Side of the Titan Orbiter in its Fully Deployed Configuration .....	2-7
Figure 2.3.1-9. Illustration of the Front Side of the Titan Orbiter in Its Fully deployed Configuration .....	2-7
Figure 2.3.1-10. Conceptual Advanced Stirling Convertor .....	2-9
Figure 2.3.1-11. Near-infrared spectra of Saturn (top) and Titan (below), showing absorption peaks due to various atmospheric constituents.. ..	2-11
Figure 2.3.1-12. Block Diagram of the Conceptual Titan Orbiter Communications System....	2-13
Figure 2.3.1-13. Block Diagram of the Conceptual Titan Orbiter Thermal Control System....	2-14
Figure 2.3.1-14. Earth-Jupiter Gravity Assist (EJGA) for the Titan Orbiter Mission Concept .....	2-15
Figure 2.3.1-15. Schematic of Conceptual Titan Orbiter Propulsion System.....	2-17
Figure 2.3.1-16. Operating Modes and Power Levels of the Titan Orbiter Mission Concept ...	2-18
Figure 2.3.1-17. Brayton Configuration of the Titan Orbiter Concept during the Science Phase.....	2-22
Figure 2.3.1-18. Advanced RTG Version of the Titan Orbiter Concept during the Science Phase.....	2-22
Figure 2.3.1-19. TPV Configuration of the Titan Orbiter Concept during the Cruise phase (Left), and Science phase (Right). .....	2-22
Figure 2.4.1-1. Europa enhanced color image from Galileo images taken in 1995 and 1998... 2-26	
Figure 2.4.1-2. Europa Lander Concept Using Advanced RTG Power Source .....	2-27
Figure 2.4.1-3. Europa Lander Mission Concept Interplanetary Trajectory.....	2-28
Figure 2.4.1-4. Europa Lander Propulsion System Diagram.....	2-34
Figure 2.4.1-5. Europa Lander Concept Nominal Power and Data Storage Profile. ....	2-35

---

Figure 2.4.1-6. Europa Lander Concept Configuration Options: Advanced Stirling, TPV, and Brayton (left to right).....	2-38
Figure 2.5.1-1. First Color View of Titan’s Surface (Cassini-Huygens).....	2-41
Figure 2.5.1-2. Cassini-Huygens Descent Image Mosaic. Drainage channels presumably cut by liquid methane rainfall and runoff dissect the elevated highlands in the upper part of the image.....	2-42
Figure 2.5.1-3. Conceptual Titan Rover WEB (Left) and Fully Deployed Rover (Right). .....	2-43
Figure 2.5.1-4. Titan Rover Concept Stowed Inside a 4.5-m Viking-Type Aeroshell. ....	2-45
Figure 2.5.1-5. Deployment of the Conceptual Titan Rover from Stowed Configuration (Top-Left and Top-Right) through Wheel Deployment (Bottom-Left) to Inflated Wheels and Deployed Mast (Bottom-Right).....	2-46
Figure 2.5.1-6. Conceptual Titan Rover Arm and Sample Collection Mechanism. ....	2-48
Figure 2.5.1-7. Titan Rover Concept Telecom Block Diagram .....	2-50
Figure 2.5.1-8. Titan Rover Concept Power Levels.....	2-53
Figure 2.5.1-9. Conceptual Illustrations of the Titan Rover Using Advanced Stirling, Brayton, and TPV RPSs.....	2-55
Figure 2.5.2-1. Venus with False Coloring to Highlight Surface Features .....	2-58
Figure 2.5.2-2. Earth-Venus-Venus Trajectory of the Venus Rover Mission Concept.....	2-60
Figure 2.5.2-3. Venus Rover Concept Ballute Entry Sequence .....	2-61
Figure 2.5.2-4. Conceptual Venus Rover Configuration.....	2-62
Figure 2.5.2-5. TASHE and Linear Alternator Operating at NGST (Tward, 2005).....	2-63
Figure 2.5.2-6. Venus Rover Drive-Train Concept.....	2-67
Figure 2.5.2-7. Power and Energy Profile for Nominal Daily Operations for the Venus Rover Concept.....	2-69
Figure 3-1. Key Components of a Space-Based Nuclear Power System .....	3-1
Figure 3-2. General-Purpose Heat Source Module (DOE).....	3-1
Figure 3-3. Conceptual Advanced 112-We Radioisotope Thermoelectric Generator.....	3-2
Figure 3-4. Thermoelectric Figure of Merit (ZT) for P-type and N-type Materials (Snyder, 2004) as a Function of Temperature. ....	3-2
Figure 3-5. Cutaway of a Stirling Convertor Integrated with a Linear Alternator in a Hermetically Sealed Pressure Vessel. ....	3-4
Figure 3-6. Laboratory Prototype of an Advanced 80 We SunPower Stirling Engine and Linear Alternator (Wood, 2005). ....	3-5
Figure 3-7. 1-kWe Engine and Resonator Developed by NGST and LANL (Petach, 2004b)...	3-7
Figure 3-8. Cutaway Illustration of a Conceptual Thermoacoustic Stirling Engine (Petach, 2004b). ....	3-7
Figure 3-9. Performance and Operating Parameters of a Conceptual Thermoacoustic Stirling Heat Engine and Cryocooler in a Venus Surface Environment. ....	3-8
Figure 3-10. Thermodynamic Cycle of the Brayton Radioisotope Power System (Zagarola, 2003). ....	3-9

---

---

Figure 3-11. Turbo-Alternator-Compressor Used in the Creare Brayton Generator Design (Zagarola, 2005).....	3-10
Figure 3-12. Conceptual 110-We Brayton RPS System by Creare Using Two Redundant Converters and two GPHS Modules (Zagarola, 2005). ....	3-10
Figure 3-13. Conceptual Illustration of a TPV Generator (Courtesy of OSC). ....	3-11
Figure 3-14. Fundamental Operating Concept of a TPV Generator (Crowley, 2003). ....	3-12
Figure 3-15. Two Conceptual TPV RPS Systems Studied by JPL (Ewell, 1993) (Top), and Fairchild Space (Schock, 1994) (Bottom). Note the different radiator fin configurations.....	3-13
Figure 3-16. Relative Sizes of Four Conceptual Advanced RPS Systems Configured for Operation in a Deep Space Environment (Clockwise from Left):.....	3-16
Figure 3-17. Conversion Efficiency versus Specific Power for the Four Conceptual Advanced RPS Systems Used in the Mission Studies. Assumes Radiator Fins are Sized for Deep Space. ....	3-17
Figure 3-18. Generator Mass versus Electrical Power Output for the Four Conceptual Advanced RPS Systems Used in the Mission Studies. Assumes Radiator Fins are Sized for Deep Space. ....	3-17
Figure 3-19. Estimated Power Degradation Rates for Each of the Four Conceptual Advanced RPS Systems Used in the Mission Studies. ....	3-18

**LIST OF TABLES**

Table 1-1. Previous U.S. Space Missions Using Nuclear Power (Bennett, 1984; Bennett, 1989; Bennett, 1995; Furlong, 1999; Hyder, 2000)..... 1-2

Table 1-2. Science and Exploration Missions Potentially Requiring Radioisotope Power Systems ..... 1-3

Table 1-3. Assessment of Advanced RPS Systems Relative to Selected Mission-Related Criteria\* ..... 1-7

Table 1-4. General Assessment of Advanced RPS Systems for a Range of Space Applications\* ..... 1-8

Table 2.3.1-1. Performance Characteristics of the Conceptual Advanced Stirling RPS for the Titan Orbiter Concept ..... 2-8

Table 2.3.1-2. Science Payload and Instrument Descriptions for the Conceptual Titan Orbiter Mission ..... 2-10

Table 2.3.1-3. Data Rates and Data Volume of the Titan Orbiter Instrument Suite..... 2-12

Table 2.3.1-4. Heat Generation Rates and Required PCM Mass for Four Different Advanced RPS Systems for the Conceptual Titan Orbiter Mission..... 2-15

Table 2.3.1-5.  $\Delta V$  Estimates for the Conceptual Titan Orbiter Mission ..... 2-16

Table 2.3.1-6. Operating Modes and Power Levels for the Titan Orbiter Mission Concept ..... 2-19

Table 2.3.1-7. Mass Estimates for the Titan Orbiter, Aeroshell, and Probe..... 2-20

Table 2.3.1-8. Titan Orbiter and Probe Mass Comparison as a Function of Advanced RPS Technology Used (Includes Contingency)..... 2-21

Table 2.3.1-9. Comparison of ARPS Systems for the Titan Orbiter Mission Concept..... 2-24

Table 2.4.1-1. Europa Lander Concept Science Payload and Instrument Descriptions..... 2-30

Table 2.4.1-2. Europa Lander Concept Instrument Data Rates and Volumes..... 2-32

Table 2.4.1-3. Europa Lander Concept Mass Breakdown (Advanced RTG Option)..... 2-36

Table 2.4.1-4. Europa Lander Concept Mass Comparison (with contingency)..... 2-37

Table 2.4.1-5. Comparison of ARPS Systems for the Europa Lander Concept..... 2-39

Table 2.5.1-1. Representative Trajectory Trade Space ..... 2-44

Table 2.5.1-2. Titan Rover Science Payload and Instrument Descriptions..... 2-49

Table 2.5.1-3. Titan Rover Concept Data Rates..... 2-50

Table 2.5.1-4. Titan Rover Power Modes ..... 2-52

Table 2.5.1-5. Titan Rover Concept Mass Breakdown ..... 2-53

Table 2.5.1-6. ARPS System Mass Comparison for the Titan Rover Mission Concept\* ..... 2-54

Table 2.5.1-7. ARPS Radiator Sizes for the Conceptual Titan Rover..... 2-55

Table 2.5.1-8. Comparison of ARPS Systems for the Titan Rover Concept ..... 2-56

Table 2.5.2-1. Mission Overview for the Venus Rover Concept ..... 2-60

Table 2.5.2-2. Baseline Science Instrument Summary for the Venus Rover Concept..... 2-64

Table 2.5.2-3. Data Rates and Data Volumes for the Venus Rover Instruments..... 2-65

Table 2.5.2-4. Parasitic Heat Loads for the Venus Rover Concept.....	2-66
Table 2.5.2-5. Power Modes and Levels for the Venus Rover Concept .....	2-69
Table 2.5.2-6. Venus Rover Concept Mass Budget.....	2-70
Table 3-1. Performance Estimates for a Conceptual Skutterudite-Based Advanced RTG* .....	3-3
Table 3-2. Performance Estimates for a Conceptual Advanced Stirling Generator* .....	3-6
Table 3-3. Performance Estimates for a Conceptual Brayton Generator* .....	3-11
Table 3-4. Performance Estimates for a Conceptual TPV Generator* .....	3-14
Table 3-5. Overall Performance Estimates of the Conceptual Advanced RPS Systems Considered in this Report (within a Deep Space Environment)* .....	3-15

---

## 1. SUMMARY

### 1.1 INTRODUCTION

---

Nuclear power has played a significant role in the exploration of the solar system, in many cases enabling missions that could not have been achieved otherwise. First flown by the United States in 1961 (Table 1-1), radioisotope power systems (RPSs) possess unique capabilities relative to other types of space power systems. RPSs generate electrical power by converting the heat released from the nuclear decay of radioactive isotopes (typically  $^{238}\text{Pu}$ ) into electricity via one of many power conversion processes. Potential advantages of RPSs are their long life, robustness, compact size, and high reliability. They are able to operate continuously, largely independent of orientation to and distance from the Sun, and can be designed to be relatively insensitive to radiation and other environmental effects. These properties have made RPSs ideally suited for many robotic missions in the extreme environments of outer space and on planetary and satellite surfaces.

The current RPS unit used in the United States is the General Purpose Heat Source—Radioisotope Thermoelectric Generator (GPHS-RTG), which has been used with great success on the Galileo, Ulysses, and Cassini missions. This unit nominally generates ~290 We of electric power at time of launch, and has a specific power of ~5.2 We/kg at the beginning of mission (BOM [U.S. Department of Energy, 1987]). However, the GPHS-RTG is designed for deep space operations only, and is not intended for operations in planetary atmospheres. Nor is it designed to withstand the higher launch loads associated with the newest launch vehicles being used by NASA or the landing loads associated with airbag-style landing systems. To address this, development has begun on two next-generation RPSs with enhanced multi-mission capabilities, that is, the Multi-Mission Radioisotope Thermoelectric Generator (MMRTG) and the Stirling Radioisotope Generator (SRG). The MMRTG is expected to be available for space missions later this decade, with the SRG becoming available by early next decade. The MMRTG and SRG both have the ability to operate in the vacuum of space and in a range of planetary environments, and are capable of handling launch and landing loads beyond those of the GPHS-RTG; however, this multi-mission capability comes at the price of lower specific power (2.8 We/kg for MMRTG, and ~3.4 We/kg for SRG). To address this, NASA is researching a number of advanced RPS technologies with the goal of increasing the specific power beyond that of the MMRTG and SRG.

Four advanced RPS technologies have recently been funded under NASA's Radioisotope Power Conversion Technology (RPCT) and Segmented Thermoelectric (STE) programs. These programs are intended to mature the advanced RPS technologies up to technology readiness level 5 (TRL 5), whereupon one or more of the technologies could be selected for further development by the Department of Energy (DOE) into a full-scale RPS system. The RPS technologies include advanced RTG, advanced Stirling, Brayton, and thermophotovoltaics (TPV). Advanced RPS development is still in its early stages, and thus, flight-qualified advanced RPS systems are not expected to become available until around the middle of the next decade. The goal is to develop an RPS system with a specific power closer to that of the GPHS-RTG while retaining all of the capabilities of NASA's multi-mission RPSs. This includes the ability to support missions in deep space and planetary atmospheres, the capability of being launched on all current launch vehicles without modification, and the ability to withstand landing loads commensurate with typical Entry, Descent, and Landing (EDL) systems including airbags.

**Table 1-1. Previous U.S. Space Missions Using Nuclear Power**  
(Bennett, 1984; Bennett, 1989; Bennett, 1995; Furlong, 1999; Hyder, 2000)

Spacecraft	Principal Energy Source (#)	Initial Avg Power / Unit (We)	Destination/ Application	Launch Date	Status
Transit 4A	SNAP-3B7 RTG (1)	2.7	Earth Orbit/ Navigation Satellite	29 Jun 1961	RTG operated for 15 yr. Satellite now shut down.
Transit 4B	SNAP-3B8 RTG (1)	2.7	Earth Orbit/ Navigation Satellite	15 Nov 1961	RTG operated for 9 yr. Operation intermittent after 1962 high alt test. Last signal in 1971.
Transit 5BN-1	SNAP-9A RTG (1)	>25.2	Earth Orbit/ Navigation Satellite	28 Sep 1963	RTG operated as planned. Non-RTG electrical problems on satellite caused failure after 9 months.
Transit 5BN-2	SNAP-9A RTG (1)	26.8	Earth Orbit/ Navigation Satellite	5 Dec 1963	RTG operated for over 6 yr. Satellite lost navigational capability after 1.5 yr.
Transit 5BN-3 <sup>1</sup>	SNAP-9A RTG (1)	Aborted	Earth Orbit/ Navigation Satellite	21 Apr 1964	Mission aborted because of launch vehicle failure.
SNAPSHOT	SNAP-10A	>500	Experimental	3 Apr 1965	Reactor operated for 43 days until shut down by an electrical component failure on the spacecraft.
Nimbus B-1 <sup>2</sup>	SNAP-19B2 RTG (2)	Aborted	Earth Orbit/ Navigation Satellite	18 May 1968	Mission aborted because of range safety destruct. RTG heat sources recovered and recycled.
Nimbus III	SNAP-19B3 RTG (2)	28.2	Earth Orbit/ Navigation Satellite	14 Apr 1969	RTGs operated for over 2.5 yr. No data taken after that.
Apollo 11	ALRH Heater	Heater Only	Lunar Surface/ Science Payload	16 Jul 1969	Heater units for seismic experimental package. Station shut down Aug 3, 1969.
Apollo 12	SNAP-27 RTG (1)	73.6	Lunar Surface/ Science Payload	14 Nov 1969	RTG operated for about 8 yr until station was shut down.
Apollo 13 <sup>3</sup>	SNAP-27 RTG (1)	Aborted	Lunar Surface/ Science Payload	13 Apr 1970	Mission aborted. RTG reentered intact with no release of <sup>238</sup> Pu. Currently located at bottom of Tonga Trench.
Apollo 14	SNAP-27 RTG (1)	72.5	Lunar Surface / Science Payload	31 Jan 1971	RTG operated for over 6.5 yr until station was shut down.
Apollo 15	SNAP-27 RTG (1)	74.7	Lunar Surface / Science Payload	26 Jul 1971	RTG operated for over 6 yr until station was shut down.
Pioneer 10	SNAP-19 RTG (4)	40.7	Planetary / Payload & Spacecraft	2 Mar 1972	Last signal received on January 23, 2003. Spacecraft now well beyond orbit of Pluto.
Apollo 16	SNAP-27 RTG (1)	70.9	Lunar Surface/ Science Payload	16 Apr 1972	RTG operated for about 5.5 yr until station was shut down.
Triad-01-1X	Transit-RTG (1)	35.6	Earth Orbit/ Navigation Satellite	2 Sep 1972	RTG operating as of mid-1990s.
Apollo 17	SNAP-27 RTG (1)	75.4	Lunar Surface/ Science Payload	7 Dec 1972	RTG operated for almost 5 yr until station was shut down.
Pioneer 11	SNAP-19 RTG (4)	39.9	Planetary / Payload & Spacecraft	5 Apr 1973	Last signal received on September 30, 1995. Spacecraft now well beyond orbit of Pluto.
Viking 1	SNAP-19 RTG (2)	42.3	Mars Lander / Payload & Spacecraft	20 Aug 1975	RTGs operated for over 6 yr until lander was shut down.
Viking 2	SNAP-19 RTG (2)	43.1	Mars Lander / Payload & Spacecraft	9 Sep 1975	RTGs operated for over 4 yr until relay link was lost.
LES 8, LES 9 <sup>4</sup>	MHW-RTG (4)	153	Earth Orbit / Com Satellites	14 Mar 1976	LES 8 was shutdown in 2004. LES 9 continues to operate.
Voyager 2	MHW-RTG (3)	159.2	Planetary / Payload & Spacecraft	20 Aug 1977	RTGs still operating. Spacecraft operated successfully at Jupiter, Saturn, Uranus, Neptune, and beyond.
Voyager 1	MHW-RTG (3)	156.7	Planetary / Payload & Spacecraft	5 Sep 1977	RTGs still operating. Spacecraft operated successfully at Jupiter, Saturn, and beyond.
Galileo	GPHS-RTG (2) RHU Heater (120)	292	Jupiter Orbiter / Payload & Spacecraft	18 Oct 1989	RTGs continued to operate until 2003, when spacecraft was deorbited into Jupiter atmosphere.
Ulysses	GPHS-RTG (1)	282	Polar Solar Orbiter / Payload & Spacecraft	6 Oct 1990	RTG continues to operate successfully after 15 yr. Spacecraft conducting polar solar orbits.
Mars Pathfinder	RHU Heater (3)	Heater Only	Mars Surface Rover / Electronics	4 Dec 1996	Heater units used to maintain payload temperature. Units still presumed active.
Cassini	GPHS-RTG (3) RHU Heater (117)	293	Saturn Orbiter / Payload & Spacecraft	15 Oct 1997	RTGs continue to operate successfully after 8 yr. Spacecraft entered Saturn orbit in 2004.
Mars Rover Spirit	RHU Heater (8)	Heater Only	Mars Surface Rover / Batteries and Electronics	10 Jun 2003	Heater units still operational and used to maintain vehicle operating temperatures.
Mars Rover Opportunity	RHU Heater (8)	Heater Only	Mars Surface Rover / Batteries and Electronics	7 July 2003	Heater units still operational and used to maintain vehicle operating temperatures.

1. Mission was aborted due to launch vehicle failure. RTG burned up on reentry as designed.  
2. Mission was aborted due to launch vehicle failure. RTG heat sources recovered, recycled, and used on subsequent mission.  
3. Mission aborted on way to Moon. RTG reentered Earth atmosphere intact with no release of <sup>238</sup>Pu. It is currently located deep in the Tonga Trench in the South Pacific Ocean.  
4. Mission consisted of two RPS-powered communications satellites (LES 8 and 9) launched on a single launch vehicle.

**1.2 PURPOSE AND BACKGROUND**

The science and exploration communities have identified a broad range of high-priority missions for the next two decades, many of which may require radioisotope power sources (Table 1-2). Advanced RPS systems have the potential to enhance, and possibly enable these missions by virtue of their greater specific power and higher conversion efficiencies compared with those of the MMRTG and SRG. The purpose of this report is to introduce and describe the advanced RPS technologies currently being considered by NASA for future space mission applications, and to assess their relevant merits from a mission and system engineering perspective over a range of potential mission applications.

The technologies considered in this study are

- Advanced thermoelectrics
- Advanced Stirling
- Brayton
- Thermophotovoltaics

**Table 1-2. Science and Exploration Missions Potentially Requiring Radioisotope Power Systems**

Missions Potentially Enabled by <sup>1</sup> Radioisotope Power Systems	SSEDS <sup>2</sup> Time Frame	SSESRM <sup>3</sup> Time Frame	VSE <sup>4</sup> Time Frame	Source
Venus Surface Explorer		2015–2025		SSESRM
Lunar Lander			≥2009	VSE
Lunar Rover			≥2011	VSE
Lunar Base			>2020	VSE
Mars Long-Lived Lander Network	2003–2013			SSEDS
Mars Science Laboratory	2003–2013			SSEDS
Mars Astrobiology Field Laboratory				MEPAG <sup>5</sup>
Io Observer	>2013			SSEDS
Europa Geophysical Explorer/Observer	2003–2013	2005–2015		SSEDS and SSESRM
Europa Lander	>2013	2015–2025		SSEDS and SSESRM
Ganymede Observer	>2013			SSEDS
Saturn Ring Observer	>2013			SSEDS
Titan Explorer	>2013	2015–2025		SSEDS and SSESRM
Uranus Orbiter with Probes	>2013			SSEDS
Neptune Orbiter with Probes	>2013	2015–2025		SSEDS and SSESRM
Neptune Orbiter with Triton Explorer	>2013	2015–2025		SSEDS and SSESRM
New Horizons—Kuiper Belt-Pluto Explorer	2003–2013			SSEDS
Trojan Asteroid/Centaur Reconnaissance	>2013			SSEDS

1. Missions are in order of Sun proximity (not in science priority)
2. SSEDS = Solar System Exploration Decadal Survey (Space Studies Board, 2003)
3. SSESRM = Solar System Exploration Strategic Roadmap (NASA, 2005)
4. VSE = Vision for Space Exploration (Bush, 2004)
5. MEPAG = Mars Exploration Program Analysis Group

## PURPOSE AND BACKGROUND

Key characteristics of each technology are presented, along with assessments of their relative advantages and disadvantages for general and mission-specific applications. High-level studies were performed for four mission concepts to understand the system and mission impacts and relative trades of using each advanced RPS technology. The mission concept studies include a Titan orbiter with probe, Titan rover, Europa lander, and long-lived Venus rover. The science goals of each mission study are based on the priorities of the Solar System Exploration Decadal Survey (Space Studies Board, 2003) and the Solar System Exploration Strategic Roadmap (NASA, 2005).

The advanced RPS systems discussed in this report are currently in the research and development phase, and thus flight-like advanced RPS systems do not currently exist. To permit comparisons between the different advanced RPS systems selected for consideration, preliminary performance estimates were generated by the Jet Propulsion Laboratory (JPL) for each of the technologies based on extrapolations from subsystem-level test results, theoretical performance predictions, and comparisons with RPS systems currently in an advanced state of development (MMRTG and SRG). In order to be approximately commensurate with the power levels of the MMRTG and SRG, all of the generator concepts were assumed to have power levels between 80 and 112 We.

The conceptual advanced RTG is based on an upgraded MMRTG design using higher performance skutterudite thermoelectrics with an estimated conversion efficiency of ~9% (Ewell, 2005a), specific power of ~4.3 We/kg, and a power output of ~112 We at BOM<sup>1</sup> (Fig. 1-1). Two conceptual advanced Stirling generators were considered, the first based on the high-temperature, low-mass SunPower free-piston Stirling engine and linear alternator (Wood, 2005) with an estimated efficiency of 32%, specific power of ~5.9 We/kg, and power output of ~80 We

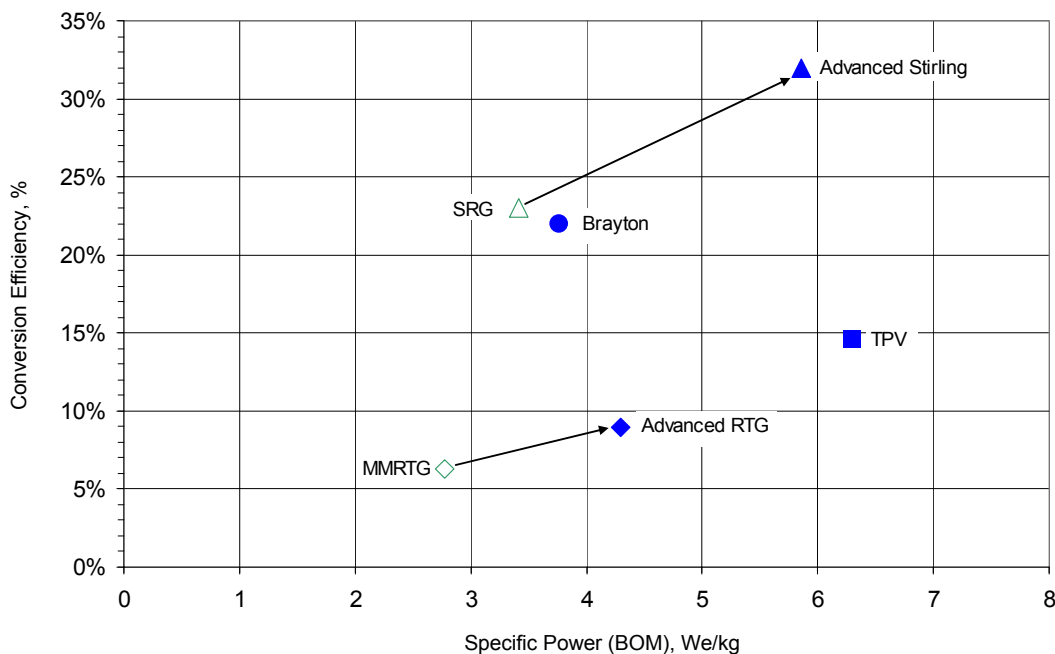


**Figure 1-1.** Conversion Efficiency versus Specific Power for Standard and Conceptual Advanced RPS Systems

<sup>1</sup> Analysis will begin in 2006 on a deep-space only version of a higher power ( $\geq 200$  We) advanced RTG with the goal of achieving a specific power of  $\geq 6$  We/kg using advanced high temperature thermoelectrics.

at BOM<sup>2</sup>. The second conceptual Stirling generator considered was specifically tailored for a long-duration Venus surface application. It is based on the thermoacoustic Stirling heat engine with integrated pulse tube refrigerator (PTR) being designed by Northrop Grumman Space Technologies (NGST [Petach, 2004b]) and Los Alamos National Labs (LANL). A conceptual Brayton generator was considered based on a Creare Brayton design (Zagarola, 2005) with an estimated conversion efficiency of 22%, specific power of ~3.8 We/kg, and a power output of ~110 W. A conceptual TPV generator based on a JPL design (Ewell, 1993) was considered with an estimated conversion efficiency of 15%, specific power of 6.3 We/kg, and power output of ~110 We at BOM. Advanced RPS performance was assessed over a range of operating environments that include deep space, the surface of Titan, and Venus at 60-km altitude (e.g., for an aerobot-type application).

This report assumed that these RPS technologies could be made available for use by flight projects as early as ~2015 given appropriate developmental funding. Thus, the present mission studies considered launch dates no earlier than 2015.

This report is divided into three sections. Section 1 summarizes the results of the advanced RPS comparative assessment and presents the relative benefits of each technology from an overall and mission-specific perspective. Section 2 presents the results of the four mission concept studies and illustrate the power system trades, power system implementation, and relative benefits of each advanced RPS technology. Section 3 summarizes the technical characteristics and performance of the conceptual advanced RTG, advanced Stirling, Brayton, and TPV RPSs considered in this report.

### 1.3 RESULTS

The relative capabilities of each advanced RPS were assessed over a broad spectrum of mission-relevant criteria with the results illustrated in Table 1-3. The criteria include *Unit-Level Specific Power*, *Volume*, *Heritage*, *Integration*, *Environmental Emissions*, *Robustness*, *RPS Complexity*, *Power Degradation Rate*, and *Plutonium Usage*. *Unit-Level Specific Power* is the ratio of DC electrical output power to generator mass for one RPS unit, and is a useful metric for comparing RPS systems. *Volume* refers to the physical dimensions of the RPS unit and any required support systems, including radiator fins, etc. *Heritage* accounts for the commonality of each advanced RPS with similar systems that have been designed, built, tested, and/or flown. *Integration* refers to the complexity associated with integrating each advanced RPS system on a spacecraft, and considers such factors as the physical size and configuration of the RPS system. *Environmental Emissions* refers to the emitted electromagnetic radiation and vibration environment associated with each RPS and their potential mission impact. *Robustness* describes the inherent ability of each RPS to gracefully handle fault conditions, and considers factors such as built-in redundancy, cross-strapped series/parallel connectivity, and the potential for single-point failures. RPS complexity considers whether the RPS uses solid-state or moving parts, passive versus active control, and simple versus sophisticated electronics. Lastly, *Plutonium Usage* assesses the relative amount of <sup>238</sup>Pu each RPS system uses and is related to the RPS conversion efficiency.

Each RPS system was ranked for its potential ability to support a range of space applications, including rovers, landers, and orbiter and flyby spacecraft. The results are dependent on the mission power level (as discussed in the text), and thus rankings are provided for low-power missions ( $\leq 200$  We) and those requiring higher power levels ( $> 200$  We). The RPS concepts were

---

<sup>2</sup> Recent analysis by the Orbital Science Corporation (OSC) suggests that a specific power of up to 8 We/kg may be possible for a higher power (~150 We) SunPower-based advanced Stirling generator.

also ranked for a number of special cases, including missions on the surface of Venus, missions using aerocapture, missions including seismometry or fields and particles-based instrumentation, missions in high-radiation environments, and long-duration missions. The results of this assessment are summarized in Table 1-4. Color coding is used to indicate the relative ranking of how well each RPS meets each criterion—green is higher, yellow is moderate, and red is lower. All of the advanced RPS technologies were assumed to meet all mission safety requirements to an equal degree.

### ***Advanced RTG***

The conceptual advanced RTG is a 112-We (BOM) device with an estimated unit mass of ~26.2 kg and specific power of 4.3 We/kg. This value is approximately 54% higher than that of the MMRTG, but is somewhat lower than the specific power of the advanced Stirling and TPV systems considered in this study (both are on the order of ~6 We/kg). The advanced RTG design would have a moderately-sized physical envelope relative to other advanced RPS concepts studied, with dimensions similar to those of the MMRTG but using only five GPHS modules compared with the MMRTG's eight, due to the higher efficiency of skutterudite thermoelectrics. RTG integration with a spacecraft is expected to be straightforward, with minimal complexity as demonstrated by previous missions using RTG technology (Table 1-1). RTGs produce no vibration, noise, or AC electromagnetic (EM) fields, giving them an inherent advantage relative to dynamic power systems for missions making sensitive fields and particles measurements or having tight pointing and/or stability requirements. Though RTGs produce DC electromagnetic fields, the process of mitigating these fields is well understood and not expected to be any more difficult than with existing RTG devices. RTGs have a high level of robustness and inherent reliability, using cross-strapped series/parallel electrical connectivity, passive power production, and no sophisticated electronics or controllers. The conceptual RTG considered in this study is assumed to share significant heritage with the MMRTG, using a similar design and components with the exception of the uncouples (skutterudites vs. PbTe/TAGS) and a shorter generator housing as previously discussed. The failure modes of RTGs are generally well known and understood from over 30 yrs of flight, minimizing the risk associated with using thermoelectric technology. RTGs are inherently radiation tolerant (e.g., the MMRTG is rated for a dose of 1 Mrad behind 100 mils of aluminum [Boeing, 2005]), and the advanced RTG is expected to have similar radiation tolerance. This is a significant advantage for missions in high-radiation environments (such as within Jupiter's radiation belts) where higher radiation tolerance translates into less shielding, potentially resulting in a less-massive power system. The lack of need for a controller also eliminates the concern of single-event upsets, which could be an issue for dynamic power systems. Though the relatively modest conversion efficiency of the advanced RTG requires the use of more <sup>238</sup>Pu fuel compared with dynamic systems, additional heat is generated that could potentially be used to warm spacecraft systems in place of electric heaters.

Based on the assessments summarized in Tables 1-3 and 1-4, the advanced RTG would be an attractive choice for a wide range of space missions and applications assuming <sup>238</sup>Pu availability is not an issue. The combination of the RTG's robustness, reliability, flight system heritage, lack of AC electromagnetic fields or vibration, and high radiation tolerance maximizes the number of missions that could be supported with this power system. While the advanced RTG has a lower unit-specific power than the advanced Stirling or TPV, the effective specific power of the advanced RTG would be approximately equal to or greater than that of the advanced Stirling at low spacecraft power levels (~100 to 200 We) due to the latter's need for a redundant unit consistent with *JPL Design Principles* (Yarnell, 2003), Figure 1-2. This would make the advanced RTG more attractive than the Stirling from a mass perspective for low-power spacecraft such as small orbiters or probes, MSL-class rovers, aerobots, etc.

Table 1-3. Assessment of Advanced RPS Systems Relative to Selected Mission-Related Criteria\*

Criteria	Adv RTG	Adv Stirling	TPV	Brayton	Rationale
Unit-Level Specific Power	Yellow	Green	Green	Yellow	Ranking based on advanced Stirling and TPV having specific powers on the order of 6 We/kg, and Brayton and advanced RTG having a specific power of about 4 We/kg. Note that the advanced Stirling assessment does not include the mass associated with a redundant unit(s) required for a mission.
Volume	Yellow	Green	Red	Yellow	High efficiency and heat rejection temperature of the advanced Stirling makes for the smallest size unit. The low heat rejection temperature of the TPV results in the need for large radiators, which may make the TPS option less attractive from a volume perspective.
Heritage	Green	Yellow	Red	Red	The advanced RTG is assumed to share significant design heritage with the MMRTG and previous RTGs (SNAP-19), thus making it the preferred option from a heritage perspective. The advanced Stirling has some heritage with terrestrial-based systems of similar design and potentially from the SRG. The TPV and Brayton systems are assumed to share little relevant heritage with existing flight systems.
Integration	Green	Green	Yellow	Green	The large size of the TPV radiators could complicate RPS integration with the spacecraft.
Environmental Emissions	Green	Yellow	Green	Yellow	Dynamic power systems generate AC electromagnetic fields and vibration that could be an issue for certain mission categories.
Robustness	Green	Yellow	Green	Green	The advanced RTG and TPV are assumed to use cross-strapped series/parallel electrical connections such that an individual uncouple or cell failure does not take down the entire system. The Brayton system is assumed to use a fully redundant architecture. The advanced Stirling is assumed single string, making it less attractive in terms of robustness.
RPS Complexity	Green	Yellow	Green	Yellow	The advanced RTG and TPV are fundamentally simpler systems compared with advanced Stirling and Brayton due to their passive operation, lack of moving parts, and lack of active electronics or sophisticated controllers.
Power Degradation Rate	Yellow	Green	Yellow	Green	Dynamic power systems are estimated to have a power degradation rate of 0.8%/yr due only to <sup>238</sup> Pu decay. Advanced RTG and TPV are estimated to have power degradation rates of approximately 1.6%/yr and 2%/yr, respectively. Note that degradation modes of dynamic systems have not been fully characterized - additional modes may exist that are not accounted for here.
<sup>238</sup> Pu Usage	Yellow	Green	Yellow	Green	The higher efficiency of the dynamic power systems (advanced Stirling and Brayton) make them preferable from the perspective of reduced <sup>238</sup> Pu fuel usage. This could be a significant driver if fuel availability is an issue.

**\*Legend**

Green = RPS system has a high relative ranking with respect to the specified criterion.  
 Yellow = RPS system has a moderate relative ranking with respect to the specified criterion.  
 Red = RPS system has a low relative ranking with respect to the specified criterion.

**Table 1-4. General Assessment of Advanced RPS Systems for a Range of Space Applications\***

Comparison Criteria	Adv RTG	Adv Stirling	TPV	Brayton	Rationale
<b>Mission Types</b>					
Rovers Low Power ( $\leq 200$ We)	Green	Yellow	Yellow	Green	Stirling systems require a redundant unit for missions, increasing overall power system mass. Large TPV radiator results in large TPV volume and greater integration complexity.
Rovers Higher Power ( $> 200$ We)	Green	Green	Yellow	Green	Large TPV radiator may result in greater integration complexity. Higher power missions gain the mass advantage of the advanced Stirling even with a redundant unit.
Landers Low Power ( $\leq 200$ We)	Green	Yellow	Yellow	Green	Stirling systems require a redundant unit for missions, increasing overall power system mass. Large TPV radiator size results in large RPS volume and greater integration complexity.
Landers Higher Power ( $> 200$ We)	Green	Green	Yellow	Green	Large TPV radiator may result in greater integration complexity. Higher power missions gain the mass advantage of the advanced Stirling even with a redundant unit.
Orbiters/Flybys Low Power ( $\leq 200$ We)	Green	Yellow	Yellow	Green	Stirling systems require a redundant unit for missions, increasing overall power system mass. TPV radiator size not expected to be a major issue for low-power Orbiter/Flyby.
Orbiters/Flybys Higher Power ( $> 200$ We)	Green	Green	Yellow	Green	Large TPV radiator size may result greater integration complexity. Higher-power missions gain the mass advantage of the advanced Stirling even with a redundant unit.
Surface Power Supply (Multiple kWe)	Yellow	Green	Yellow	Green	Higher-efficiency systems require less $^{238}\text{Pu}$ , which is significant for high-power applications.
<b>Special Cases</b>					
Venus Surface Missions	Red See Note	Green	Red	Yellow	Dynamic systems can directly drive cryocoolers to provide both electrical and cooling power. Stirling is more efficient than Brayton. This Stirling is based on the NGST TASHE engine (Section 3). RTG could be used to produce electricity, but providing refrigeration would be very inefficient. Is questionable whether TPV could operate at Venus-surface temperature, and would still need to provide cooling and deal with large fins.
Aerocapture Missions	Yellow	Green	Yellow	Green	Need to manage RPS heat during aerocapture. Higher-efficiency converters require less fuel, which produces less heat, equating to a simpler, lighter thermal control system.
Seismometry Payload	Green	Yellow	Green	Yellow	Dynamic RPSs produce vibration that could interfere with seismic measurements - would require isolating the seismometer from RPS, increasing system complexity.
High Radiation Environments	Green	Red	Red	Red	RTGs are inherently rad-hard. Stirling and Brayton controllers, and PV arrays are rad-soft.
Sensitive Fields and Particles Missions	Green	Yellow	Green	Yellow	The advanced Stirling and Brayton produced AC electromagnetic fields that may interfere with fields and particles measurements, potentially requiring Mu-metal shielding, booms and/or notch filtering to mitigate, increasing spacecraft complexity.
Long-Duration Missions	Green	Yellow	Green	Yellow	The advanced Stirling and Brayton have moving parts, active electronics, and less graceful degradation modes, making them less preferred for long-duration missions compared with RTG and TPV.
<b>*Legend</b>	Green = RPS system has a high relative ranking with respect to the specified criterion. Yellow = RPS system has a moderate relative ranking with respect to the specified criterion. Red = RPS system has a low relative ranking with respect to the specified criterion.				
<b>Note:</b>	Rating based on the lower overall efficiency of an RTG system compared with that of dynamic RPS systems. However, dynamic systems may not be compatible with surface seismic applications. An RTG/sorption refrigerator may be enabling for this type of application.				

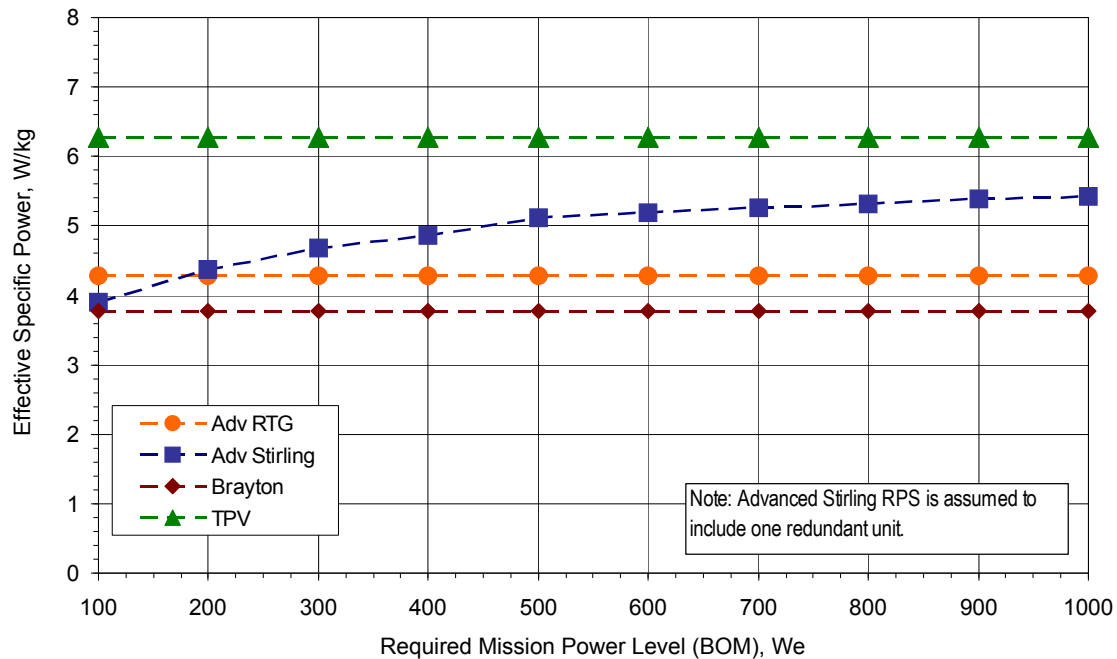


Figure 1-2. Effective Specific Power versus Mission Power Requirement

The advanced RTG could also be used on higher-power missions, but would be less attractive from a mass perspective compared with the advanced Stirling or TPV systems. Note, however, that this study did not consider the launch load requirements of the advanced Stirling, TPV, and Brayton RPSs, or whether the launch vehicle (LV) would need to be modified to accommodate the launch load requirements of each of these power systems. This could be a significant mass driver, as it was for the Cassini mission, which required ~200 kg of acoustic tiles to attenuate the launch environment of the Titan IV LV to a tolerable level of the GPHS-RTG (Hoffman, 2005).

The advanced RTG concept in this report is assumed to be based on the MMRTG, which is designed to launch on LVs up to and including the Delta IV-Heavy (4050H-19). On the other hand, the launch limits of the advanced Stirling, Brayton, and TPV are unknown and may require significant generator modifications and/or acoustic tile mass to launch on the largest of LVs, thus potentially decreasing their effective specific powers to below those estimated here. The lower efficiency of the advanced RTG makes it less suitable for aerocapture missions, potentially requiring a heavier and more complex thermal energy management system compared with the more efficient Stirling and Brayton systems. Similarly, the advanced RTG would be less attractive from a <sup>238</sup>Pu usage perspective.

A long-lived Venus surface mission is considered beyond the capability of the advanced RTG considered in this report due to the extreme pressure and temperature that would be encountered there (90 bar and 460°C) - a mission-specific RPS generator would be required for this application. Electrical power production on the surface of Venus may be possible using thermoelectrics made from silicon germanium (SiGe), or even high-temperature skutterudites. However, the spacecraft cooling requirements can exceed the electrical power requirements by several times, and powering a cryocooler using RTG electrical power would be much less efficient compared with directly-coupled dynamic RPS systems (e.g., Stirling or Brayton). Sorption refrigeration systems are a potential option that would require little or no electrical power to operate and use GPHS modules as the high temperature heat source; however, preliminary analysis indicates that the cooling efficiency of such systems would be very low

(~0.1% to 1% [Jones, 2005]) compared with Stirling-based cooling systems (several percent, [Petach, 2004b]). On the other hand, a long-lived Venus seismometry mission may not be compatible with the vibration environment produced by a dynamic RPS/cryocooler system. Were this the case, then the inherently vibration-free RTG/sorption refrigeration concept could be an enabling technology for a long duration Venus surface seismic application.

In summary, though the advanced RTG has a lower efficiency and unit specific power compared with other advanced RPS systems considered in this report, it possesses many desirable characteristics, including robustness, simpler design, flight heritage, lack of AC EM fields or vibration, and high radiation tolerance, that make it a preferred choice for many mission applications requiring radioisotope power.

### *Advanced Stirling*

The conceptual advanced Stirling generator assessed in this report is an 80-We (BOM) device based on a single Stirling Converter Assembly (SCA) with a unit mass of 13.7 kg. The unit-specific power is estimated at 5.9 We/kg, which is ~74% greater than that of the SRG. The advanced Stirling RPS has the second highest unit-level specific power value of all the RPS types considered herein, with only the TPV estimated to have a higher unit-level specific power level of ~6.3 We/kg. The advanced Stirling is a block-redundant device, requiring at least one redundant generator for missions using this technology (Yarnell, 2003). As a result, the effective specific power of the advanced Stirling system is lower than its unit-level value, with the actual value dependent upon the power level of the mission and the number of redundant systems required. For example, a mission requiring 80 We at BOM would require two advanced Stirling generators (one prime and one redundant), resulting in an effective specific power of ~3 We/kg; a mission requiring 400 We at BOM would require a minimum of six advanced Stirling units (five prime and one redundant), with an effective specific power of ~4.9 We/kg (Fig. 1-2). In practice, high-power missions may require more than one redundant Stirling generator, which could further reduce its effective specific power. The relatively small size of the SunPower Stirling engine and linear alternator results in this conceptual Stirling system having the smallest physical dimensions of any of the RPS types considered in this report. Integration of this generator concept into a spacecraft is expected to be relatively straightforward due to the small volume and compact physical layout of each unit, along with an integrated electronic controller assumed to be contained within the generator housing. Stirling convertors produce vibration from their oscillating displacer and power pistons, and AC and DC electromagnetic fields from their linear alternator and controller. For this conceptual design, vibration mitigation would be performed using an actively controlled opposing-phase counter mass. No isolation system is completely effective, however, and residual vibration could pose a challenge to missions with very sensitive pointing and stability requirements (e.g., spacecraft with long focal-length optics and long-exposure durations, etc.). Management of the Stirling generator's DC fields would likely be similar to that used for RTGs (e.g., using magnets to counter the fields, clocking the RPSs to create a null zone, etc.). Management of the Stirling generator's AC fields, however, is a greater challenge and could require a complex combination of Mu-metal shielding, booms, and notch filtering to meet the EM cleanliness requirements of the most sensitive fields and particles missions. Such missions may be better served by static RPSs that produce no AC field component. The conceptual Stirling considered in this report assumes single-string electronics and controller (consistent with the current SRG design). The use of moving parts, active electronics, and the need for a sophisticated controller make the Stirling system more complex than static power systems that have intrinsic redundancy and no active electronics.

The advanced Stirling system considered here is assumed to share limited heritage with the SRG currently under development by NASA and DOE and with other terrestrially-based Stirling

systems being designed by SunPower. The failure modes of the advanced Stirling RPS are not yet fully understood, and are not all graceful; thus the advanced Stirling RPS's robustness is considered less attractive compared with static power systems. The advanced Stirling system uses electronics that were assumed radiation tolerant to between 20 krad to 100 krad (behind 100 mils of aluminum), consistent with the SRG design. This is likely adequate for the majority of missions that would operate in the relatively benign radiation environment of deep space and on many planetary bodies; however, extensive shielding would be required to support missions in the strong radiation fields of Jupiter's magnetosphere. For example, a 30-day Europa orbiter mission would receive a total ionizing dose as high as 1.8 Mrad (behind 100 mils of aluminum). The amount of shielding required in this type of environment could decrease the effective specific power of the Stirling system below that of the radiation-hardened advanced RTG. Single-event upsets (SEUs) are another potential issue in high radiation environments and would require the controller to be designed with radiation tolerance and SEU recovery in mind. These factors make the advanced Stirling RPS relatively less attractive for missions in high radiation environments. The conversion efficiency of the advanced Stirling was the highest (32%) of all the RPS systems considered in this work, translating into less  $^{238}\text{Pu}$  fuel required to generate a given power-level compared with less efficient systems. This makes the advanced Stirling the most attractive system from a fuel usage perspective, and could be a deciding factor were fuel availability an issue.

The second type of Stirling generator considered in this report is specifically intended for a long-duration Venus surface mission. Such a mission would require a dedicated RPS system specifically designed to survive the extreme Venus environment (460°C and 90 bar) and to provide active cooling to the exploratory vehicle. The Stirling system has an inherent advantage relative to static power systems for a Venus surface mission in that it can be integrated with a cryocooler to provide both electrical power and cooling. A specially-modified Thermoacoustic Stirling Heat Engine (TASHE) with integrated cryocooler (Section 3.5) was considered in this report for a Venus surface application. This system is being developed by NGST and LANL for operation in terrestrial environments, but could potentially be designed to operate in a Venus surface environment (Petach, 2004b), with modifications. The TASHE has no moving parts, and uses thermoacoustic energy to drive a linear alternator to produce electricity. A key advantage of the TASHE system is that it can be directly coupled to a pulse tube refrigerator (e.g., cryocooler) to provide higher efficiency cooling than is possible with traditional mechanically-coupled Stirling cryocooler systems. Though prototype TASHE units have been built and tested under laboratory conditions, the integrated TASHE and cryocooler system considered in this report is conceptual only and specifically designed for a Venus surface application. It would generate 80 We of electrical power and ~410 Wth of cooling power from 53 GPHS modules. Thermoacoustic Stirling technology has the additional benefit of potentially higher system reliability due to fewer moving parts compared with traditional free-piston Stirling engines. Though the TASHE was considered only for a Venus application, numerous other space missions and applications could benefit from this technology with and without using the integrated cryocooler. However, the limited scope of this report precluded consideration of TASHE technology beyond its use for a conceptual long-duration Venus surface mission.

The high specific power of the SunPower-based advanced Stirling generator makes it an attractive candidate for missions with higher power requirements (>200 We), such as medium to large orbiter and flyby spacecraft, and large landers or rovers (e.g., >2 times the power of MSL). Though the Stirling generator could be used for lower-power missions ( $\leq 200$  We), the need to include at least one redundant unit would result in a heavier power system relative to the advanced RTG and TPV systems (Fig. 1-3). The high efficiency of the advanced Stirling also

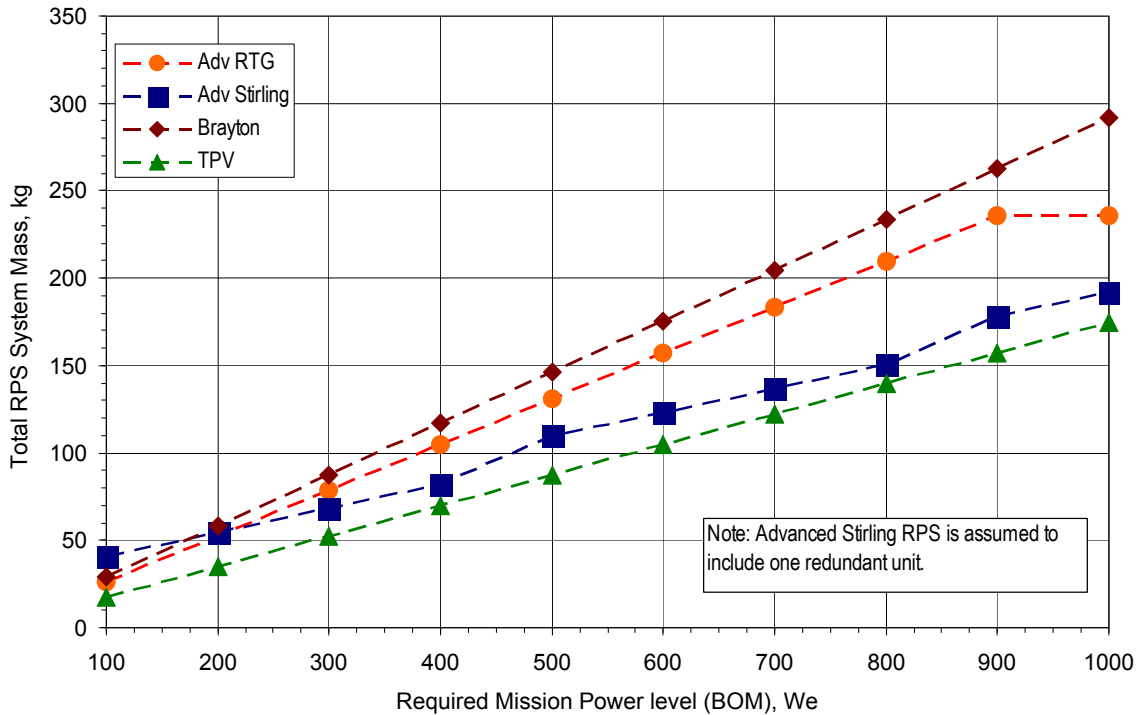


**Figure 1-3.** RPS System Mass versus Mission Power Requirement

makes it attractive for aerocapture missions, where its lower heat output would potentially lead to a lighter and less complex thermal energy storage system. An important benefit of Stirling technology is that a mission-dedicated RPS (based on the TASHE RPS) with integrated cryocooler has the potential to enable a long duration Venus surface mission, a key priority of the Solar System Exploration Strategic Roadmap (NASA, 2005). Though a Venus-specific Brayton system based on a Creare design (Zagarola, 2004) may also be a viable option, preliminary analyses indicates that a Stirling-based unit would be more efficient. The advanced Stirling would be less attractive for missions using seismic monitoring instrumentation as such payloads could be adversely affected by the vibrations induced by the generator.

Likewise, the production of AC electromagnetic fields could make the Stirling less suitable for missions with sensitive fields and particles instrumentations, though Mu-metal shielding, booms, and/or notch filtering may be able to help mitigate this. The advanced Stirling’s relatively lower radiation tolerance makes it less attractive for missions operating in high radiation environments such as the Jovian system and near the Sun. Such missions would potentially require large amounts of shielding and special electronics to mitigate SEUs. The advanced Stirling would be less preferred for long duration missions (at least initially) due to its lower robustness and greater system complexity. However, advanced Stirling RPSs would be attractive for shorter duration missions (~few years) with high power requirements (e.g., lunar surface power supplies). Such missions could also serve to demonstrate the long-term performance and reliability of the advanced Stirling in a flight environment, a necessary step before using them on long-duration missions to the outer solar system.

In summary, the advanced Stirling is attractive from the perspective of high unit-level specific power, high efficiency, and small size. This is balanced by its relatively lower robustness and greater RPS complexity compared with static power systems, its generation of AC EM fields, vibration, and its sensitivity to high radiation fields. As such, the advanced Stirling could be

suitable for shorter duration, higher power (>200 We) applications including rovers, landers, aerobots, and orbiter/flyby spacecraft that operate in benign radiation environments. The high efficiency of the advanced Stirling makes it attractive for aerocapture missions and for surface power supplies (though a higher power version of the advanced Stirling could be more practical for this application). Lastly, a mission-specific variant of the Stirling with integrated cryocooler could be enabling for a long duration (a few weeks to a few months) Venus surface mission.

### ***Brayton***

A conceptual Brayton RPS was considered that would generate 110 We at BOM from two GPHS modules (Zagarola, 2005), and have a unit mass of approximately 29.2 kg. The unit-level specific power is estimated at 3.8 We/kg. This Brayton system includes a fully redundant power system built upon two counter-rotating turbo-alternator-compressors, each nominally operating at 50% power and able to be spooled up to the full 110 We in case one unit fails (Zagarola, 2005). Due to this internal redundancy, it is assumed that additional redundant Brayton systems would not be required. As a result, the total mass of the Brayton RPS system would be less than that of the advanced Stirling system for low power applications (<200 We). See Figure 1-3. The conceptual Brayton RPS would have a physical size similar to that of the advanced RTG, which is larger than that of the advanced Stirling unit, but significantly smaller than the TPV generator. Integration of this generator into a spacecraft is expected to be relatively straightforward due to the moderate volume and physical layout of each unit and the assumption of internally integrated controllers within the generator housing. The Brayton is expected to produce some residual vibration from its rotating turbo-alternator-compressor (TAC), and to generate AC and DC electromagnetic fields from its alternator and controller. Depending on its magnitude and frequency, the induced vibration could potentially pose a challenge to missions with very sensitive pointing and/or stability requirements (e.g., for high-resolution remote sensing or seismometry). Management of the Brayton generator's DC fields would likely be similar to that of the advanced RTG and advanced Stirling generators. The Brayton's AC fields, however, could prove more difficult to manage and require a combination of Mu-metal shielding, booms, and notch filtering to meet the EM cleanliness requirements of the most sensitive fields and particles missions. Such missions may be better served by static RPSs that produce no AC field component. The Brayton's high-speed rotating TACs have the potential to generate undesired torque on the spacecraft. Torque mitigation would nominally be performed by counter rotating each of the two TACs to produce zero net torque; however, failure of one TAC would allow the remaining TAC to induce torques on the spacecraft during acceleration and attitude change maneuvers (in the case of orbiters and flyby spacecraft), potentially complicating the operation of the spacecraft attitude and control system (ACS). The Brayton RPS includes moving parts, active electronics, and a sophisticated controller, making it inherently more complex than static power systems. While Brayton systems have been used for decades for terrestrial power generation, no Brayton RPS systems have flown in space, and there is minimal (if any) applicable heritage for the space-based Brayton RPS. As with the advanced Stirling RPS, the failure modes of this system have yet to be fully understood and quantified, and are not all graceful; thus, the robustness of the Brayton RPS is considered less attractive compared with static RPS concepts. The electronics used in the Brayton RPS are assumed to be radiation tolerant to between 20 to 100 krad (behind 100 mils of aluminum) similar to the current SRG design. This is potentially adequate for the majority of space missions in more benign radiation environments, but limits the utility of the Brayton RPS for missions in high-radiation environments as previously discussed, making it less attractive compared with the radiation-hard advanced RTG. The conversion efficiency of the Brayton was the second highest (22%) of all the RPS systems considered in this report, translating into less  $^{238}\text{Pu}$  fuel required relative to both the

advanced RTG and TPV concepts. The higher conversion efficiency of the Brayton is attractive from a fuel usage perspective, and for potentially simplifying thermal energy management for missions that do not need large amounts of heat to maintain operating system temperatures.

The Brayton RPS system considered in this study would make a reasonable alternative to the advanced Stirling for a fairly wide range of space missions and applications. An attractive feature of this system is its built-in redundant TACs and controllers, making it more robust than the single-string advanced Stirling system. This internal redundancy also makes the Brayton lighter than the advanced Stirling system for lower power applications (<200 We), though it is heavier than an equivalent RTG or TPV system. The Brayton's relatively modest size is not expected to pose a challenge for spacecraft integration as is likely on par with integration complexity of the advanced RTG. The higher conversion efficiency of this system makes it more attractive than static systems for surface power supply applications. Missions using aerocapture could benefit from the Brayton's low heat output relative to static power systems by using a simpler and potentially lighter thermal energy management system. As with the advanced Stirling RPS, the vibration and AC electromagnetic fields produced by the Brayton RPS could make it less attractive for missions using seismic instrumentation and making sensitive fields and particles measurements. However, the AC field strength for the Brayton is expected to be greatest at the higher frequencies (tens of kHz) due to the high TAC rotational speed (hundreds of thousands of RPMs), thus potentially permitting measurements at the lower frequencies (tens to few thousands of Hz). The Brayton RPS would be less attractive for missions in high-radiation environments (e.g., the Jovian system and near the Sun) relative to the radiation-hard advanced RTG. Use of the Brayton RPS in high-dose environments could require significant amounts of shielding for its electronics, and its controller would need to be specially designed to tolerate SEUs. A mission-specific variant of the Creare-based Brayton RPS was considered for a Venus surface mission using an integrated cryocooler; however, preliminary estimates (personal communication with Zagarola, 2005) indicate that the efficiency of such a system would be less than the thermoacoustic heat engine and cryocooler concept previously discussed, requiring approximately three times more <sup>238</sup>Pu fuel for the same level of electrical and cooling power. As with the advanced Stirling system, the greater complexity of the Brayton RPS (due to its moving parts and active electronics) make it less attractive for long-duration missions relative to static power systems. Successful flight demonstrations of the Brayton on shorter missions (few yrs) would likely be necessary before this system would be used for a long-duration mission to the outer solar system.

In summary, the Brayton could be preferred relative to static power systems for short-duration, high-power missions in lower-radiation environments with payloads that can tolerate the Brayton's AC EM fields and vibration. The Brayton could also be preferred over static systems for spacecraft using aeroshells, where its higher efficiency translates into relatively lower fuel usage and heat generation. Though the Brayton system is estimated to have lower efficiency than the advanced Stirling RPS, the Brayton's built-in redundancy gives it greater robustness relative to the Stirling system. This potentially eliminates the need to carry a redundant Brayton RPS unit, yielding a greater effective specific power at lower power levels (<200 W) than that of the advanced Stirling concept.

### ***TPV***

A conceptual TPV RPS generator assessed in this study is based on a JPL design scaled to a 110 We (BOM) device with an estimated unit mass of 17.5 kg. The unit-level specific power of this system was estimated at ~6.3 We/kg—the highest value of all the advanced RPS systems assessed in this report. The TPV system requires a low heat rejection temperature, and thus needs large radiator fins to maximize its power conversion efficiency. As a result, the TPV generator

has a large physical envelope, with a fin area of  $\sim 2.5 \text{ m}^2$  predicted for a 110-We device. Though different fin configurations have been studied (Section 3.7), the large size of the TPV radiators is expected to generally complicate spacecraft integration and limit its practicality on smaller spacecraft and vehicles. An exception is the use of TPV in Titan's cold, dense atmosphere which would allow for significantly smaller radiator fins, potentially making TPV a viable option for atmospheric and surface vehicles on Titan; however, heat rejection during the cruise stage in deep space could require a second set of large fins that would increase the overall RPS system mass and potentially complicate spacecraft integration. TPV power conversion produces no vibration, noise, or AC electromagnetic fields, which like the advanced RTG, gives it an inherent advantage compared with dynamic power systems for missions with sensitive fields and particles instruments or tight pointing and stability requirements. The TPV would produce a DC electromagnetic field, but mitigation strategies that would likely be similar to that for the advanced RTG. The photovoltaic cells of the TPV generator would be cross-strapped with series/parallel electronically connectivity such that failure of a single cell would reduce the system power by only that of the failed cell. This, in combination with passive power production, and lack of active electronics or controllers potentially makes the TPV less complex and potentially more reliable and robust than dynamic power systems. However, no TPV generators have flown in space, and thus heritage for a TPV flight unit is considered low compared with RTG power systems. Photovoltaic modules are generally sensitive to radiation, with their performance decreasing with received fluence level (personal communications with Mardesich, Mueller, Stella, and Timmerman, 2005). Shielding is likely required for missions with higher fluence levels (such as those encountered in Jupiter's radiation belts) that would make the TPV option less favorable from a mass perspective. The conceptual TPV generator considered in this report has a conversion efficiency of  $\sim 15\%$  (Ewell, 1993), which is greater than that of the advanced RTG, but lower than that of the advanced Stirling and Brayton concepts.

The TPV system could be an attractive alternative for low power orbiter/flyby spacecraft (e.g.,  $\leq 200 \text{ We}$ ) where its radiator fins would still be small enough to more readily integrate with a spacecraft. Missions with sensitive fields and particles payloads and tight pointing and stability requirements could take advantage of the TPV's lack of AC electromagnetic fields or vibration. The inherent robustness and inherent reliability of the TPV generator make it attractive for long-duration missions. However, the relatively large fins of the TPV make this power system potentially less attractive for rovers, landers, and aerobot vehicles where the sizable fins could impede the field of view of science instruments, interfere with mobility, etc. The lower conversion efficiency and large size of the TPV system compared with dynamic systems makes TPV relatively less attractive for surface power-supply applications. TPV is also less suitable for aeroshell missions as two sets of potentially large fins would be required (one inside the aeroshell and one outside it, as illustrated in Section 2.3.1-15), thus increasing system and integration complexity, and adding more mass relative to other power systems with smaller fins.

The TPV system would be a poor choice for a Venus surface mission due to the incompatibility of the high surface temperature ( $460^\circ\text{C}$ ) and need for a low TPV heat rejection temperature (few tens of  $^\circ\text{C}$ ) to achieve high efficiencies. Additionally, a separate cooling system would be required to maintain spacecraft operating temperatures. TPV electrical power could potentially be used to drive a cryocooler, or a sorption refrigeration system could be incorporated using GPHS modules as a heat source. In both cases, however, the cooling efficiency would be much lower than for dynamic power systems (e.g., Stirling or Brayton).

The inherent sensitivity of photovoltaics to radiation makes the TPV unattractive for missions in high-radiation environments with high total fluences, such as the Jovian system and in proximity to the Sun. Such missions would be better off using the inherently radiation-hard RTG system.

Were  $^{238}\text{Pu}$  availability an issue and a static power system preferred (e.g., for robustness, AC EM cleanliness, and/or lack of vibration), the TPV concept could be an attractive option.

In summary, the TPV has several attractive features compared with other advanced RPS systems considered in this report, including high specific power, moderately high conversion efficiency, a lack of moving parts and active electronics, a lack of AC EM fields or vibration, and inherent robustness and inherent reliability. The main disadvantage of TPV is its large fin size, making it less attractive compared to the advanced RTG, advanced Stirling, and Brayton for all but low-power ( $\leq 200$  W) orbiters or flyby spacecraft. The TPV's low radiation tolerance is also a limiting factor for a number of scientifically valuable missions. TPV may be an attractive alternative for missions to Titan's cold, convective atmosphere (e.g., for a lander, rover, or aerobot) where its fins size could be made significantly smaller ( $\sim 1/5$ ) compared with deep space; however, a larger second set of fins would be required during the cruise phase, that would add mass, and potentially complicate the overall spacecraft system.

## **1.4 CONCLUSIONS**

Five conceptual advanced RPSs were assessed from a mission perspective based on power converter technology being developed by NASA, DOE, and their industry partners. These systems included an advanced RTG, two types of advanced Stirling generators, a Brayton generator, and a TPV generator. Four detailed mission studies were conducted to better understand the power system trades and define the potential power requirements, mass constraints, and integration issues associated with each advanced RPS. The mission studies were all based on the priority missions defined in the SSEDs and the SSESr, and include a Titan orbiter with probe, Titan rover, Europa lander, and Venus surface explorer. The RPS converter technologies described in this report are in an early state of development, and do not yet exist in a flight-like configuration. Thus, in order to perform power system trades, preliminary system analyses were conducted by JPL to estimate the potential performance characteristics of each advanced RPS system based on the subsystem-level analyses and tests performed by NASA, SunPower, Creare, NGST and LANL. The balance of each advanced RPS system (i.e., housing, insulation, controllers, etc.) was based on RPS systems currently in development (MMRTG and SRG) in order to achieve more realistic results.

The conceptual advanced RTG has many key characteristics including robustness, lack of moving parts or active electronics, heritage, a lack of AC EM fields or vibration, and high radiation tolerance that make it an attractive choice for many mission applications. These applications include rovers, landers, aerobots, and orbiter/flyby spacecraft. Though the advanced RTG considered here has a lower efficiency and unit specific power compared with other advanced systems discussed in this report, it possesses other key characteristics that are at least as important (e.g., robustness, simplicity of design, and heritage) making it a preferred choice for a wide range of space missions over a broad range of power levels and environments.

The conceptual advanced Stirling had the highest conversion efficiency and second highest unit specific power of all the conceptual RPS systems considered. This is tempered, however, by its lower robustness (assumed single string) and greater complexity compared with static power systems, its generation of AC EM fields and vibration, and its greater sensitivity to high radiation fields. Thus, the advanced Stirling was considered to be more suitable (at least initially) for shorter duration missions with higher power ( $>200$  We) applications including rovers, landers, aerobots, and orbiter/flyby spacecraft that operate in benign radiation environments. Once its performance had been verified in a flight environment, the advanced Stirling could be an attractive choice for longer-duration missions. This RPS system is also suitable for aerocapture missions, and potentially for high-power surface power supplies. A mission-specific variant of

---

the advanced Stirling with integrated cryocooler could also be enabling for a long duration Venus surface mission.

The conceptual Brayton system shared many characteristics with the advanced Stirling in terms of environmental emissions, RPS complexity, and radiation tolerance, but possessed a lower unit specific power and conversion efficiency than the advanced Stirling system. The Brayton RPS was assumed to use an internally redundant power system, making it potentially more robust than the single string Stirling; however, its use of moving parts and active electronics makes it less preferable for long duration missions compared with simpler static power systems until such time as its long-term performance had been verified. Were  $^{238}\text{Pu}$  availability a serious driver, the Brayton would be an attractive alternative to the advanced RTG for short duration, low power applications such as rovers, landers, and aerobots. Likewise, the Brayton could be preferred over static power systems (and is potentially a viable alternative to the advanced Stirling) for short duration, and high power missions such as surface power supplies. However, the Brayton's AC EM field and vibration levels may limit the types of payloads it could support. A mission-specific Brayton system with integrated cryocooler was considered for a Venus surface application; however, preliminary analyses indicate that the advanced Stirling would be more attractive from the perspective of higher efficiency.

The TPV has many attractive features including high specific power, moderately high conversion efficiency, a lack of moving parts and active electronics, a lack of AC EM fields or vibration, and inherent robustness and lower complexity. The main disadvantage of TPV is the need to maintain a relatively low cold-side temperature in order to achieve higher conversion efficiency. This results in the need for large fins, making TPV relatively less attractive for all but low power (less than a couple of hundred watts) orbiters or flyby spacecraft. Possible exceptions to this are missions that operate in Titan's cold, convective atmosphere where the fins size could be made significantly smaller compared with deep space; thus, potentially making TPV a viable option for a Titan lander, rover, or aerobot mission.

In conclusion, the higher specific power and conversion efficiency of the advanced RPS systems studied in this report were found to be mission-enhancing compared to the MMRTG and SRG, potentially enabling greater mission payloads or the use of smaller launch vehicles with the benefit of lower mission cost. Though low-power applications would see a moderate mass advantage from using advanced RPSs, it is really the higher power Galileo- and Cassini-class missions that would benefit the most from the higher specific power of these power systems. Lastly, advanced RPSs would be mission-enabling for a long-lived Venus surface mission, as none of NASA's current RPS systems have the capability to operate in this extreme environment.



---

## 2. MISSION CONCEPTS AND APPLICATIONS

### 2.1 INTRODUCTION

---

JPL performed studies to identify and assess mission concepts that could be enhanced or enabled by a new generation of advanced RPSs currently being developed by NASA, DOE, and their industrial partners. These systems include the advanced RTG, advanced Stirling, Brayton, and TPV. While analyses and/or subsystem tests have been performed to varying degrees for each of these systems, no flight-like systems currently exist. Thus, preliminary estimates of converter configuration and specific power were formulated by JPL to facilitate their use in the mission studies.

The goal of this report was to (1) identify high-value missions and applications that could be enhanced or enabled by this new RPS technology, (2) perform high-level analyses of selected concepts to demonstrate overall feasibility, (3) assess the preliminary mission power requirements, and (4) identify the potential benefits and advanced RPS preference as a function of key mission parameters.

### 2.2 BACKGROUND AND MISSION CATEGORIES

---

Studies were performed to identify how advanced RPS systems could enhance or enable a range of conceptual missions that employ orbiters, landers, and rovers. Integrated mission design teams were formed that included a core group of scientists and mission design architects, and used JPL's concurrent engineering design teams with their broad range of subsystem domain expertise. Each concurrent engineering team included experts in systems, communications, thermal, power, avionics, guidance, navigation and control, propulsion, mission design, and structures. Many of these team members have experience on flight projects and use that expertise to maximize the realism and accuracy of the mission design.

The scientists on the core team defined a preliminary set of science goals for each mission based on the National Research Council (NRC) Solar System Exploration Roadmap and Decadal Survey. The mission architects worked with the scientists to define the mission requirements and overall architecture, and led the concurrent design team sessions. JPL's Team-A and Team-P were used in the development of the mission concepts presented in this report.

Four mission concepts were selected for investigation and assessment in the present study; these included a Titan orbiter with probe, Europa lander, Titan rover, and a long-duration Venus rover. The results obtained from each of these studies was then extrapolated to other, similar missions such that an overall assessment could be made of the benefits of advanced RPSs for a broad range of missions and applications. Though no lunar-based missions studies were explicitly considered in this activity, preliminary trades were made regarding the benefits of each type of advanced RPS for lunar exploration-based applications and missions including high-energy surface power supplies.

## 2.3 SATELLITE MISSIONS

### 2.3.1 Titan Orbiter with Probe Mission

With the remarkable success of the Cassini-Huygens mission, considerable new knowledge has been obtained regarding the surface topography, composition, and atmospheric characteristics of Titan (Fig. 2.3.1-1). However, Cassini-Huygens represents only a bold beginning for the exploration of Titan, as high-resolution mapping will have been performed for only a small fraction of the surface of Titan by the end of the nominal mission. Large gaps in knowledge will remain in key scientific areas, including global surface topography; atmospheric and surface composition; precipitation rates; and the density, thickness, and formation processes of clouds.

This study details a conceptual follow-on Titan orbiter mission that would provide full global topographic coverage, surface imaging, and meteorological characterization of the atmosphere over a nominal 2-yr science mission. The baseline power requirement is ~1 kWe at EOM and is driven by a high-power radar instrument that would provide 3-dimensional measurements of atmospheric clouds, precipitation, and surface topography. While this power level is moderately higher than that of the Cassini spacecraft, higher-efficiency advanced RPSs could potentially reduce  $^{238}\text{Pu}$  usage to less than one-third that used on the Cassini spacecraft.

The Titan orbiter mission is assumed to launch in 2015. It would utilize advanced RPSs to provide all onboard power, and would employ an aeroshell to aerocapture into Titan orbit. Additionally, a 500-kg “black box” deployed probe, with unspecified science instrumentation, was included in the design.

Four conceptual advanced RPS concepts were considered for this mission, specifically, advanced RTG, advanced Stirling, Brayton, and TPV technologies. For the baseline mission, the advanced Stirling RPS was selected due to its greater specific power and higher conversion efficiency, enabling the ability to include a 500-kg probe (only the advanced Stirling option permitted this capability; see Section 2.3.1-15). The advanced Stirling was considered viable for this mission, since the baseline Titan orbiter payload did not include any fields and particles instruments that could be adversely affected by the Stirling’s AC electromagnetic fields. Had a fields and particles mission been selected, it is possible that the AC fields produced by the Stirling and Brayton systems could have precluded their use on such a mission; in such a case, the advanced RTG would be the preferred RPS power system.

This study also summarizes the key results for the remaining three advanced RPS systems not included in the baseline mission, and describes the resulting benefits and issues for each advanced RPS technology with respect to the Titan orbiter mission. For purposes of comparison, results are also provided using the MMRTG and SRG RPSs.

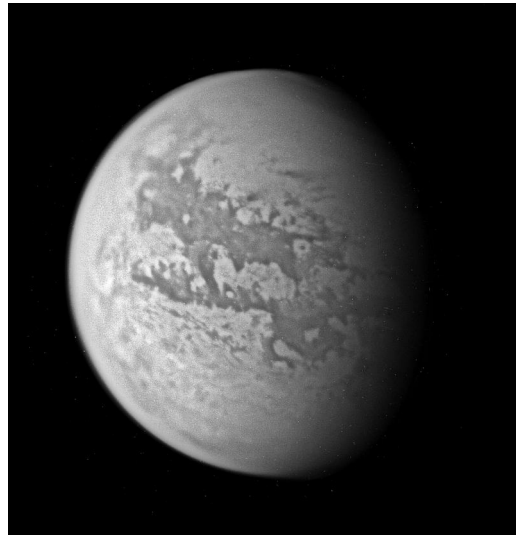


Figure 2.3.1-1. Image of Titan Taken from the Cassini Spacecraft in 2005.

### 2.3.1.2 Science Goals

Saturn's large satellite Titan is the only body in the solar system other than the Earth that has a substantial atmosphere (Earth-like density or greater) dominated by molecular nitrogen. Therefore, the similarities and differences of atmospheric processes on Earth and Titan are of considerable interest to the scientific community. In addition, the prebiotic organic chemistry expected to be found at Titan's surface is of great interest for scientists concerned with the origins of life. The Solar System Exploration Decadal Survey identified Titan as the second highest-priority target for future missions to the outer solar system, after Europa. Early Cassini and Huygens observations of Titan have only increased the level of interest. Follow-on missions to the Saturn system to explore Titan's mysteries in more detail are being studied both in the U.S.A. and in Europe.

Because Titan's thick, hazy atmosphere prevents making certain observations from orbit, some of the highest priority objectives for future missions to Titan can best be addressed from lander, rover, or aerial platforms. Global surface composition, the distribution and nature of surface organics, and current chemical interactions of the surface and atmosphere are among these. There are also a number of key Titan science objectives that are best addressed from an orbiting platform. Among these are (1) understanding global atmospheric dynamics, including the global meteorology of clouds and precipitation on Titan; (2) understanding global topography and the distribution of geomorphic features across the body; understanding global atmospheric composition and its interactions with Saturn's magnetosphere; and (3) completing the global high-resolution imaging of the surface. The mission concept study reported here focuses on these four potential orbiter mission objectives, while providing cruise support and delivery of an entry probe for in situ science.

**Objective 1 is to understand the meteorology and dynamics of the atmosphere.** Observations of Titan have resolved clouds in polar regions and elsewhere on the body, that are thought to be composed of methane. The structure and evolution of clouds with time, and the precipitation of drops of liquid methane from the clouds, are of considerable scientific interest. The presence of features of fluvial origin on the surface, detected by Cassini and Huygens, imply surface modification by occasional rainstorms. Virtually every aspect of this alien meteorology (occurring at temperatures below 100 K) has the potential to yield new insights that may apply to atmospheric processes on Earth. One of the primary science objectives of the Cassini mission was to "study the time variability of Titan's clouds and hazes"; however, the intermittent nature of Cassini's Titan observations allows only minimal observing time. Thus, Cassini will provide only snapshots to help us understand these dynamic features and processes. Measurements of atmospheric rainfall and cloud density and thickness addressing the first objective would be made by a sophisticated dual-frequency radar instrument known as the Titan Cloud/Precipitation Radar and Altimeter (TCPRA; Im, 2003).

**Objective 2 is to measure the global topography of Titan, in order to understand the nature of the surface and its evolution with time; to understand the results of meteorological processes and the effects of fluid flows over the surface; and to understand the crustal structure and strength of crustal materials.** To meet this objective, the orbiter discussed here would take measurements of two types: radar altimetry, as obtained by the TCPRA instrument; and additional Synthetic Aperture Radar (SAR) measurements in selected regions. The radar system carried on the Cassini orbiter will be able to obtain altimetry data for only about 5% of the satellite's surface. Cassini's SAR capability will be employed more often, but even so, the majority of the surface of Titan will not be sampled during the Cassini mission. The TCPRA instrument (the primary science instrument for the present mission) would fill the need for global topographic coverage. The SAR instrument for the present study would be based on the Cassini

version. The Titan orbiter's TCPRA, in conjunction with its SAR, would provide extensive high-resolution regional imagery of this interesting and diverse moon.

**Objective 3 is to characterize (1) the atmospheric composition of Titan and its variability with latitude and solar phase angle and (2) the interaction of Titan's atmosphere with Saturn's magnetosphere.** Measurements addressing this objective would be made by two instruments on board the orbiter. The first, an ion and neutral mass spectrometer (INMS), would make in situ compositional measurements at the orbiter altitude of 1400 km that would allow us to make wide ranging (vertical and horizontal) inferences of atmospheric chemistry and magnetosphere-atmosphere interactions. The second, a near-infrared imager similar to the Compact Reconnaissance Imaging Spectrometers for Mars (CRISM) used on the Mars Reconnaissance Orbiter, would provide considerable information on atmospheric composition and its variability while allowing imaging of the surface through atmospheric windows where the transparency of the atmosphere is greatest.

**Objective 4 is to obtain global imaging coverage of the surface of Titan.** Although Titan's surface is obscured by thick hazes at visible wavelengths (Fig. 2.3.1-2), there are windows of greater transparency in near-infrared wavelengths. Imaging of the surface at moderate resolution would be accomplished by the near-infrared mapping instrument described in Objective 3.

### **2.3.1.3 Mission Goals**

The goals of the Titan orbiter mission are to spend a minimum of two yrs in orbit around Titan, where the orbiter would perform detailed global mapping of Titan's surface topography, IR reflection characteristics, cloud structure and dynamics, precipitation rates, and atmospheric composition. A black box entry probe would be included to perform in situ measurements. The instrument complement selected for the Titan orbiter, in conjunction with advanced RPSs, would



**Figure 2.3.1-2.** Shifting Haze Layers on Titan Imaged by the Cassini Imaging Science System.

provide a level of coverage and detail far exceeding that possible with the Cassini-Huygens spacecraft. The data obtained from such a mission would provide new insights into the evolution and current state of this remarkable moon.

**2.3.1.4 Mission Architecture Overview and Assumptions**

The Titan orbiter mission would be a logical follow-on to Cassini-Huygens, and a potential precursor to a dedicated rover or aerobot mission once full surface mapping had been completed. The technology cutoff date for this mission was assumed to be 2011, with a launch date of 2015. The Titan orbiter spacecraft would consist of an orbiter stage and a deployable entry probe—however, the details of the probe were not explored in this study. The orbiter stage would initially be housed with a lifting body aeroshell used for aerocapture at Titan, with the probe mounted externally to the back side of the aeroshell (Figs. 2.3.1-3 and 2.3.1-4). A blunt body aeroshell with a lift to drag ratio (L/D) of 0.2-0.25 would be used for aerocapture at Titan based on the analyses and results of NASA’s Aerocapture Systems Analysis Team (ASAT). Aerocapture was selected for this mission due to the significant mass savings obtained versus the use of conventional chemical propulsion to perform Titan orbital insertion (Fig. 2.3.1-5). The tentative 2015 launch date is significant in that the large delivered mass to Titan (~5000 kg) using a Delta IV-Heavy LV allows carrying a 500-kg Titan entry probe as an auxiliary payload. Besides its heavy lift capability, this LV offers a 5-m-diameter fairing that allows the simplest possible accommodation of the 4-m radar instrument antenna and 4-m Ka/X-band high-gain antenna. The reference trajectory launches to a  $C_3$  of  $25.7 \text{ km}^2/\text{s}^2$  and uses Earth and Jupiter flybys to maximize launch mass and minimize trip duration to Titan.

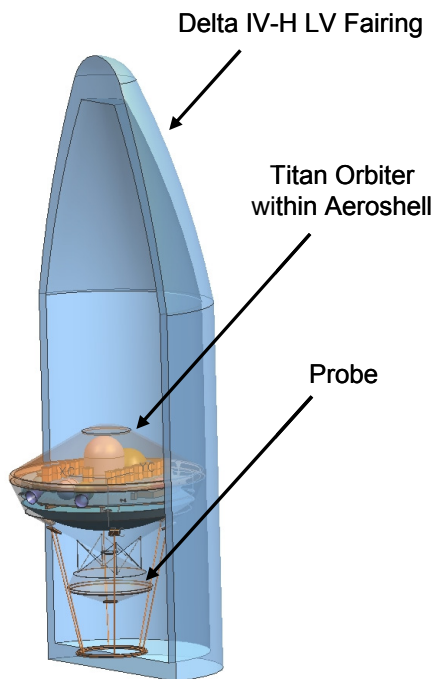


**Figure 2.3.1-3.** Configuration of the Titan Orbiter, Aeroshell, and Probe within a Delta IV-Heavy Launch Vehicle Fairing

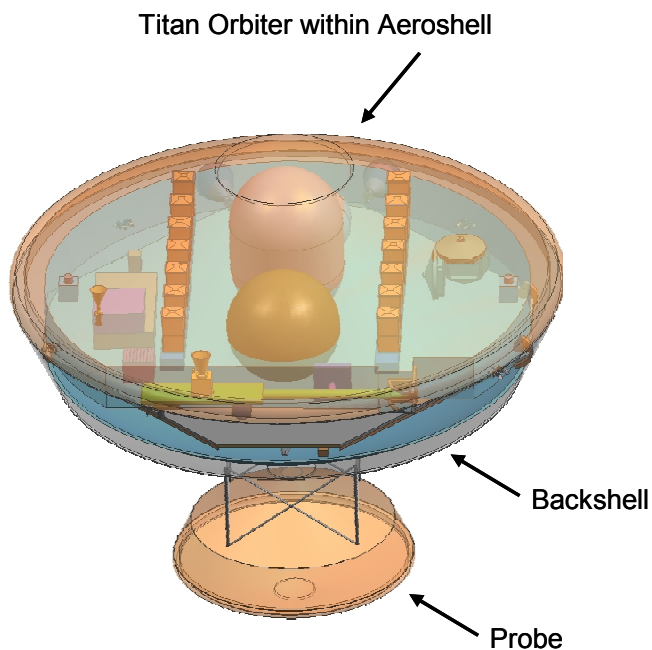


**Figure 2.3.1-4.** Titan Orbiter Spacecraft (shown within an aeroshell) and Externally Mounted Probe

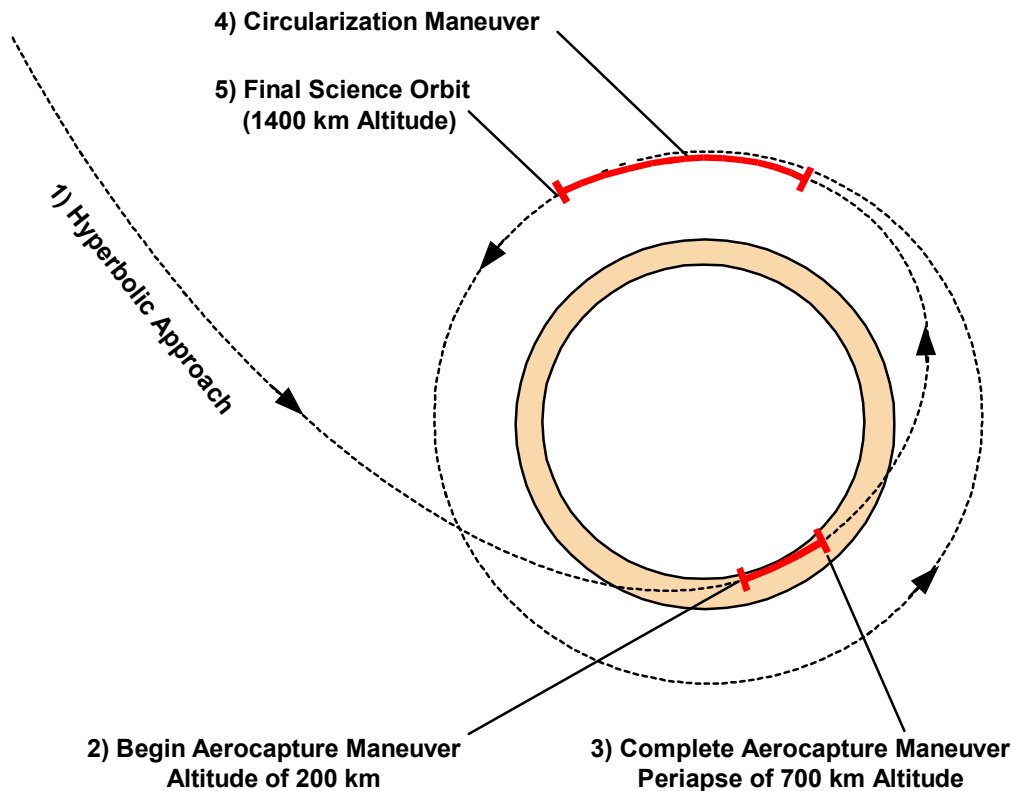


**Figure 2.3.1-5.** Aerocapture and Circularization Maneuver of the Conceptual Titan Orbiter

During the cruise phase, the clamshell-configured aeroshell would be open, exposing the RPSs to deep space (Figs. 2.3.1-6 and 2.3.1-7). This would permit passive thermal control of the RPSs and eliminate the need for an auxiliary set of externally mounted radiators. Upon Titan approach, the spacecraft would be maneuvered to properly orient the probe for release. Once released, the probe would continue independently and enter Titan's atmosphere directly. (The subsequent probe entry, descent, landing, and science mission were not addressed in this study, but a 500-kg probe offers many options.) As the orbiter approached Titan's atmosphere, the aeroshell would be closed and locked in preparation for aerocapture into a polar orbit. Once closed, phase change material (PCM) would store the heat of the RPSs.

The spacecraft would enter Titan's atmosphere with a periapse of 200 km altitude, maneuver to a periapse of 700 km using its lifting body aeroshell, and exit with an apoapse of 1400 km (Fig. 2.3.1-5). The duration of the aerocapture maneuver is estimated at ~15 min, and the total time between closure of the aeroshell and subsequent reopening is estimated at 1 hr for purposes of sizing the thermal control system. Upon completion of aerocapture, the Titan orbiter would be deployed from the aeroshell, and the RPSs thereafter allowed to passively radiate to deep space. Subsequent engine firings would be performed to circularize the spacecraft orbit to 1400 km.

Upon reaching its final circular polar orbit, the Titan orbiter would deploy its 4-m high-gain antenna (HGA) and 4-m TCPRA antenna, which had been folded and stowed under the HGA since launch, as shown in Figures 2.3.1-8 and 2.3.1-9. Following instrument checkout and calibration, the nominal 2-yr science mission would commence. Science would be collected in

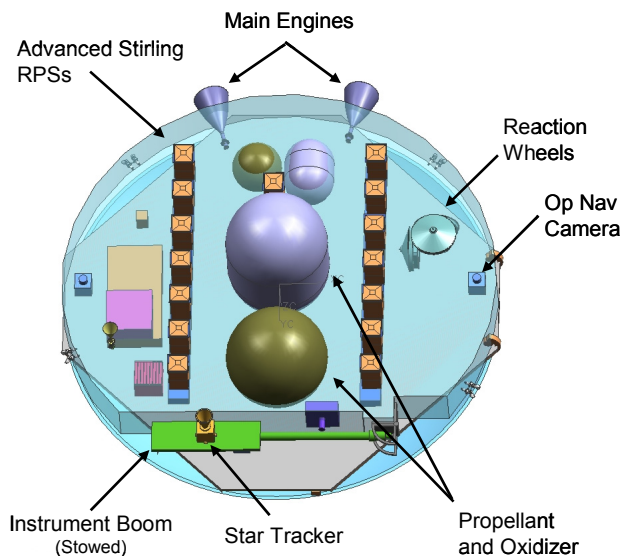


**Figure 2.3.1-6.** Top View of Titan Orbiter Illustrating Placement of Key Subsystems

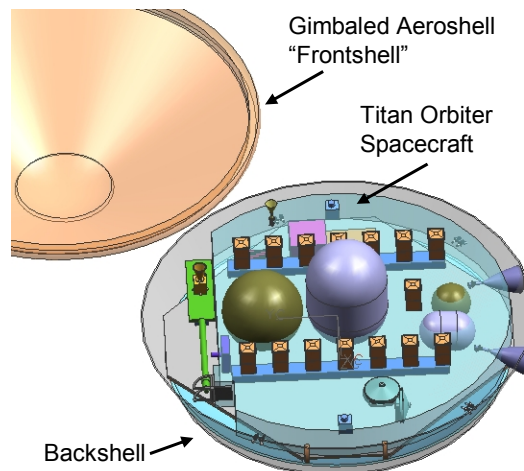


**Figure 2.3.1-7.** Titan Orbiter Spacecraft with Aeroshell Opened During the Cruise Phase

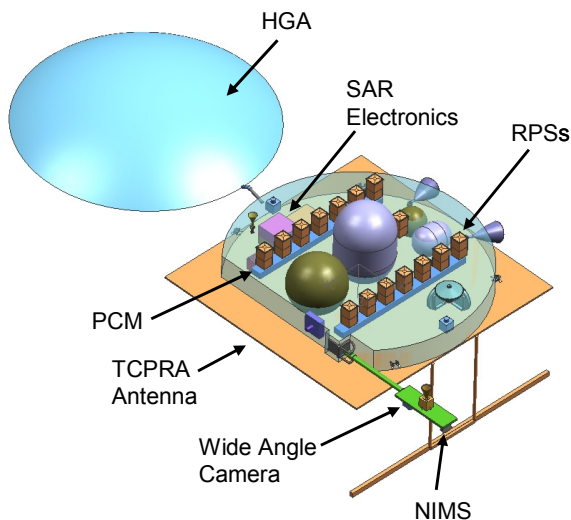


**Figure 2.3.1-8.** Illustration of the Back Side of the Titan Orbiter in its Fully Deployed Configuration

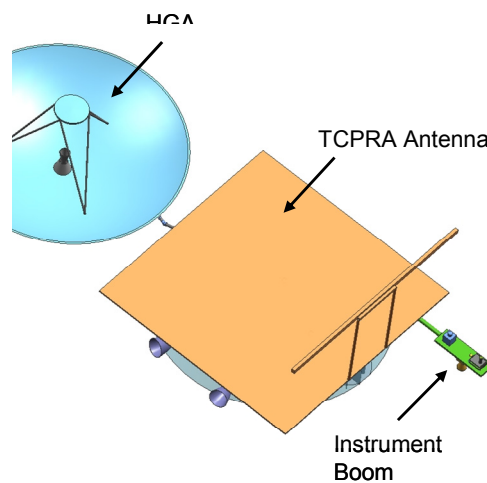


**Figure 2.3.1-9.** Illustration of the Front Side of the Titan Orbiter in Its Fully Deployed Configuration

two distinct modes—the first geared towards radar mapping of Titan’s surface topography atmosphere, clouds, and precipitation using the TCPRA. The requirement for this mode is a nominal 25% duty cycle, meaning that the TCPRA would take measurements for 25% of each orbit (from the equator to the pole or vice versa) and use the remainder of the orbital period for downlinking the data to Earth and recharging its batteries for the next orbital period (the peak power draw of the TCPRA exceeds the steady-state power output of the RPSs; thus, secondary batteries are required). The power level and duty cycle of the TCPRA instrument are the key drivers for the ~1 kWe (EOM) power requirement of the orbiter. A shorter duty cycle could reduce the required number of RPSs, but at the expense of reduced coverage during each orbital period. All other instruments would be kept in a standby state during this mode of operation. In the second mode of operation, the TCPRA would be placed in standby state during and the near-

infrared mapping spectrometer (NIMS), SAR, INMS, and radio science subsystem (RSS) would be used.

Changes in science modes could be performed as determined by the mission science team for this study, and were tentatively assumed to occur once a week. The orbiter has a tight pointing requirement based on the NIMS field of view, assessed at 16 arcsec for control, 6 arcsec for knowledge, and 0.5 arcsec for pointing stability.

**2.3.1.5 Power Source Trade Study**

Different power system options were considered for the Titan orbiter concept study, including solar power and radioisotope power systems. Key factors considered in the power system trade study were the power system’s mass, physical size, tolerance to the space environment, and overall feasibility. In the final analysis, RPSs were considered the only viable technology for this class of mission for the following reasons: Titan is ~9.5 AU distant from the Sun, resulting in the Orbiter receiving only about ~1.1% of the insolation at Earth’s orbit. This corresponds to ~15 W/m<sup>2</sup>. Assuming that a new generation of Low-Intensity Low-Temperature (LILT) tolerant solar arrays could be developed and qualified in time for this mission, and using reasonable assumptions for specific mass and volume of the arrays, the total amount of solar array (SA) area required to power the orbiter would be on the order of 320 m<sup>2</sup>. This corresponds to a SA mass exceeding 800 kg. The SA system mass would be further increased by the addition of batteries for operations during eclipse, as well as gimbals, cabling, and power converters. These orbiter SAs would need to be folded within the aeroshell during the cruise phase, and thus would be inoperable during the first 8 yrs of the mission. Thus, a second solar array system would be required that could be externally mounted to the aeroshell and ejected prior to aerocapture at Titan, further increasing the spacecraft mass. In comparison, the mass of an advanced Stirling RPS system with batteries is estimated at ~250 kg without contingency, which is approximately 30% of the mass of the solar array option. Considering that any mass added to the spacecraft has a multiplicative effect on the amount of propellant that must be carried and the size of the aeroshell, it becomes clear that RPS would be the only practical option for this mission.

**2.3.1.6 Advanced RPS Characteristics**

The baseline Titan orbiter mission would use conceptual advanced Stirling RPSs for all electrical power generation. While other advanced RPS options were also considered for this mission (i.e., advanced RTG, TPV, and Brayton), the higher efficiency and specific power of the advanced Stirling system yielded the lightest overall orbiter configuration and, subsequently, the largest probe size. The performance characteristics of the advanced Stirling RPS are summarized here—the reader is referred to Section 3 for a detailed discussion all four advanced RPS devices.

Each advanced Stirling RPS is assumed to generate 80 We at BOM with a conversion efficiency of 32% (Table 2.3.1-1). A single 250 Wth (BOM) GPHS module would be used for this RPS design. Thermal control would be performed via heat rejection from the Stirling housing and small external fins, and via an

**Table 2.3.1-1. Performance Characteristics of the Conceptual Advanced Stirling RPS for the Titan Orbiter Concept**

<b>Advanced RPS Parameter</b>	<b>Value</b>
# of RPSs (not including redundancy)	14
Total # of RPSs (including redundancy)	15
Number of GPHS modules per RPS	1
Mass per advanced Stirling RPS, kg	13.7
Total Number of GPHS modules	15
Total Thermal Power at BOM, Wth	3750
Conversion Efficiency, %	32
Electrical Power per RPS at BOM, We	80
Total Design Power at BOM, We	1120
Degradation Rate per yr, %	0.8
Mission Duration, Yrs	10
<b>Design Electrical Power at EOM, We</b>	<b>1033</b>

integrated cooling loop that interfaces with the Titan orbiter spacecraft cooling system for maintaining spacecraft operating temperatures and for energy storage during the aerocapture maneuver.

An active vibration compensator would be used to limit vibration levels associated with a single convertor system (i.e., as opposed to the balanced two-convertor system of the SRG, which would nominally not require a compensator). A conceptual drawing of the Stirling convertor is shown in Figure 2.3.1-10. A total of 15 advanced RPSs would be used on the Titan orbiter, 14 required for the mission design power level of 1120 We at BOM, and 1 included for redundancy. The electrical power produced by the redundant RPS unit does not count towards the design power level, but could be used to enhance the mission were the 14 prime RPSs operating nominally; however, the spacecraft thermal control system must account for the heat generated by all 15 RPSs. The design EOM power level is estimated at ~1033 We after 10 yrs, and assumes a  $^{238}\text{Pu}$  fuel decay of ~0.8%/yr and no generator degradation during the mission (Wong, 2004).

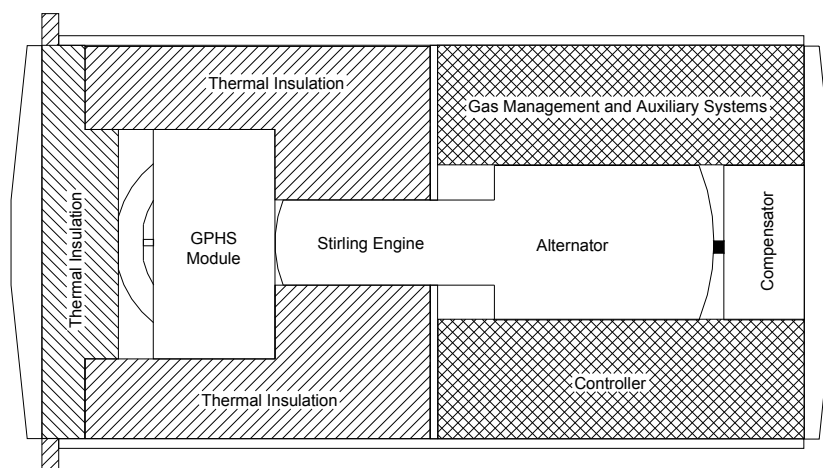


Figure 2.3.1-10. Conceptual Advanced Stirling Convertor

### 2.3.1.7 Science Instruments

The most innovative and powerful instrument of the conceptual Titan orbiter payload would be the TCPRA (Im, 2003), Table 2.3.1-2. This dual-frequency (35- and 94-GHz) radar would allow simultaneous imaging of both clouds and precipitation, enabling the 3-D imaging of convective weather systems. Based on a number of proven technologies from Earth observing systems, the TCPRA could resolve atmospheric clouds and precipitation with 250-m vertical resolution over a 50-km altitude window, providing completely new insights into the dynamics and circulation of Titan's atmosphere. In altimeter mode, TCPRA could acquire surface height measurements with 10-m vertical resolution, completing the global topographic coverage of Titan only partly addressed by the Cassini mission. The TCPRA would be a high-capability instrument whose operating average power consumption (1.2 kWe), large mass (400 kg) and high data rate (10 Mb/s) would be driving factors in the spacecraft design.

The Titan orbiter would carry an NIMS similar to CRISM on the Mars Reconnaissance Orbiter (MRO), but optimized for the Titan environment and requirements. This instrument observes individual absorption features to infer abundances of various atmospheric species, (Fig. 2.3.1-11). A SAR similar to that on Cassini would be included in the Titan orbiter payload to provide radar imaging and altimetry that complements and extends the radar altimetry performed by the

**Table 2.3.1-2. Science Payload and Instrument Descriptions for the Conceptual Titan Orbiter Mission**

Instrument Name	Purpose	Science Objectives Addressed	Heritage
1. Titan Cloud/Precipitation Radar Altimeter (TCPRA)	Radar altimetry mode for global topographic mapping; atmospheric 3-D imaging of clouds and precipitation	Objective 1, to understand the meteorology and dynamics of the atmosphere; Objective 2, to resolve the global topography of Titan.	New
2. Near-Infrared Mapping Spectrometer (NIMS)	Obtain global infrared (~1.8 to 5 um) surface imaging and measure atmospheric composition	Objective 3, to characterize the atmospheric composition of Titan, and its variability; Objective 4, to obtain global imaging coverage of Titan's surface.	Mars CRISM
3. Wide-Angle Camera (WAC)	Context imaging and public outreach—(Near IR, imaging at ~980 or ~2200 nm)	Contributes to Objectives 1, 3, and 4 by providing wide-area context images for interpreting the higher resolution radar, near-IR, and mass spectrometer compositional data.	Multiple Missions
4. Radio Science Subsystem (RSS)	Provide detailed information on Titan's gravitational fields and mass.	Contributes to understanding of the state of Titan's interior, which is relevant to the scientific questions addressed by Objective 2 (surface topography).	Cassini
5. Synthetic Aperture Radar (SAR)	High-resolution radar mapping of surface morphology and surface properties	Objective 2, to resolve the global topography of Titan, to understand the fluvial and other processes that modify Titan's surface.	Cassini
6. Ion and Neutral Mass Spectrometer (INMS)	Measure upper atmospheric chemistry and quantify magnetospheric interactions.	Objective 3, to characterize the atmospheric composition of Titan, and its variability with latitude and with time.	Cassini

TCPRA. Surface properties such as texture (on a wide range of scales) and material dielectric constant affect the returned signal, allowing scientists to obtain additional key information about surface roughness and other properties.

Titan's atmosphere is relatively thicker (or "deeper") than that of the Earth, due to its lower surface gravity, so the spacecraft's science orbit would be at an altitude of 1400 km to avoid excessive atmospheric drag. At this altitude, the INMS could continuously monitor high-altitude neutral atmospheric composition while also resolving ions produced by various mechanisms with Titan's atmosphere. The orbiter would also carry a wide-angle camera, for context imaging and for imaging targets of opportunity during the orbiter mission. Although no dedicated instrument package is included on the orbiter for gravitational mapping, standard radio science celestial mechanics techniques would yield improved information on Titan's gravity field and internal mass distribution.

### 2.3.1.8 Data

The Titan orbiter mission would be divided into separate cruise and science phases. During the cruise phase, data volume would generally be limited to health and status information of key subsystems, and the resulting data volume would be relatively low and easily manageable by the spacecraft communications system. During the science phase, however, the data volume would be significant, particularly during operation of the TCPRA instrument, which drives the data

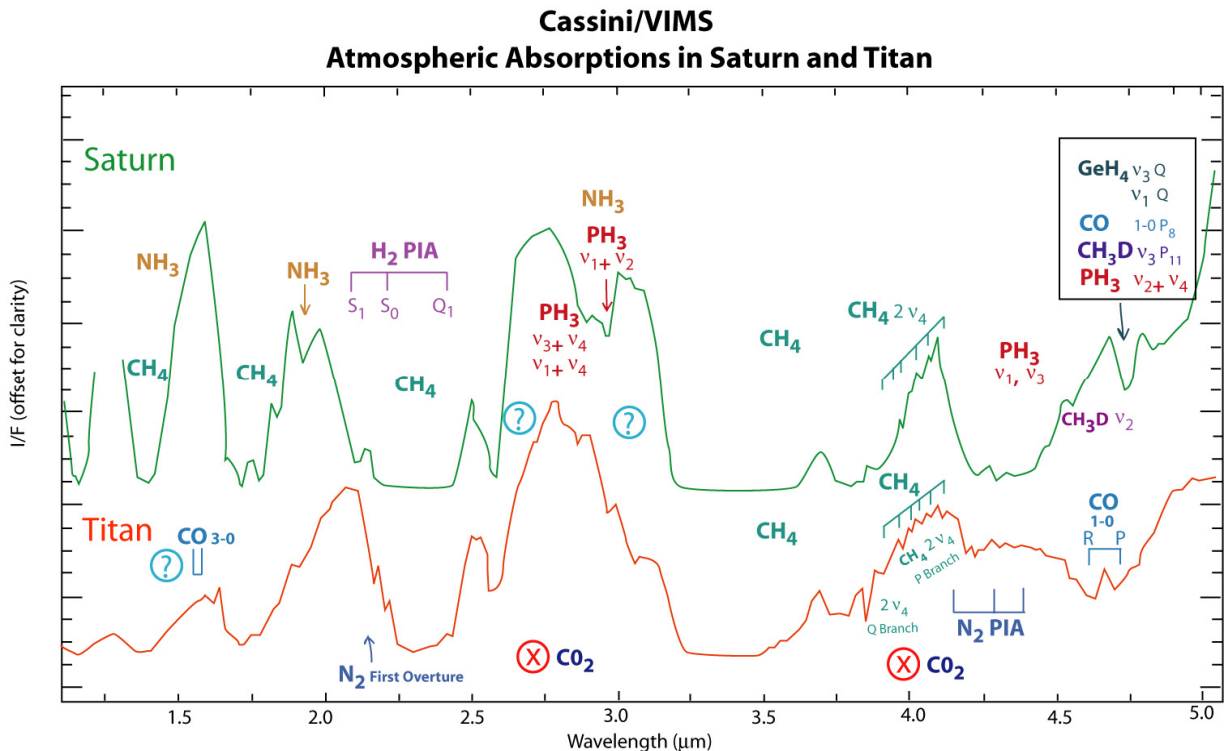


**Figure 2.3.1-11.** Near-infrared spectra of Saturn (top) and Titan (below), showing absorption peaks due to various atmospheric constituents. The low points of the curve at 2.25 and 3.25 μm are “windows” through which it is possible to image the surface (Baines, 2005).

storage and communications design of the vehicle. The TCPRA has an estimated raw data rate of 10 Mb/s, generating about ~42 Gb per orbital pass using a 25% duty cycle (see Table 2.3.1-3). Lossless data compression would be used (e.g., Rice or Huffman methods) to reduce the stored data volume by a factor of 2.25, yielding ~18.6 Gb/orbit. A solid-state recorder (SSR) would be used to store this data during TCPRA operations, and play it back during the subsequent 2.5-hr downlink mode each orbit. A 100% memory margin would be included in the SSR design to guard against missed or failed downlinks, permitting storage of two orbit’s worth of TCPRA data. Data storage during the second science mode (SAR/NIMS/INMS) would be 6.7 Gb/orbit raw and ~3 Gb/orbit compressed, which is well within the capability of the 40-Gb SSR design.

### 2.3.1.9 Communications

The spacecraft communications architecture requires a high-performance, high-bandwidth communications system, both onboard the Titan orbiter and on Earth, in order to meet the science data volume requirements specified in the previous section. The orbiter design would use a deployable 4-m Ka-/X-band HGA that is nominally stowed during the cruise phase and only deployed once in orbit about Titan. During the cruise phase, an articulated X-band medium gain antenna (MGA) would be used for downlinking nominal engineering and optical navigation data. Two X-band low-gain antennas (LGAs) are included for omni-directional communication with Earth during launch and near-Earth operations. The LGAs would be mounted externally on the aeroshell structure, permitting communications with the orbiter following LV separation and prior to opening the aeroshell. The HGA, MGA and a second pair of LGAs would be mounted directly on the Titan orbiter (Fig. 2.3.1-12). An upgraded Deep Space Network (DSN) of 180

Table 2.3.1-3. Data Rates and Data Volume of the Titan Orbiter Instrument Suite

Instrument	Science Mode	Measurement Duration per Orbit	Data Rate or kb/sample	Raw Data Volume/Orbit (Mb)
1. Titan Cloud/Precipitation Radar Altimeter	TCPRA	1.16 hrs (25% duty cycle)	10 Mb/s	41,760
2. Infrared Spectrometer	SAR/NIMS/INMS	4.2 hrs (91% duty cycle)	72 kb/s	1089
3. Wide-Angle Camera	SAR/NIMS/INMS	Same	10 Mb/frame Infrequent	50
4. Synthetic Aperture Radar	SAR/NIMS/INMS	Same	365 kb/s	5519
5. Ion and Neutral Mass Spectrometer	SAR/NIMS/INMS	Same	1.5 kb/s	23
6. Radio Science Subsystem	TCPRA and SAR/NIMS/INMS	During communication periods	None	None
Total Raw Data Volume (Mode A) per Orbit, Gb				41.8
Total Raw Data Volume (Mode B) per Orbit, Gb				6.7
Lossless Compression Ratio				2.25:1
<b>Compressed Data Volume (Mode A) per Orbit, Gb</b>				<b>18.6</b>
<b>Compressed Data Volume (Mode B) per Orbit, Gb</b>				<b>2.98</b>
Solid State Recorder Requirement, Gb				40
<b>Data Storage Design Margin, %</b>				<b>115%</b>

12-m diameter antennas is assumed in this study, and is consistent with the concepts currently being considered for development in the 2015 and 2020 time frame. The Titan orbiter would not start its science mission until ~2023, and thus could use the existing DSN during the cruise phase while the upgraded DSN was constructed and checked out.

The 4-m Ka-/X-band HGA would use redundant 125-W (RF) amplifiers at 32 GHz to transmit data at 2.3 Mb/s at a maximum range of 10.5 AU from Earth. The HGA is assumed to be 50% efficient and requires 0.02° pointing accuracy. The articulated 0.2-m (20-dBi) Ka-/X-band MGA would include redundant 35-W and 200-W (RF) transmitters to provide dual-rate data downlink during cruise phase and for emergency events. The 200-W (RF) transmitter provides 1.2 kb/s downlink at 10.5 AU distance from Earth (using the upgraded DSN), and would be used for playback of Optical Navigational (Op/Nav) telemetry. The 35-W (RF) transmitter would be used for emergency downlinks, with a maximum data rate of 10 b/s at 10.5 AU range distance.

The Titan orbiter would have a nominal communications window of 1.16 hrs per orbit while operating in the TCPRA science mode, corresponding to ~13 hrs per Earth day in this mode. In the less stressing SAR/NIMS/INMS science mode, the communications window is 0.4 hrs per orbit, or ~2 hrs per Earth day.

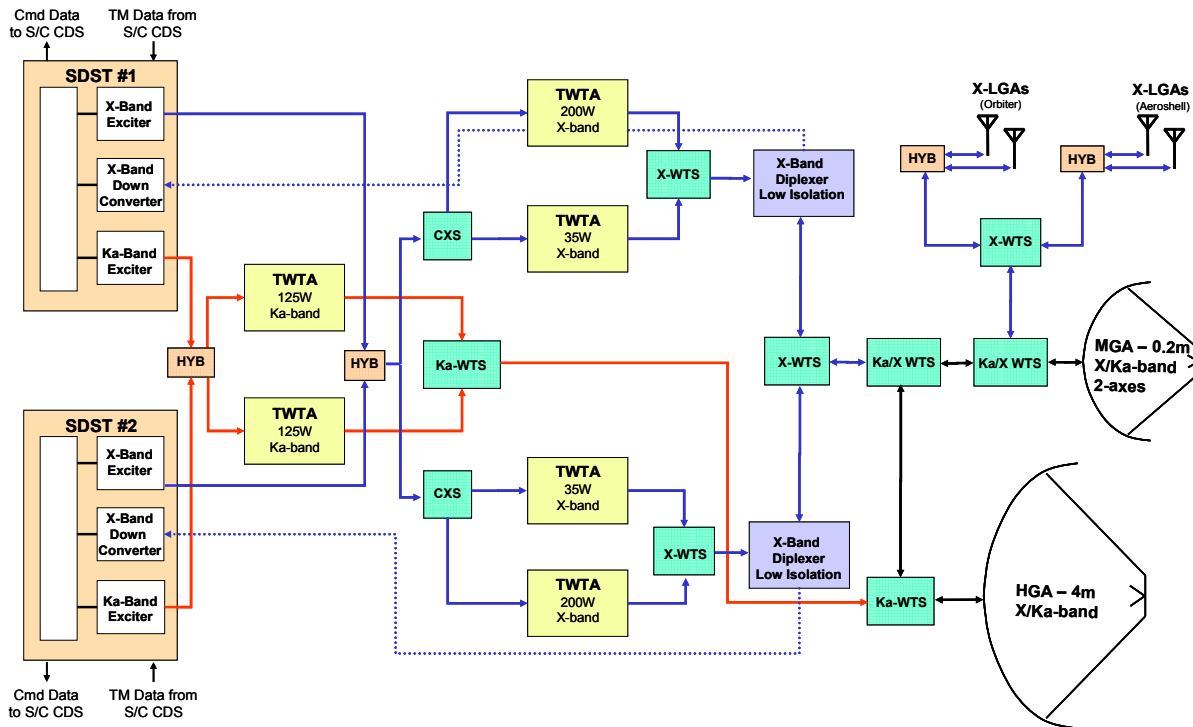


Figure 2.3.1-12. Block Diagram of the Conceptual Titan Orbiter Communications System

### 2.3.1.10 Thermal

The Titan orbiter would use a combination of passive and active thermal control systems to maintain operating and survival temperatures during the mission (Fig. 2.3.1-13). A key challenge of the orbiter thermal control system is the rejection of the heat from the RPS power systems. A significant advantage of the advanced Stirling-based RPS is its higher power-conversion efficiency relative to other RPS concepts, translating into less heat required to generate the same power level. The 15 advanced Stirling systems required by the spacecraft would cumulatively generate 3750 W of thermal power at BOM; this is compared with 5500 Wth for Brayton, 9000 Wth for TPV, and 13,750 Wth for advanced thermoelectrics. Effective management of this heat is critical during all phases of the mission.

While on the launch pad, cooling of the spacecraft would be supplied by on-pad resources (i.e., chillers). During launch and up through fairing jettison, cooling would be accomplished by heating and phase change of the residual pad cooling fluid. Once the spacecraft was free and clear from the fairing, the clamshell-style aeroshell would open (Fig. 2.3.1-7), permitting the RPSs to radiate directly to deep space using their integrated radiators. The concept of an opening/closing aeroshell is not new, as both the NASA Genesis and StarDust missions used a back shell that could perform this function. However, in their case, the open back shell was used to expose the science collection plates, and was subsequently closed for aero-entry at Earth. During the ~8-yr cruise phase, the RPSs would be passively cooled, with loop heat pipes used to transfer some of their heat in order to warm spacecraft subsystems.

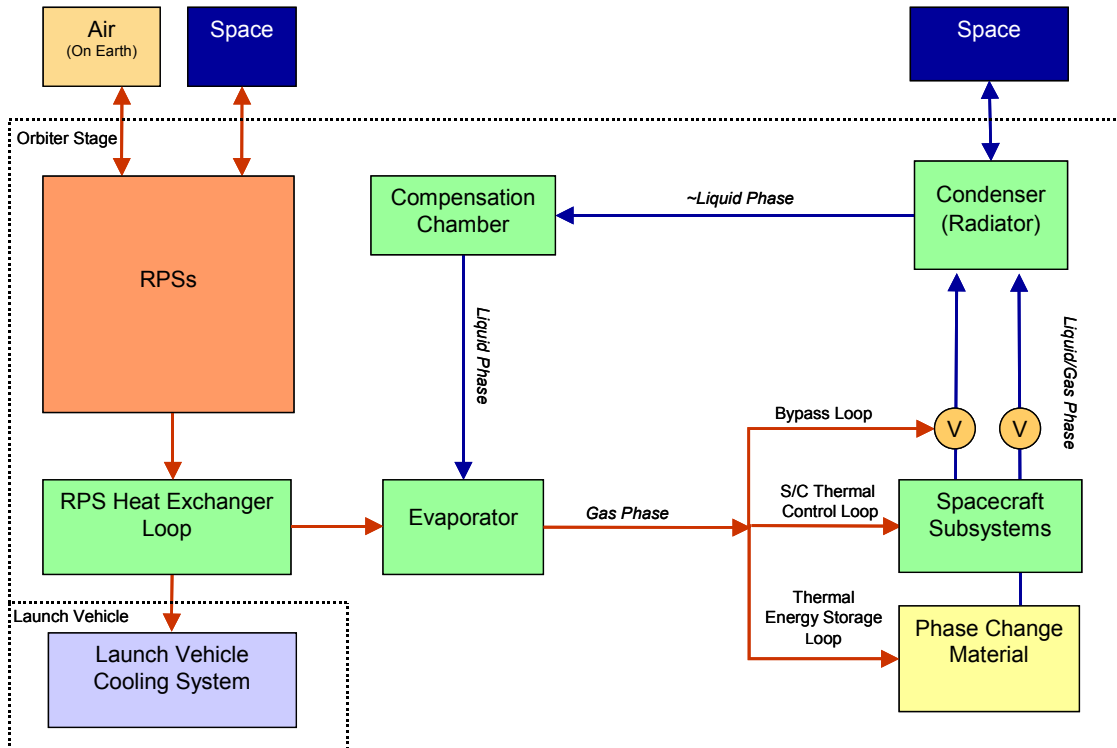


Figure 2.3.1-13. Block Diagram of the Conceptual Titan Orbiter Thermal Control System

Additionally, the RPSs would be physically located around the propellant tanks to provide radiative heating of the fuel and oxidizer, thus reducing the required power needed for electrical heaters. Just prior to aerocapture at Titan, the aeroshell would be closed, requiring that the RPS thermal energy be stored for approximately 1 hr. PCM would be used in conjunction with passive heat pipes to manage this thermal energy. PCMs are effective, flight-proven materials for maintaining prescribed temperature levels, and have been successfully used on numerous space missions (Gilmore, 2002). Water was selected for its relative high heat of fusion (333 kJ/kg) and well-known thermophysical properties. In general, the heat storage capability of a PCM is proportional to its heat of fusion and the quantity of material. Using advanced Stirling RPSs, ~41 kg of PCM is required (Table 2.3.1-4). This is compared with 59 kg for Brayton, 97 kg for TPV, and 149 kg for the advanced RTG. The significant difference in PCM mass illustrates the importance of higher efficiency RPS systems for missions using aerocapture. Thermal control of the aeroshell would be performed primarily via ablation of the phenolic-impregnated carbon ablator (PICA) heat shield and secondarily via radiative heat transfer from the heat shield surface to deep space.

Once the aeroshell has been jettisoned following aerocapture, the RPSs would be exposed to deep space, permitting passive thermal control as during the cruise phase. Passive thermal management would be maintained using a combination of multi-layer insulation (MLI), thermal surfaces, thermal conduction controller, and passive heat pipes. Active thermal control would use electric heaters for propulsion elements and other temperature-sensitive elements. A shunt radiator would be used to reject excess electric power not used by the spacecraft.

**Table 2.3.1-4. Heat Generation Rates and Required PCM Mass for Four Different Advanced RPS Systems for the Conceptual Titan Orbiter Mission**

RPS Configuration	Total # of GPHS Modules	Thermal Power, We (BOM)	Thermal Energy Generated in 1 hr, kJ	Required Mass of Phase Change Material, kg
Advanced Stirling	15	3750	13,500	41
Brayton	22	5500	19,800	59
Thermophotovoltaic	36	9000	32,400	97
Advanced RTG	55	13,750	49,500	149

**2.3.1.11 Propulsion**

The Titan orbiter propulsion system would perform all the deep space and attitude control maneuvers of the spacecraft. These maneuvers would include trajectory correction maneuvers (TCMs) and deep space maneuvers (DSMs) required for the gravity-assisted flybys of Earth and Jupiter (Fig. 2.3.1-14), as well as orbit circularization and cleanup burns following aerocapture (Fig. 2.3.1-5), reaction wheel desaturation and drag makeup while in Titan orbit. All thrusters and propellant systems are integrated on the conceptual Titan orbiter spacecraft to reduce unnecessary redundancy and decrease mass. These systems are needed for all phases of the mission (i.e., prior to, during, and following aerocapture), and thus cannot be mounted on the aeroshell as they would likely be damaged from the heat of entry and subsequently be jettisoned with the aeroshell following the aerocapture maneuver.

The total  $\Delta V$  requirement for the Titan orbiter mission concept is  $\sim 890$  m/s, with approximately 710 m/s allocated to DSMs. The total mass of propellant (fuel, oxidizer, and pressurant) is estimated at  $\sim 1300$  kg (Table 2.3.1-5). The Titan orbiter propulsion system would consist of separate high, intermediate, and low-thrust engines. As conceived, the high-thrust system would be composed of two bipropellant 450-N HiPAT thrusters (Isp  $\sim 325$  s) using hydrazine ( $N_2H_4$ ) and nitrogen tetroxide (NTO). The intermediate-thrust system would be composed of eight 90-N MR-120 monoprop thrusters (Isp  $\sim 226$  s), and the low-thrust system would be composed of 16 Aerojet 0.7-N MIT monoprop thrusters (Isp  $\sim 210$  s; Fig. 2.3.1-15). Separate pressurization tanks would be used for the bipropellant and monopropellant systems. The aeroshell would include penetrations in its back-side, permitting the orbiter-based thrusters to operate with the aeroshell in place (i.e., during the cruise and aerocapture phases of the mission). The propulsion system is assumed to utilize existing heritage technology, and as such, would be inherently low risk. All thrusters would have functional redundancy including a backup main engine, four backup MR-120 engines, and eight back-up MIT thrusters.

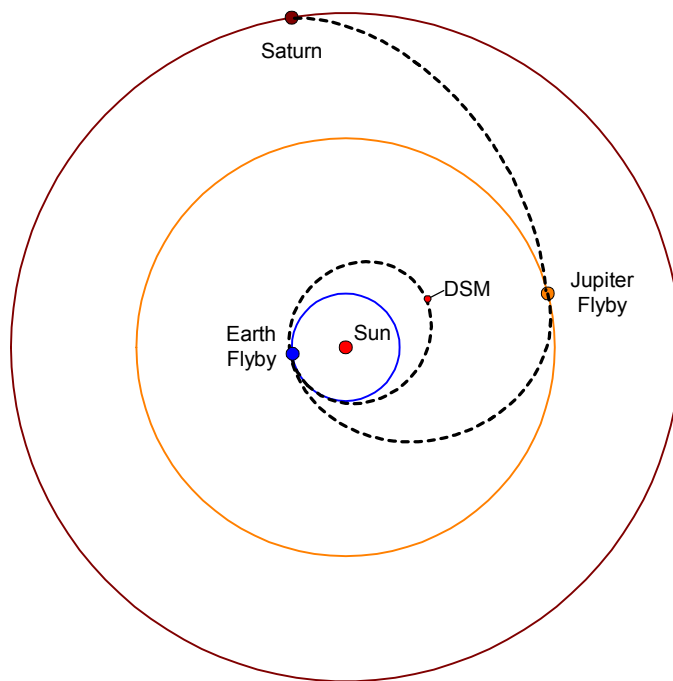


**Figure 2.3.1-14. Earth-Jupiter Gravity Assist (EJGA) for the Titan Orbiter Mission Concept**

Table 2.3.1-5.  $\Delta V$  Estimates for the Conceptual Titan Orbiter Mission

Activity	$\Delta V$ (m/s)	Prop Mass (kg)	Description
TCMs	10	17	Trajectory correction maneuvers during cruise phase.
Deep Space Maneuvers	706	1070	Deep space maneuvers during cruise phase.
Approach (Earth and Jupiter)	45	61	Trajectory corrections during Earth and Jupiter approach.
Orbiter Maneuver during Probe Release	30	35	Avoidance maneuvers during the deployment of the entry probe.
Bank Angle Control	20	39	Orbiter attitude control during Titan aerocapture maneuver.
Periapse Raise and Cleanup	76	52	$\Delta V$ required for orbit circularization and cleanup maneuvers following aerocapture maneuver.
Atmospheric Drag Compensation	1	1.2	Periodic atmospheric drag compensation to maintain 1400-km elevation during 2-yr science mission.
Oxidizer and Residual Propellant		22	Holdup volume/residual margin of propellant and oxidizer.
<b>Total <math>\Delta V</math> / Propellant Mass</b>	<b>888</b>	<b>1297</b>	

The high-thrust system would be used for TCMs, DSMs, flybys of Earth and Jupiter, probe release, and orbit circularization. The intermediate-thrust system would provide bank attitude control during aerocapture. The low-thrust system would provide coupled three-axis control during all phases of the mission for fine attitude control (e.g., for pointing of instruments), desaturation of reaction wheels, and atmospheric drag makeup during the science mission.

Propellant use during the science phase for atmospheric drag makeup would be minimal, as the atmosphere is extremely thin at 1400-km elevation. Left uncompensated, the spacecraft altitude and velocity would be reduced by  $\sim 1$  m/yr and  $\sim 0.3$  m/s/yr, respectively.

The temperature of the  $N_2H_4$  and NTO tanks would need to be maintained at  $\sim 25^\circ C$  for the entire mission in order to use this type of propellant. Temperature management would be performed using heat from the RPS system supplemented by auxiliary tank heaters. Were this temperature control not possible, lower performing MMH (i.e., lower Isp) could be used with a subsequent increase in propellant mass and volume.

For the purposes of this study, the oxidizer tank was assumed to be a 1.0-m sphere, while the fuel tank would measure 1.0 m in diameter and 1.3 m long. The oxidizer pressurant tank would be a 0.5-m diameter sphere, while the fuel pressurant tank would be 0.5 m in diameter and 0.65 m long. Although a single oxidizer tank and a single fuel tank were used for this simplified system, a balanced multiple tank design would be required in a more advanced design. The aerocapture maneuver would require balanced tanks and an evenly distributed (and known) center of gravity (CG). Space limitations within the aeroshell and backshell along with structural support requirements may drive the design to multiple fuel and oxidizer tanks evenly spaced within the spacecraft structure.

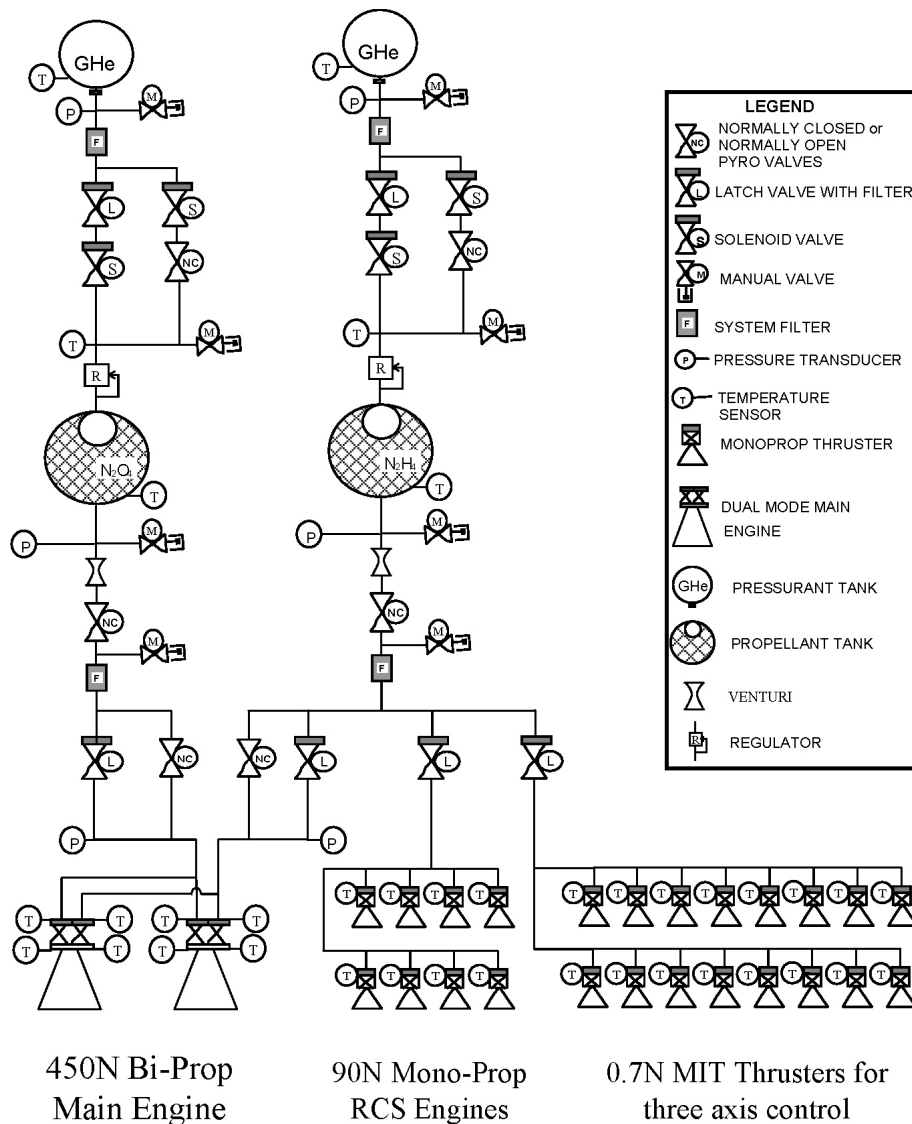


Figure 2.3.1-15. Schematic of Conceptual Titan Orbiter Propulsion System

Lastly, a lifting body aeroshell was baselined for this concept as it enabled the mission due to its tremendous mass savings compared with conventional chemical propulsive techniques. Using the Delta IV-Heavy LV with  $C_3$  of  $25.7 \text{ km}^2/\text{s}^2$  and Earth-Jupiter gravity assist, the Titan approach velocity would be 5.9 km/s. The desired science orbit for this mission would be a circular 1400-km orbit, with an orbital velocity of 1.5 km/s. Thus, a  $\Delta V$  of  $\sim 4.8 \text{ km/s}$  (not including attitude control and correction burns) must be imparted on the spacecraft in order to achieve the target orbit. A lifting body aeroshell, conservatively assumed to weigh 35% of the approach mass (Hall, 2005), corresponding to a  $\sim 1300 \text{ kg}$  aeroshell, could provide the requisite  $\Delta V$ , whereas a bipropellant chemical propulsion system would require over 8500 kg of propellant for the same approach mass, significantly exceeding the launch capability of the Delta IV-Heavy. Thus, the aeroshell would provide a mass savings of over 6000 kg compared with a purely chemical system, enabling the use of an existing launch vehicle for this mission.

2.3.1.12 Power

The conceptual Titan orbiter would nominally require ~1 kWe at EOM in order to meet the science and mission objectives of this study. This corresponds to 14 advanced Stirling RPSs (each generating 80 We at BOM). Consistent with JPL design principles (Yarnell, 2003), a redundant advanced Stirling RPS would be added, yielding a total of 15 Stirling RPSs for this concept. The spacecraft power system would be located on the orbiter; there are no power requirements for the aeroshell, and the entry probe is assumed to be self powered. To meet the peak energy demands of the TCPRA instrument and communications modes, secondary batteries are required and would be recharged during low-power system activities.

The Titan orbiter would have eight mutually exclusive operating modes (Fig. 2.3.1-16 and Table 2.3.1-6) corresponding to key sequences and activities during the mission. The modes are designed to maintain the energy balance of the orbiter power system.

The power modes are divided into three distinct transit-phase modes and five science-phase modes. The three transit-phase modes are (1) Launch, (2) Cruise, and (3) Aerocapture and Circularize. The five science-phase modes are (1) TCPRA Science, (2) TCPRA Communications, (3) TCPRA Standby, (4) SAR/NIMS/INMS Science, and (5) SAR/NIMS/INMS and Communications.

The TCPRA science mode is the peak power driver of the mission, requiring a total of ~1900 We (including 30% contingency) for the entire spacecraft. As the end-of-mission RPS power level is 1033 We, batteries are required to make up the balance of electrical power (867 We) used during

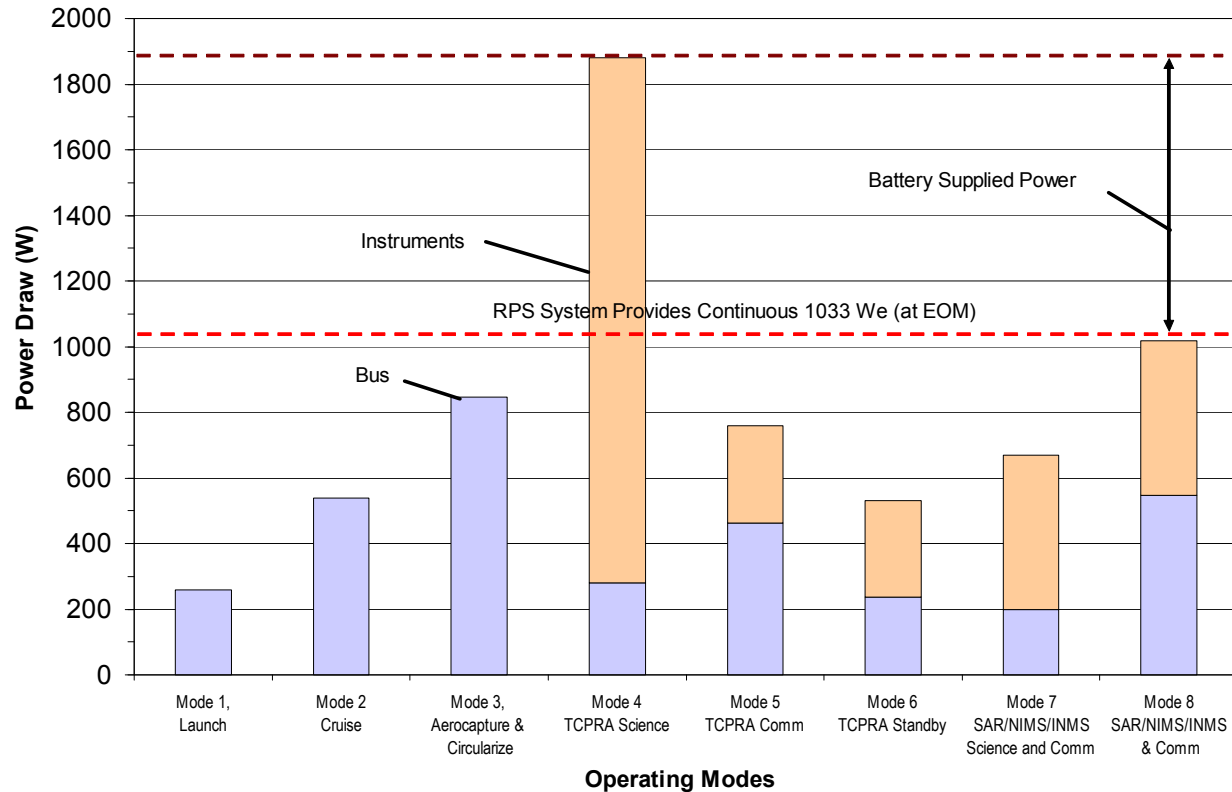


Figure 2.3.1-16. Operating Modes and Power Levels of the Titan Orbiter Mission Concept

Table 2.3.1-6. Operating Modes and Power Levels for the Titan Orbiter Mission Concept

Subsystem	Cruise Phase Power Modes, We			Science Phase Power Modes, We				
	Mode 1	Mode 2	Mode 3	Mode 4	Mode 5	Mode 6	Mode 7	Mode 8
	Launch	Cruise	Aerocapture & Circularize	TCPRA Science	TCPRA Comm	TCPRA Standby	SAR/NIMS/INMS Science	SAR/NIMS/INMS & Comm
<b>Instruments</b>	<b>0</b>	<b>0</b>	<b>0</b>	<b>1231</b>	<b>228</b>	<b>227</b>	<b>360.9</b>	<b>360.9</b>
TCPRA	0	0	0	1200	200	200	200	200
NIMS	0	0	0	5	5	5	40.9	40.9
Wide-Angle Camera	0	0	0	5	1	1	5	5
RSS	0	0	0	0	1	0	1	1
SAR	0	0	0	15	15	15	86	86
INMS	0	0	0	6	6	6	28	28
<b>Bus Total</b>	<b>199.6</b>	<b>414.3</b>	<b>651.1</b>	<b>215.2</b>	<b>355.8</b>	<b>181.3</b>	<b>153.3</b>	<b>421.4</b>
ACS	27	35.5	31	34.8	34.8	24	34.8	34.8
C&DH	20	20	20	20	20	20	20	20
Power	12.3	10.7	39.8	88.4	35.7	25	31.3	47.7
Propulsion	51.3	3.3	298.3	3.3	3.3	3.3	3.3	3.3
Telecom	72.1	307.9	225.1	31.8	225.1	72.1	27	278.7
Thermal	16.9	36.9	36.9	36.9	36.9	36.9	36.9	36.9
<b>Total</b>	<b>199.6</b>	<b>414.3</b>	<b>651.1</b>	<b>1446.2</b>	<b>583.8</b>	<b>408.3</b>	<b>514.2</b>	<b>782.3</b>
Contingency (30%)	59.9	124.3	195.3	433.9	175.1	122.5	154.3	234.7
<b>Total (w/Contingency)</b>	<b>259.5</b>	<b>538.6</b>	<b>846.4</b>	<b>1880.1</b>	<b>758.9</b>	<b>530.8</b>	<b>668.5</b>	<b>1017.0</b>

this mode. Three 30 A-hr lithium-ion batteries are baselined for this mission, which includes one redundant unit. The total battery mass is ~33 kg (with 30% contingency), and is sized by the energy requirements of the TCPRA science mode. A single-string nickel-hydrogen battery system was studied, but not selected as it was >18 kg heavier than the lithium-ion system.

The batteries would nominally be used only during the TCPRA science mode to cover peak power usage. The power requirements of all other modes are within the capabilities of the RPS power system, and thus would not need battery power.

### 2.3.1.13 Mass

The total wet mass of the conceptual Titan orbiter spacecraft, including the aeroshell and probe is ~5730 kg with contingency. The orbiter dry mass, excluding aeroshell or probe, is ~2130 kg (Table 2.3.1-7). The propellant and pressurant mass is ~1300 kg, with the majority of the fuel used to perform DSMs (706 kg). The Titan orbiter instrument suite would weigh 626 kg including 30% contingency, and would be driven by the 520-kg TCPRA instrument used to perform detailed topographic altimetry and resolve atmospheric clouds and precipitation.

The aeroshell mass is estimated at ~35% of the approach mass at Titan (Hall, 2005), i.e., ~1300 kg. The approach mass is minimized by deploying the probe prior to aerocapture. For comparison purposes, a purely chemical propulsion system (i.e., no aeroshell) was studied for the same size spacecraft. Such a system would weigh >6000 kg more (assuming a two-stage propulsion system) than the baseline spacecraft using aerocapture, placing it beyond

Table 2.3.1-7. Mass Estimates for the Titan Orbiter, Aeroshell, and Probe

Subsystem	Mass, (kg)		
	All Units w/o Contingency	Contingency, %	All Units w/ Contingency
<b>Orbiter Stage (Dry)</b>	<b>1662</b>		<b>2129</b>
<b>Orbiter Stage (Wet)</b>	<b>2958</b>		<b>3425</b>
<b>Instruments</b>	<b>481</b>	<b>30%</b>	<b>626</b>
TCPRA	400	30%	520
NIMS	28	30%	36
WAC	3	30%	4
RSS	1	30%	1
SAR	41	30%	53
INMS	9	30%	12
<b>Attitude Control System</b>	<b>34</b>	<b>25%</b>	<b>43</b>
<b>Command and Data Handling</b>	<b>10</b>	<b>30%</b>	<b>13</b>
<b>Structures and Mechanisms</b>	<b>361</b>	<b>30%</b>	<b>469</b>
<b>Spacecraft Adapter</b>	<b>37</b>	<b>30%</b>	<b>48</b>
<b>Power</b>	<b>254</b>	<b>30%</b>	<b>330</b>
Li-Ion Battery System	25	30%	33
Advanced Stirling RPSs	210	30%	273
Power Conditioning	18	30%	24
<b>Cabling</b>	<b>99</b>	<b>30%</b>	<b>128</b>
<b>Thermal</b>	<b>104</b>	<b>25%</b>	<b>135</b>
<b>Telecom</b>	<b>125</b>	<b>20%</b>	<b>150</b>
<b>Propulsion</b>	<b>136</b>	<b>20%</b>	<b>165</b>
<b>Propellant and Pressurant</b>	<b>1297</b>	<b>N/A</b>	<b>1297</b>
<b>System Contingency</b>	<b>22</b>	<b>N/A</b>	<b>22</b>
<b>LV Adapter</b>	<b>324</b>		<b>324</b>
<b>Probe</b>	<b>500</b>		<b>500</b>
<b>Additional Unallocated Mass</b>	<b>189</b>		<b>189</b>
<b>Aeroshell (35% of Approach Mass)</b>	<b>1292</b>		<b>1292</b>
<b>Total Launch Mass (Dry)</b>	<b>3760</b>		<b>4434</b>
<b>Total Launch Mass (Wet)</b>	<b>5057</b>		<b>5730</b>

the reach of existing launch vehicles (the mass savings using a single-stage propulsion system is even greater at >10,500 kg). Clearly, aerocapture technology is enabling for the Titan orbiter mission.

The minimum probe mass requirement of 500 kg was selected to adequately cover the mass of the probe itself and its associated support structure. The combination of the Delta IV-Heavy LV and advanced Stirling-based Titan orbiter provides enough injected mass capability to enable the addition of a 500-kg probe, and ~200 kg of additional unallocated mass that could be used for an increased capability probe, more orbiter instruments, or for system growth.

**2.3.1.14 Radiation**

The Titan orbiter spacecraft would be exposed to both external and internal sources of radiation during the course of its mission. While shielding would be required to protect spacecraft electronics and key subsystems, the total radiation dose would be expected to be relatively mild compared with other successful planetary missions (e.g., Galileo), and in line with that experienced by the Cassini spacecraft. External sources of radiation include solar wind, belts of charged particles trapped in planetary magnetic fields, galactic cosmic rays, and high-energy particles generated by solar events. The total external radiation dose received by subsystems and instruments would not be expected to exceed ~20 krads (Si) behind 100 mils of aluminum shielding (Langley, 1993; Hoffmann, 2004). Radiation would also be produced by the decay of <sup>238</sup>Pu within the advanced RPSs consisting of gammas, neutrons, and alpha particles (alpha particles are trapped within the GPHS modules and are not an issue.) The maximum internal radiation dose received by the instruments and sensitive subsystems is estimated at <10 krads over mission lifetime. The total radiation dose due both to external and internal sources is thus estimated at ~30 krads (Si). Employing a radiation safety factor of 2, the Titan orbiter would use subsystem components rated for a minimum of 60 krads, well within the capability of existing technology (Galileo spacecraft components were rated significantly higher than those for the conceptual Titan orbiter mission). The fact that the Cassini spacecraft continues to orbit about Saturn illustrates that radiation shielding is not a significant driver for this mission concept.

**2.3.1.15 Alternate RPS Power System**

Trade studies were performed for four conceptual advanced RPS (ARPS) systems, including the advanced RTG, advanced Stirling, TPV, and Brayton. The estimated performance characteristics of each ARPS system are presented in Section 3. The spacecraft mass was evaluated for each ARPS technology, with the results are summarized in Table 2.3.1-8.

The advanced Stirling option has the lowest mass of all the ARPS systems, enabling the inclusion of a 500-kg probe along with ~200 kg of additional unallocated mass.

Next is the Brayton converter (Fig. 2.3.1-17), which utilizes 11 Brayton generators (22 GPHS modules total) to produce ~1 kWe (EOM). Though the specific power of the Brayton system is low relative to other ARPS technologies (~3.8 We/kg), the relatively high conversion efficiency (22%) yields a lighter thermal control system (i.e., less PCM), which makes the Brayton preferred over the advanced RTG and TPV systems from a mass perspective. However, the

**Table 2.3.1-8. Titan Orbiter and Probe Mass Comparison as a Function of Advanced RPS Technology Used (Includes Contingency).**

RPS Type	Mass, kg					
	Orbiter, Dry (No Aeroshell, Adapter, or Probe)	Propellant and Pressurant	Orbiter, Wet (No Aeroshell, Adapter, or Probe)	Aeroshell	LV Adapter	Mass Available for a Probe
Adv. Stirling	2129	1296	3425	1292	324	<b>689</b>
Brayton	2357	1307	3663	1366	324	<b>377</b>
Adv. RTG	2450	1311	3760	1396	324	<b>250</b>
TPV	2538	1314	3852	1425	324	<b>129</b>
SRG	2458	1311	3769	1400	324	<b>236</b>
Std. MMRTG	2814	1316	4131	1555	324	<b>-280</b>

Brayton-powered spacecraft would yield only ~380 kg for a probe, insufficient to meet the 500-kg mass requirement, but potentially enough for a smaller, less capable probe.

Third is the advanced RTG (Fig. 2.3.1-18), which would use 11 RPSs (55 GPHS modules total) to produce all spacecraft power. Though the advanced RTG represents a significant leap forward in capability relative to the standard MMRTG, the advanced RTG has the lowest conversion efficiency of the ARPS considered in this study (9%), which drives the need for a heavier thermal control system to store the RTG's heat during aerocapture. The combination of higher PCM mass (~150 kg) and lower specific power yields only ~250 kg of mass for a probe.

The fourth ARPS option is TPV (Fig. 2.3.1-19), which would use 12 RPSs, each employing 3 GPHS modules (36 modules total). The TPV has the highest specific power (6.2 We/kg) of all

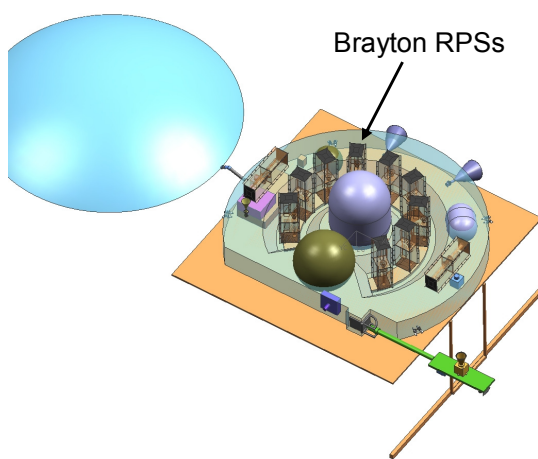


**Figure 2.3.1-17.** Brayton Configuration of the Titan Orbiter Concept during the Science Phase.

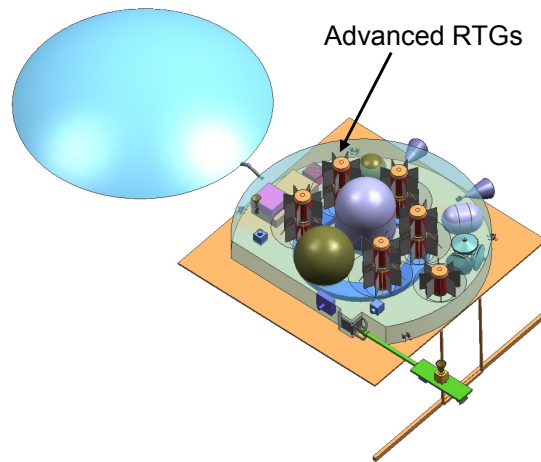


**Figure 2.3.1-18.** Advanced RTG Version of the Titan Orbiter Concept during the Science Phase.

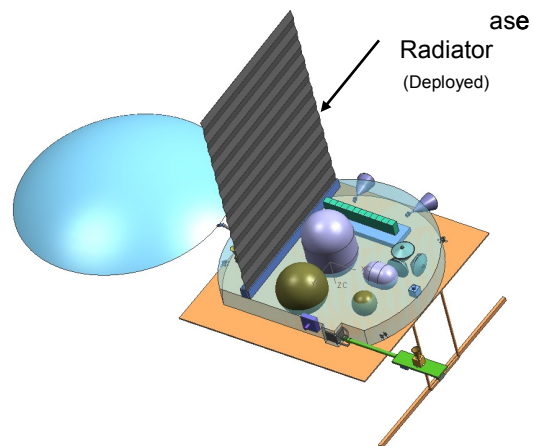
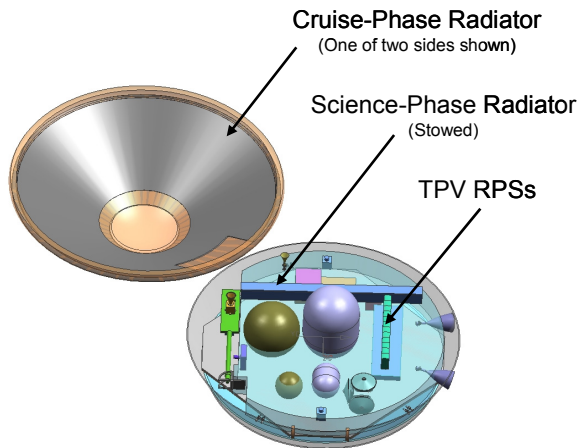


**Figure 2.3.1-19.** TPV Configuration of the Titan Orbiter Concept during the Cruise phase (Left), and Science phase (Right). Note the Thermal Radiators Integrated with the Aeroshell Cover used during Cruise, and the Separate Deployed Radiators Used during the Science Phase of the Mission.

advanced RPS systems considered; however, the PV cells must be operated at a low temperature, which requires relatively large radiators. For the Titan orbiter spacecraft configuration, two sets of radiators are required—one for the cruise phase that is mounted to the aeroshell, and a second set that is integrated with the bus, and deployed following aerocapture. The extra mass of the TPV thermal control system overwhelms the mass savings from the TPV's higher specific power for this application, resulting in the TPV being the heaviest of the ARPS systems for this mission (yields only ~130 kg of available mass). The MMRTG and SRG were also assessed for the Titan orbiter mission. The lower efficiency and specific power of the standard MMRTG (6.3% and 2.8 We/kg, respectively) was found to be incompatible with the mission from a mass perspective, yielding a negative mass margin of ~280 kg. On the other hand, the more efficient SRG with its higher specific power (23% and 3.4 We/kg, respectively), could potentially support the orbiter, but provides only ~240 kg of available mass, which is insufficient to meet the probe mass requirements. Thus, from an overall mass perspective, the advanced Stirling is the only RPS system that is able to meet the mission requirements for an orbiter spacecraft with  $\geq 500$  kg probe.

Mass trades are only one piece of the total picture regarding the suitability of an RPS system for the Titan orbiter mission. Other key parameters include RPS integration, complexity, robustness, heritage, and, potentially,  $^{238}\text{Pu}$  usage. Table 2.3.1-9 illustrates this ARPS assessment for 10 key criteria. Color shading is used to indicate the relative merits of each ARPS system for a given criterion, with green indicating the highest level of preference, yellow an intermediate level, and red indicating the least preferred for this Titan orbiter mission. Red does not necessarily mean that a specific ARPS could not be used for the mission, only that other green or yellow ARPS options would be preferred for that criterion.

The rationale for each rating is provided in the right-most column of the table. Definitions of each criterion were presented in Section 1 (Table 1-3). The result of the assessment is that the advanced Stirling has the highest ranking for this mission as it is strong in many key areas (mass, conversion efficiency, volume, integration, power degradation rate, and  $^{238}\text{Pu}$  usage) as well as being the only ARPS system able to meet the mission requirement of including a  $\geq 500$  kg probe for the mission. The advanced Stirling is considered to have less robustness and greater system complexity than solid-state ARPS systems; however, this is partially compensated for by including a spare advanced Stirling system to mitigate the potentially higher risk associated with this technology. The advanced RTG and Brayton would be the next preferred ARPS systems for this mission, both being roughly equally preferred. The TPV is the least preferred ARPS for this mission, as it has the greatest mass, volume, and integration complexity of all the ARPS systems. This suggests that a TPV system is not a good match for high-power spacecraft missions, especially for those using aerocapture.

### **2.3.1.16 Summary and Conclusions**

The Titan orbiter mission would provide a valuable follow-on to Cassini-Huygens, performing detailed global measurements of Titan's surface topography, cloud structure and dynamics, precipitation rates, and atmospheric composition. The spacecraft is designed around the high-power TCPRA, which drives the power requirement of ~1 kWe (EOM) and data rate requirement of 2.3 Mb/s. The Titan orbiter would be enabled by rigid-body aerocapture into Titan orbit. The use of aerocapture reduces the required propellant mass by over 6000 kg, making it possible to use the Delta IV-Heavy LV. The baseline Titan orbiter would use 15 advanced Stirling generators to produce all onboard power, corresponding to 15 GPHS modules, or  $<1/3$  of the fuel used by the Cassini spacecraft.

Table 2.3.1-9. Comparison of ARPS Systems for the Titan Orbiter Mission Concept

Criteria	Adv RTG	Adv Stirling	TPV	Brayton	Rationale
Power	Green	Yellow	Green	Green	Advanced RTG, TPV, and Brayton designs considered had similar power outputs of ~110 We. The advanced Stirling has an output of ~80 We, requiring units to generate the spacecraft power output of ~1 kW (EOM).
Mass	Yellow	Green	Red	Yellow	The advanced Stirling has the highest unit-specific power of the four ARPS concepts considered. Additionally, the high efficiency of the advanced Stirling results in the lightest spacecraft energy storage system (i.e., less phase change material is needed.) These two factors make the adv. Stirling the preference here.
Volume	Yellow	Green	Red	Green	The low heat rejection temperature of the TPV results in the need for large radiators, making the TPS option less preferred from a volume perspective.
Heritage	Green	Yellow	Red	Red	The advanced RTG shares significant design heritage with the MMRTG, and would utilize many of its subsystems and components. The advanced Stirling has some heritage with terrestrial-based systems of similar design. The remaining two ARPS systems share little, if any, relevant heritage.
Integration	Green	Green	Red	Green	The large size of the TPV radiators significantly complicates integration of the TPV with the spacecraft (i.e., two sets of radiators are required: one during the cruise phase and jettisoned before aerocapture, and the other deployed following aerocapture).
Environmental Emissions	Green	Green	Green	Green	Do not expect the vibration or EMI fields generated by the ARPS systems to be a significant issue for this mission (assuming proper EMI shielding for all units and active vibration compensation for the advanced Stirling).
Robustness	Green	Yellow	Green	Green	The adv. RTG and TPV use cross-strapped series/parallel electrical connections such that an individual uncouple or cell failure does not take down the entire system. The Brayton system uses a fully redundant architecture to reduce single-point-failure modes. The advanced Stirling is single string, requiring additional Stirling units for block redundancy.
RPS Complexity	Green	Yellow	Green	Yellow	The advanced RTG and TPV are fundamentally simpler systems compared with adv. Stirling and Brayton due to their passive operation, lack of moving parts, and lack of active electronics or sophisticated controllers.
Power Degradation Rate	Yellow	Green	Yellow	Green	Lower power degradation rates are generally preferable.
<sup>238</sup> Pu Usage	Yellow	Green	Yellow	Green	The higher efficiency of the dynamic power systems (adv. Stirling and Brayton) make them preferable from the perspective of reduced <sup>238</sup> Pu usage. This could be a driver were fuel availability an issue.
ARPS Ranking for the Titan Orbiter Mission Concept	Yellow	Green	Red	Yellow	The advanced Stirling offers a significant mass savings over all other ARPS systems for this mission (even with the inclusion of a redundant RPS unit.) This mass savings enables the mission to include 500-kg probe, which is a key requirement.

The higher efficiency of the advanced Stirling generator is a key benefit to the Titan orbiter mission from the perspective of fuel availability and in that less heat is produced, thus minimizing the amount of PCM required to store the RPS heat during the ~1-hr aerocapture maneuver. For comparison, the advanced RTG system required >100 kg more PCM than the advanced Stirling due to the difference in conversion efficiency. The higher specific power of the advanced Stirling (~5.9 We/kg) and its relatively small fin size are other key factors that helped to minimize system mass and overall system volume. The advanced Stirling RPS was the only ARPS system that provided enough mass savings to enable the mission to meet its requirement of including a  $\geq 500$ -kg probe. The TPV option was the least attractive ARPS option from an overall mass and volume perspective, requiring two sets of large radiators to maintain its low cold-side operating temperature during the cruise and science phases of the mission. The use of the MMRTG was analyzed and found to produce a system with negative mass margin; the SRG, on the other hand, could support an Orbiter-only mission (though with less mass margin than the Brayton or advanced RTG), but could not include a 500-kg probe.

In conclusion, the Titan orbiter mission is designed to address the key scientific goals of the Solar System Exploration Decadal Survey, and could be enabled by advanced RPS technology and rigid-body aerocapture. Due to the limited scope of this study, several areas were not addressed that warrant consideration in future studies. These areas include Planetary Protection and mission assurance.

## 2.4 LANDER MISSIONS

### 2.4.1 Europa Lander Mission

A Europa Geophysical Explorer mission was identified in the Solar System Exploration Decadal Survey (Space Studies Board, 2003) as the highest-priority flagship-class outer solar system mission for the next decade. While that recommendation was for an orbiter mission, it is widely recognized that a landed science package would dramatically increase the value of any Europa mission. Europa, shown in Figure 2.4.1-1, presents unique challenges for in situ exploration. Any landed science platform would have to survive the intense levels of trapped radiation, land safely on the extremely rugged surface, and provide sufficient electric power and thermal control for surviving in the frozen environment. This study demonstrates that long-lived in situ surface exploration would greatly benefit from the use of advanced RPS technologies. A static lander concept is described that would drop to the surface of Europa and perform scientific measurements for a period of 30 days. This lander concept could potentially be included in a Europa orbiter mission during the next decade, but may be more appropriately targeted for a dedicated Europa astrobiological lander mission as outlined in the Solar System Exploration Strategic Roadmap (NASA, 2005).

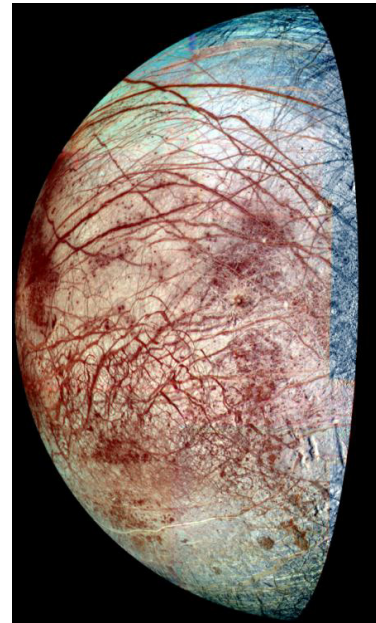


Figure 2.4.1-1. Europa enhanced color image from Galileo images taken in 1995 and 1998

The primary goal of this document is to compare the suitability of four different ARPS technologies for use on a Europa lander mission. The details of these ARPS alternatives are described further in Section 2.4.1.16 and Section 3. A key advantage of advanced RPS systems for a Europa lander mission is their higher specific power, thus providing a mass savings that could be used to increase payload capability or lander design margins. RPSs in general are suitable for Europa in that they do not require solar insolation; they are long lived; and they can be used to keep the lander electronics warm during the long cruise phase and on the very cold Europa surface. Certain RPSs are also inherently radiation tolerant, which is a key consideration for missions operating in the intense ionizing radiation of the Jovian system. Solar array power options would have significantly more mass and would be very sensitive to the radiation environment.

The Solar System Exploration Decadal Survey indicated that a Europa mission would contribute to two areas of scientific understanding: (1) the origin and evolution of habitable worlds and (2) how planetary systems work. The first step on that path is to detect and describe the probable subsurface ocean, as well as the icy surface. This Europa lander mission concept is designed to address these goals through in situ exploration of the surface environment. Instrumentation would perform sampling of surface ice for compositional assays, as well as passive environmental measurements. The use of RPS technologies would enable sustained geophysical measurements over several 3.55-day Europa tidal cycles.

JPL's collaborative engineering team of subject matter experts (Team P) examined this mission concept to further develop a pre-existing design and identify the sensitivities to the four ARPS options. The lander described here has a landed mass of roughly 400 kg. The enclosure houses

the lander's electronics and is wrapped around the solid rocket motor that is used for de-orbiting. The ARPS unit is mounted on top, and waste heat is used to warm the lander electronics through a conduction path within the enclosure. The two propellant tanks for the dual blow-down monopropellant systems are mounted on the sides of the enclosure. Dual UHF LGAs provide broad sky coverage for communicating with the relay orbiter at data rates between 256 kb/s and 1024 kb/s. Figure 2.4.1-2 shows the lander configuration using the advanced RTG.

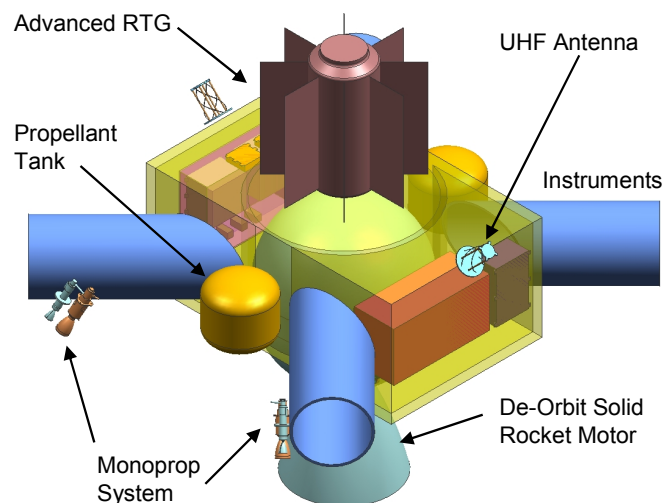


Figure 2.4.1-2. Europa Lander Concept Using Advanced RTG Power Source

#### 2.4.1.2 Science Goals

A set of likely science goals for a future Europa lander are outlined below. Most of these goals were originally formulated by the Science Definition Team for the Jupiter Icy Moons Orbiter (JIMO) mission. Beyond these direct objectives, mission planners recognize that many of the in situ measurements made by a lander would usefully complement orbiter science measurements, assisting in the interpretation of remote sensing data obtained by an orbiter.

**Objective 1 (Astrobiology): To search for signs of past and present life on Europa.** Search for organic materials and determine their composition and reveal chemical patterns that might be indicative of biological activity or biological origin.

**Objective 2 (Geophysics): To determine the local thickness and characteristics of the icy crust.** Provide in situ measurements of surface physical properties (including morphology, density, hardness, and thermal properties). Detect and measure surface gravity, tides, seismic activity, subsurface structure, ice shear modulus, and other geophysical properties. Collect measurements of tidal motion and seismic activity over several tidal cycles.

**Objective 3 (Geological-Compositional): To determine the ice and non-ice elemental and mineralogical composition of the surface.** Specific measurements include elemental composition, mineralogical characterization (including hydrated minerals), and physical properties (including morphology, thermal, and electromagnetic properties). Characterization of relevant surface processes requires measurements of ambient radiation as well.

**Objective 4: To determine the habitability of the European surface.** Measurements of surface radiation, magnetic fields, and temperature.

#### 2.4.1.3 Mission Goals

The mission concept described here seeks to address the above science objectives with a long-lived surface lander, using an ARPS system for power and heat. A 30-day surface mission would enable the collection of valuable science data, including seismometry data over several 3.55-day tidal cycles, and magnetic field and radiation measurements over several orbits of Europa around Jupiter. This study examines the impacts of the four different ARPS systems on the overall flight system and mission design of such a lander.

Landing on Europa’s surface presents unique challenges. The icy terrain varies dramatically and can be extremely rugged with feature sizes in the tens or hundreds of meters. Surface temperatures vary from ~130 K daytime to ~80 K at night. The ambient radiation is estimated to be roughly 20 rads/s. There is negligible atmosphere and the surface gravity is 1.32 m/s<sup>2</sup>. Europa’s period of rotation is 3.55 Earth days; this matches its orbital period around Jupiter.

**2.4.1.4 Mission Architecture Overview and Assumptions**

The mission design goals for this Europa lander concept would be to travel to Europa while attached to an orbiter, separate from the orbiter and descend to the surface, land and conduct scientific investigations for 30 days. Once at Europa, the orbiter would provide tele-communications relay service for all contact with Earth.

The mission architecture employs a direct launch onto a ΔV-Earth gravity assist (EGA) trajectory. The lander would be mated to, and launched with, the orbiter spacecraft. All DSMs and orbit insertion burns would be performed by the orbiter spacecraft. In order to focus on the lander concept, details of the orbiter were not explored. The launch would occur on January 29, 2015 with a C<sub>3</sub> of 26.94 km<sup>2</sup>/s<sup>2</sup>. This launch opportunity was chosen for its combination of short cruise duration and high post-Jovian orbit insertion (JOI) mass. A Delta IV-Heavy LV is capable of placing approximately 5580 kg onto this trajectory. The ΔV-EGA trajectory uses an Earth gravity assist flyby on December 12, 2016 and requires only 4.8 yrs of cruise to reach the Jovian system (Fig. 2.4.1-3). After arriving at Jupiter in November of 2019, an additional 18 months are spent in a Jovian tour to prepare for insertion into Europa orbit.

An alternative Venus-Earth-Earth gravity assist (VEEGA) trajectory, launching on June 23, 2015, would reduce the propulsion requirements by 200 m/s and increase the cruise duration to 6.08 yrs. The same launch vehicle can deliver approximately 7230 kg onto this alternative VEEGA trajectory, resulting in a 950-kg increase in mass delivered to Europa orbit.

In this mission concept, the lander would be delivered to a latitude of 30° or less at Europa. The landing sequence is straightforward and is intended to be relatively tolerant of the rugged surface features. The complete EDL sequence requires approximately 62 min. After separation from the orbiter, the lander performs a small de-orbit burn, placing it on a transfer ellipse with a periapsis at approximately 2-km altitude. A solid rocket motor (SRM) is fired causing the lander to stop and drop from an altitude of 2 km. Descent imaging is taken and transmitted in real time to the orbiter. The lander uses descent images to determine horizontal velocity cleanup requirements. Triggered by the radar altimeter, the propulsion system begins a controlled deceleration burn over the last minute of descent. Near the surface, the lander has slowed to a stop. At this point, the propulsion system shuts down allowing the lander to drop to the surface. The lander

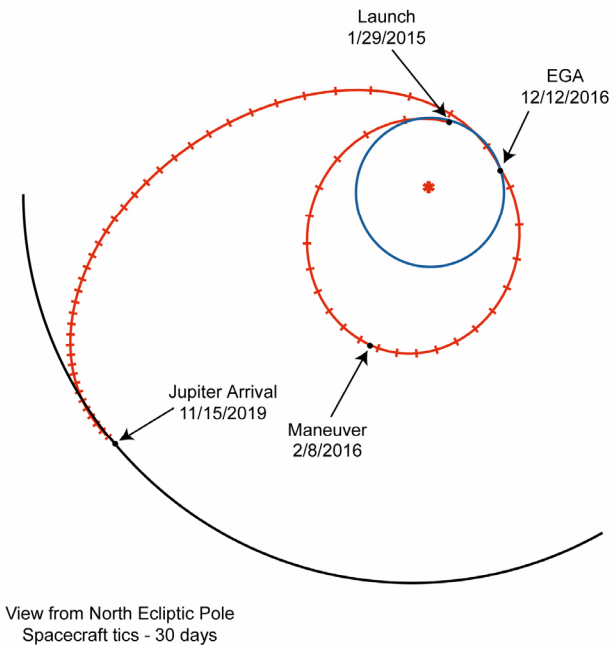


**Figure 2.4.1-3. Europa Lander Mission Concept Interplanetary Trajectory**

would touch down approximately 1 hr after separation from the orbiter.

A key design driver for this mission study is the ability to land on the surface with no greater than 40g impact acceleration. It is assumed that all four ARPS options would be capable of surviving this impact load and functioning properly afterward, consistent with the requirements of the MMRTG currently being jointly developed by DOE and NASA. The lander has 5 cm of crushable material on its bottom surface to help meet the <40 g surface impact requirement.

The relay orbiter, as studied, is assumed to have a circular equatorial orbit at an altitude of 2000 km. In that orbit, the relay orbiter will rise every 426 min (7.1 hrs). Length of contact will vary with the latitude of the landing site, with longer contacts occurring at lower latitudes. For a landing site latitude of 15°, the contact duration is 85 min, and for 30° the contacts last for 104 min. Changes in the relay orbit will certainly influence the contact duration and frequency. A low-altitude inclined relay orbit will result in shorter, less-frequent contact periods. For illustration, the JIML study used the JIMO orbiter as a relay and its 100-km inclined orbit resulted in contacts shorter than 20 min spaced as much as 35 hrs apart (Rivellini, 2004).

#### **2.4.1.5 Power Source Trade Study**

Landing on Europa presents unique challenges for power source selection. Using solar arrays at this large distance from the Sun would require relatively large arrays for the present Europa lander concept. The 3.55-day Europa orbit around Jupiter (half the time in which the lander would be in shadow), and the ~2.9-hr Jovian occultation of the Sun (once per Europa orbit), would drive the need for large, high-capacity batteries. Since the Sun angles change as Europa orbits Jupiter, an array would need to either be oversized, or would require a pointing mechanism. However, the high-radiation environment would accelerate the degradation of any solar array, requiring even more array area. Furthermore, battery power alone has been included in previous Europa lander studies and found to severely limit the mission lifetime.

Science objectives are tied to the 3.55-day orbit and tidal cycle, and several cycles are desired by the science community. RPS-based designs have several key advantages over solar arrays and batteries. Certain RPS options (i.e., RTGs) are relatively insensitive to the high-radiation environment. Also, RPS designs offer waste heat for use in keeping lander systems warm, and significantly reducing the power required for heaters. Due to the 30-day minimum surface-mission requirement, RPS systems would enable this application.

#### **2.4.1.6 Advanced RPS Characteristics**

The baseline Europa lander would use one advanced RTG to meet all its electric power requirements. Other advanced RPS power systems were considered for this mission, as discussed in Section 2.4.1-16, but the advanced RTG was preferred from an overall power system perspective that considered such criteria as mass, volume, radiation tolerance, heritage, robustness, and RPS complexity. Each advanced RTG is assumed to generate 112 We at BOM, with a conversion efficiency of 9%. The EOM power output is estimated at ~100 We. Five GPHS modules are used as the nuclear heat source for this advanced RTG design, with a BOM thermal output of 1250 W. A portion of this heat would be used to warm the lander's subsystems to maintain operating temperatures while minimizing the use of electrical heaters.

#### **2.4.1.7 Science Instruments**

The Europa lander described in this study would carry a suite of instruments for addressing the science goals described in Section 2.4.1.2. These are the same instruments that were included in the JIML study. The environmental and engineering instruments (radiation monitors, temperature sensors, accelerometer) are relatively simple and require no detailed description.

**Table 2.4.1-1. Europa Lander Concept Science Payload and Instrument Descriptions**

<b>Instrument Name</b>	<b>Purpose</b>	<b>Science Objectives Addressed</b>	<b>Heritage</b>
1. GCMS	Search for signatures of biological activity (presence of organics, non-random mass distribution, chirality, isotopic fractionation). Describe the composition of non-ice materials.	Objective 1, Astrobiology: Search for signs of past and present life on Europa. Objective 3, Geological-Compositional: Describe the composition of non-ice materials. Objective 4, Habitability: Characterize the chemical and physical habitability.	Mars Science Lander, Venus Atmos. Probe (Discovery)
2. Wet Chemistry	Characterize surface chemistry for assessing habitability.	Objective 3, Geological-Compositional: Determine the ice and non-ice elemental and mineralogical composition of the surface. Objective 4: characterize the chemical and physical habitability.	Phoenix MECA
3. Sample Acquisition System	Obtain samples for analysis by other instruments.	Objectives 1 (Astrobiology), 3 (Geological-Compositional), 4 (Habitability)	TRL 3
4. Raman Spectrometer	Nondestructively determine mineralogical composition of non-ice materials.	Objective 3: Describe the composition of non-ice materials. May also detect certain organics (Objective 1).	Mars/ Lunar RESOLVE
5. Microseismometer	Monitor acoustic energy. Characterize seismic activity level during one or more tidal cycles.	Objective 2, Geophysics: Determine the local thickness and characteristics of the icy crust.	TRL 4
6. Magnetometer	Measure the local magnetic field and its variability with time.	Objective 2, Geophysics: Help determine the local thickness and characteristics of the icy crust; provide ground truth on presence of liquid ocean beneath the ice.	TRL 5
7. Imaging System	Characterize the microphysical properties, geological context, and geomorphology of the landing site.	Objectives 1, 2, 3, 4: Provides context for all compositional measurements and for geophysical observations.	Active-Pixel Sensors
8. Temperature Sensors	Characterize the thermal properties of the surface through measurements over the diurnal cycle.	Objective 2, Geophysics: Measure thermal characteristics of the icy crust. Objective 3, Geological-Compositional and Objective 4, Habitability: Provide ground truth for orbiter measurements of surface temperatures.	Pathfinder, MER
9. Radiation Sensors	Measure incident radiation and variability over time.	Objective 4, Habitability: Characterize surface habitability. Provide ground truth for models of surface radiation levels based on orbital data.	CERN RADMON
10. Accelerometer	Measure deceleration on impact.	Objective 2 (Geophysics) and Objective 3 (Geological): Provide limited characterization of surface hardness.	Pathfinder, MER

A summary of the science payload and instrument descriptions for the proposed Europa lander mission is given in Table 2.4.1-1. A gas chromatograph mass spectrometer (GCMS) is carried as the prime science instrument because it does the best job of addressing the astrobiology science goals, particularly for the detection and characterization of organic materials. A Raman spectrometer is included for characterizing the mineralogy of non-ice surface materials, thus addressing the geology-geochemistry goals as well as the astrobiology goal. A wet chemistry instrument provides independent information on the presence and concentration of a number of major ions that are currently thought to be present on Europa (Na, K, Mg, etc.), and would characterize the habitability through measurement of pH, dissolved oxygen, and redox potential. Microseismometers would provide data on ice thickness and characterize seismic activity.

#### **2.4.1.8 Data**

A wealth of scientific data would be collected by the lander beginning with the many descent images taken before it even reaches the icy surface. At the instant of impact, the accelerometers provide valuable information about the surface hardness and features. From that point on, the suite of scientific instruments generates a constant flow of data. That data must be stored onboard the lander prior to transmission to the relay orbiter. All of the data is compressed using lossless algorithms.

The data storage requirements were sized for a nominal operational scenario with telecom contacts occurring every 14.2 hrs. This corresponds to every other pass by the orbiter, which provides contact opportunities every 426 min. The data from the group of science instruments taking measurements continuously is easily estimated. The data from the sampling science instruments is estimated by assuming each probe collects and processes one sample during each contact period. The operational scenario is driven by the energy demands and the need to recharge the battery.

The details of the data volume generated in this sizing scenario are shown in Table 2.4.1-2. The total data storage requirement for the nominal 14.2-hr period is ~138 Mb. In the event of a missed contact, the lander's programming would attempt to download stored data at the next opportunity, 426 min later. That additional time would add roughly 54 Mb of science data (no imaging would be performed in the extended period). The total data volume would be 192 Mb, and a 100% margin results in a storage sizing of ~382 Mb. This storage requirement is accommodated with 384-Mb static random-access memory (SRAM). The 192-Mb total data volume sent to the orbiter is assumed to be a very small fraction of the orbiter's storage and downlink capacity because many prior Europa orbiter studies have included data-intensive orbiter instrumentation (altimeters, radars, and imagers).

In addition to data storage, the lander's avionics equipment includes all central processing functions, power distribution, and command and data interfaces for the science instruments, communications, attitude control, and propulsion subsystems. Imager data compression is performed by the imaging instruments while the avionics processor compresses data for the other instruments. In addition, the central processing functions include science data management, power management, EDL sequence management, and attitude control during EDL. The data interface is sized for a maximum 8-Mb/s data rate originating from the imaging instruments.

The avionics suite employs a block-redundant design using rad-hard 132-MHz PowerPC processors and 384-Mb SRAM for onboard storage. A system interface assembly board provides dual 1553 interfaces, SRAM buffer, telecom interfaces, and discrete input/output (I/O) interfaces.

System I/O boards, DC/DC power-converter boards, remote engineering unit interface boards, and a cPCI backplane round out the avionics package. The design uses 6U form factor boards

Table 2.4.1-2. Europa Lander Concept Instrument Data Rates and Volumes

Instrument	Data Rate	Time Period, hrs	Volume—Raw	Compression	Volume—Compressed
<b>Passive Science Suite</b>					
MicroSeismometer	1 kb/s	14.2	51.1 Mb	2:1	25.6 Mb
Magnetometer	1 kb/s	14.2	51.1 Mb	2:1	25.6 Mb
Temperature	16 bps	14.2	818 kb	2:1	409 kb
Imager	3.2 Mb/image	1 / 14.2		5:1	3.2 Mb
Data Volume from One Passive Science Suite per Contact Period (14.2 hrs)					54.7 Mb
Data Volume from Two Passive Science Suites per Contact Period (14.2 hrs)					109.5 Mb
<b>Active Science Suite</b>					
Sampling Science	1.083 Mb/sample	1 / 14.2	1.1 Mb	2:1	542 kb
Imager	3.2 Mb/image	1 / 14.2		5:1	3.2 Mb
Data Volume from One Active Science Suite per Contact Period (14.2 hrs)					3.7 Mb
Data Volume from Two Active Science Suites per Contact Period (14.2 hrs)					7.5 Mb
<b>Other Science Instruments</b>					
Imagers (6)	3.2 Mb/image	1/cam/14.2		5:1	19.2 Mb
Temperature Sensors(2)	16 bps each	14.2	1.6 Mb	2:1	818 kb
Radiation Sensors(2)	16 bps each	14.2	1.6 Mb	2:1	818 kb
Data Volume from Other Science Instruments per Contact Period (14.2 hrs)					20.8 Mb
<b>Total Data Volume per Contact Period (14.2 hrs)</b>					<b>137.8 Mb</b>
<b>Instrument Data Volume (Non-Imaging) for One Missed Pass (Extra 426 min)</b>					<b>53.4 Mb</b>
<b>Total Data Volume Including One Missed Telecom Pass</b>					<b>191.2 Mb</b>
<b>Lander Data Storage Requirement (including 100% growth margin)</b>					<b>382.4 Mb</b>

with customized parts to achieve 300-krad radiation tolerance. Additional spot shielding is used to meet the design environment total ionizing dose (TID) requirement of 3.36 Mrad behind 100 mils Al with a radiation dose factor (RDF) of 2. The design team determined that spot shielding resulted in a mass savings over the option of using shielding vaults for enclosing all electronics.

#### 2.4.1.9 Communications

The lander telecommunications system would provide communications during EDL and surface operations. Communications during cruise would be handled by the orbiter spacecraft. The lander's dual-string design uses Electra-Lite UHF transceivers (with integrated 8-W (RF) amplifiers) and quadrifilar helix LGA. Telemetry and descent images are transmitted to the orbiter in real time during the EDL sequence. During surface operations, all data is stored onboard before being sent to the relay orbiter. Contact frequency and duration would depend on the orbit of the relay spacecraft and the lander's latitude. Due to the irregular and uncertain surface terrain, the lander's antennas are mounted on the enclosure at off-nadir angles to provide broad sky coverage and improved tolerance of non-upright resting attitudes.

Contacts with the relay orbiter can occur every 426 min, with durations depending on the lander latitude. The contact duration is 85 min at 30° latitude and 103 min at 15° latitude. These figures

assume the relay spacecraft is in a 2000-km circular equatorial orbit. Different orbits will yield different contact periods and frequencies. The JPL JIML study used the JIMO spacecraft as a relay, and its inclined 100-km orbit yielded contacts less than 20 min long and spaced as much as 35 hrs apart.

Link performance estimates were calculated using reasonable assumptions for the relay orbiter's telecommunications system. The orbiter spacecraft was assumed to use the Electra UHF transceiver and a 15-dBi steerable UHF antenna. The lander's link performance was estimated to provide between 256 kb/s and 1024 kb/s data rates for orbiter elevations of 20° and 70°, respectively. The links are designed with a minimum 10-dB margin, which is conservative for conceptual designs of deep space landers and rovers due to unpredictable terrain obstructions.

For completeness, the orbiter's downlink performance to Earth was estimated assuming the orbiter used 100-W (RF) TWTA amplifiers and a 3-m Ka-band HGA pointed to 1 mrad. At a range of 5 AU, the orbiter would achieve a minimum of 3-dB margin for data rates between 680 kb/s and 13 Mb/s, depending on ground stations used. Downlinking to one 34-m DSN station would achieve 680 kb/s. Using two 34-m stations would almost double that to 1.2 Mb/s. A rate of 2.7 Mb/s could be achieved when using a 70-m equivalent array of Ka-band stations, and 13 Mb/s are possible using 180 12-m DSN stations.

A Europa lander mission would have a high priority for DSN resources. Returning all available lander science data would therefore influence mission operations. The baseline contact schedule would plan for lander communications during each possible contact with the relay orbiter. This design supports that operational scenario, as well as returning all stored data after missing one or more contacts with the relay orbiter. The nominal scenario's 138-Mb stored science data can be transmitted at the lowest data rate of 256 kb/s in less than 9 min. Additionally, all 384 Mb of installed data storage can be transmitted in 25 min. This apparent excess link performance improves tolerance of landing in a depression or crevasse or landing with a non-upright attitude. It also provides tolerance to the shorter and/or less frequent contacts associated with inclined relay orbits at lower altitudes.

#### **2.4.1.10 Attitude Determination and Control**

Attitude determination and control capability is required to support the EDL phase. Functional requirements include attitude knowledge and control of the lander during descent, during orientation maneuvers, and during the SRM burn. Additionally, the ACS system would measure the remaining horizontal velocity of the lander after the SRM burn and support orientation and burn maneuvers for removal of that horizontal component using the monopropellant system.

Inertial attitude is determined using precision gyros and accelerometers for sensing angular rates and linear acceleration, respectively. Attitude is controlled in six degrees of freedom (6-DOF) using four 22-N and four 267-N monopropellant thrusters. Thrust vector control during the SRM burn is performed using the thrusters in pulse mode. A radar altimeter is used for controlling the descent from approximately 1.3-km altitude down to the surface. The altimeter, along with descent imaging, is used to determine the lander's horizontal velocity during descent. This use of descent imaging for horizontal velocity measurement was employed successfully on the Mars Exploration Rover (MER) project by the Descent Image Motion Estimation System (DIMES).

#### **2.4.1.11 Thermal**

The Europa lander design would employ a combination of passive and active thermal control measures for maintaining the required environments. In each design option studied, waste heat from the ARPS would be used to keep the lander's electronics warm. An estimated 100 Wth is conducted from the ARPS radiators to the top of the lander equipment housing, where it is

transferred by passive heat pipes to the internal electronics assemblies. The housing has no MLI, but does use 1.3-cm thick HiTherm insulation on the internal walls and floor of the equipment housing. This design would be balanced to passively maintain the top of the equipment box at 300 K and the bottom at 100 K. Heaters and MLI would be used in the science probes and propulsion systems. Once on the surface, the propulsion system heaters would no longer be powered.

The SRM must be heated during cruise, requiring 24 We. This is a stressing requirement and was met in this design concept by assuming this would be furnished by the orbiter spacecraft during the cruise period. The lander power system would provide this heater power during the first 60 min of EDL prior to the SRM burn.

The challenges associated with ARPS waste heat rejection during cruise and EDL are minimized due to the absence of an aeroshell. This is one advantage of landing on a body without an atmosphere. In each design option, waste heat is radiated using the ARPS fins for both cruise and EDL mission phases, as well as for surface operations. The size of those radiators match those for the deep space design variants for the ARPS technologies, with the exception of the TPV. For the TPV, the radiator fins would be reduced in area from 2.5 m<sup>2</sup> to 2.2 m<sup>2</sup>, due to shunting of 100 Wth for heating the lander electronics. The shape of the TPV radiator fins may also be modified to allow for closer mating of the unit to the lander housing. Further study is required to examine the heat rejection approach during launch phase.

**2.4.1.12 Propulsion**

The Europa lander requires propulsive capability in order to leave orbit and perform a controlled landing that would provide the low acceleration necessary for the ARPS to function. All of the traditional maneuvers associated with missions to the Jovian system are performed by the propulsion system on the relay orbiter spacecraft. These total 2644 m/s and include DSMs, TCMs, JOI, Perijove Raise maneuver (PJR), and Europa Orbit Insertion (EOI).

The functional and ΔV requirements for the propulsion system are dominated by the large stop-

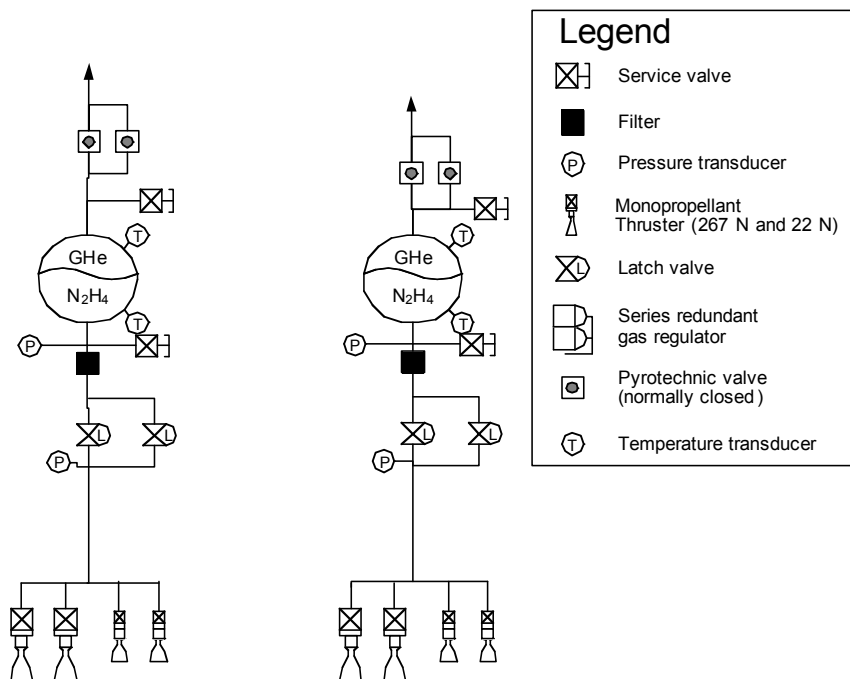


**Figure 2.4.1-4.** Europa Lander Propulsion System Diagram.

and-drop burn. A Star-27 SRM would be carried for performing this 1472 m/s burn with an Isp of 290 s. The SRM would be jettisoned after use, minimizing the landed mass and the required propellant for terminal descent and deceleration. The advanced RTG and Brayton design options required stretched versions of the Star-27, with 1.14-cm and 1.96-cm extensions, respectively.

Two identical blow-down monopropellant hydrazine propulsion systems cover the remaining functional requirements (Fig. 2.4.1-4). Two 40-cm diameter composite overwrapped tanks with elastomeric diaphragms hold the 46.3 kg N<sub>2</sub>H<sub>4</sub> and 0.2 kg pressurant. Four 267-N thrusters and four 22-N thrusters would perform all de-orbit, SRM thrust vector control, EDL orientation and deceleration burns. The thruster Isp is estimated at 230 s for the de-orbit burn system and 210 s for the terminal descent system.

Terminal descent deceleration would be performed using the four 267-N thrusters. With a thrust derating to 150-N each, due to the pressure blowdown, and a 70% pulse duty-cycle, an initial thrust-to-weight ratio greater than 2 is provided. After landing, the remaining pressurant would be vented to ambient and the propulsion system shuts down, requiring no further electric power.

**2.4.1.13 Power**

In this study, the lander is powered by a hybrid ARPS/battery direct-energy transfer system. The power control electronics, based on X2000 6U form factor boards, are dual string and manage power distribution and battery charge level. A 16 A-hr Li-Ion battery is employed in all design options. Power subsystem mass varies in each option, largely due to the difference in ARPS mass. The advanced Stirling design option requires three units, including one redundant unit in order to satisfy the power requirements.

The primary power modes and their total loads are: *Cruise* (95 We), *EDL* (343.2 We), *Continuous Science* (92.3 We), *Sampling Science* (141.2 We), and *Telecom* (175 We). *EDL* mode is the most demanding and includes heater power for the SRM and heavy ACS loads due to the

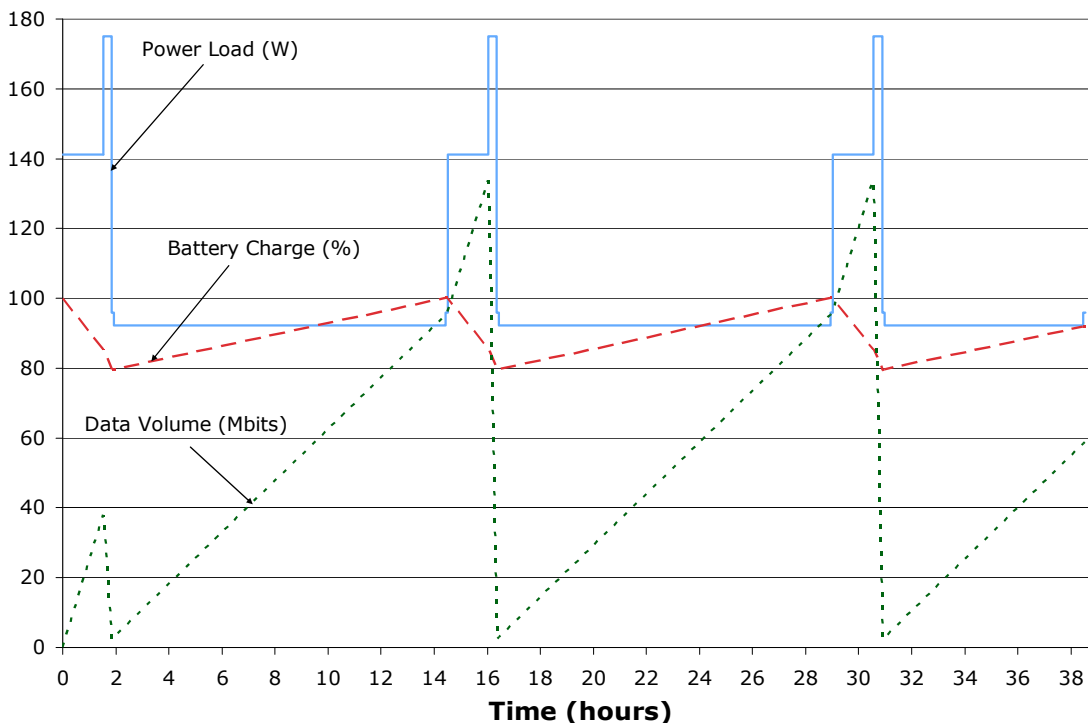


**Figure 2.4.1-5.** Europa Lander Concept Nominal Power and Data Storage Profile.

descent imaging and inertial measurement unit operation. A small primary battery is used to supplement the RPS in this mode. *Continuous Science* is the lowest mode and includes passive science measurements as well as battery recharge. *Sampling Science* mode includes the surface sampling activity and associated science measurements (from both active probes simultaneously), as well as passive science measurements. Each of the two active probes would attempt to take 15 samples over the mission and each sampling activity would span 91 min.

The power subsystem is sized using a nominal operational scenario that would begin with sampling science performed by both active probes simultaneously, followed by a telecom contact with the orbiter, then ongoing continuous science while the battery recharges. This entire scenario spans roughly 14.5 hrs, which is every other contact opportunity with the orbiter. The lander accumulates approximately 138 Mbits of compressed data during this time requiring less than 9 min for transmission to the orbiter (at the minimum 256 kb/s). Telecom contacts of 20 min are used for conservative power sizing. This nominal scenario is illustrated in Figure 2.4.1-5.

**2.4.1.14 Mass**

The mass budget for the advanced RTG design option is shown in Table 2.4.1-3. The mass of the instrument system is approximately 14.1 kg, and includes instruments, sampling mechanisms, structure, and cabling. The lander structure mass includes approximately 5 kg for the spacecraft interface adapter, as well as the mass for the tethers, reels, and tensioning systems. In this case, the propulsion SRM mass of 360.7 includes 341 kg of solid propellant. The motor would be fired at 2-km altitude, after which the motor would be ejected as the lander begins to drop to the surface. The landed mass therefore does not include the SRM mass.

Conservative mass margins of 43% were used in this study and are appropriate for early concept development designs, ensuring normal mass growth does not jeopardize mission feasibility. Mass contingencies for the SRMs are included at 5% to avoid excessive contingency mass from this dominating and well-known assembly.

**Table 2.4.1-3. Europa Lander Concept Mass Breakdown (Advanced RTG Option)**

Subsystem	Mass (kg)	Contingency %	Mass + Contingency (kg)
<b>Instrument System</b>	<b>61.2</b>	<b>43%</b>	<b>87.6</b>
<b>Lander Bus</b>	<b>562.2</b>	<b>19%</b>	<b>666.7</b>
ACS	12.0	43%	17.2
CDS	14.8	43%	21.1
Power (advanced RTG = 26.2 kg)	39.5	43%	56.5
Propulsion—Monoprop	18.9	43%	27.0
Propulsion—SRM	360.7	5%	378.7
Structures	83.9	43%	120.0
Cabling	13.6	43%	19.4
Telecom	8.8	43%	12.5
Thermal	10.0	43%	14.3
<b>Radiation Shielding</b>	<b>17.1</b>	<b>43%</b>	<b>24.5</b>
<b>Lander Total—Dry</b>	<b>640.5</b>	<b>22%</b>	<b>778.8</b>
Propellant and Pressurant	46.5	-	46.5
<b>Lander Total—Wet (Launch Mass)</b>	<b>687.0</b>	<b>20%</b>	<b>825.3</b>
<b>Lander Total—Landed Mass</b>	<b>279.8</b>	<b>43%</b>	<b>400.1</b>

**Table 2.4.1-4. Europa Lander Concept Mass Comparison (with contingency)**

Subsystem	Mass, kg			
	Adv. RTG	Adv. Stirling	TPV	Brayton
Lander Total—Dry	778.8	786.0	750.9	791.2
Propellant and Pressurant	46.5	48.7	44.8	47.2
<b>Lander Total—Launch Mass</b>	<b>825.3</b>	<b>834.7</b>	<b>795.7</b>	<b>837.7</b>
<b>Lander Total—Landed Mass</b>	<b>400.1</b>	<b>418.9</b>	<b>384.7</b>	<b>407.0</b>

Table 2.4.1-4 compares the lander mass for the four ARPS options. The TPV option has the lowest launch and landed mass; however, the TPV’s requirements for additional shielding in a high-radiation environment are not currently defined. The Stirling option is the heaviest, due to the three Stirling units required.

For the January 29, 2015 launch date, the Delta IV-Heavy (4050H-19) LV can launch approximately 5580 kg into the chosen trajectory. The required delta-V for cruise and the Jovian tour are estimated to be 2644 m/s for which an estimated 3256 kg of propellant is required. This leaves roughly 2300 kg for the orbiter dry mass and a lander. The four design options examined here result in an available orbiter dry mass of between 1460 and 1500 kg. This is significantly more than the mass of the JPL Europa Orbiter pre-project that was cancelled in 2002. The alternative VEEGA trajectory would allow an additional 950 kg of mass delivered to Europa orbit, providing even greater science value for the overall mission.

**2.4.1.15 Radiation**

All spacecraft that journey into or through the Jovian system must take precautions to protect their sensitive electronics from the intense ionizing radiation that is trapped in Jupiter’s strong magnetic fields. This trapped radiation dominates the total radiation that the Europa lander would experience. The contributions from the long interplanetary cruise period and from the ARPS are dramatically smaller.

The TID radiation values were estimated be 0.967 Mrad for the 4.8 yr cruise and Jovian tour periods, 0.284 Mrad for 10 days of systems checkout in Europa orbit, and 0.426 Mrad for 30 days on Europa’s surface (all behind 100 mils Al shielding). The surface radiation dose is conservatively estimated to be half that of the orbital dose, allowing for the shielding provided by Europa itself. Over half the entire dose is taken during the Jovian tour and 25% from the 30 day surface period. The total TID for the Europa lander mission would then be 1.68 Mrad (behind 100 mils of Al). To improve reliability and reduce risk, a safety factor of two is applied, so the concept described here is designed for a TID of 3.36 Mrad with an RDF of 2.

Shielding would be required to reduce the levels of ionizing radiation in order for the sensitive electronics to survive for the design life of this mission. A shielding vault in the housing protects the telecom and propulsion electronics to 100 krad. Spot shielding is used on the CDS chassis, ACS components, and science probe electronics to accommodate their 300 krad tolerance levels. Additionally, spot shielding is required to protect the control electronics for the Stirling and Brayton systems. Total shielding mass is estimated to be 24.5 kg.

**2.4.1.16 Alternate RPS Power Systems**

The primary goal of the study was to examine the feasibility of using each of four different ARPS technologies for a 30-day Europa lander mission concept. Several factors were considered in comparing these options, including design configuration, total mass, <sup>238</sup>Pu fuel usage, RPS complexity, and radiation sensitivity. The baseline configuration of the Europa lander uses a

single advanced RTG as its power source. The mission might also be accomplished with the alternative ARPS options with modifications to the design. The Stirling option was the only ARPS system requiring more than one unit. In fact, three Stirling units were required to satisfy the mission power demands and redundancy requirements (Yarnell, 2003). For all ARPS design options, the ARPS unit is mounted in the same location on top of the lander housing (Fig. 2.4.1-6). This minimizes the impact on the lander's configuration while maintaining a consistent thermal conduction path to warm the electronics box.

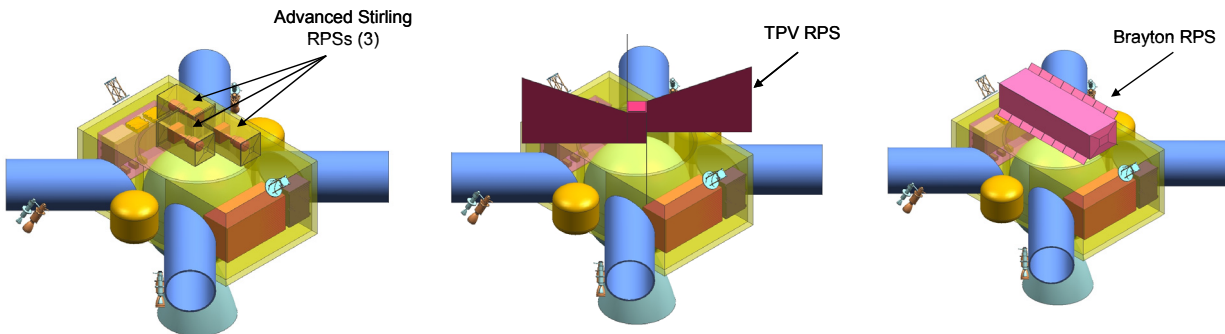


Figure 2.4.1-6. Europa Lander Concept Configuration Options: Advanced Stirling, TPV, and Brayton (left to right).

While all ARPS options use nuclear fuel, the lower efficiency of the advanced RTG option (compared with TPV and dynamic systems) requires the use of the greatest amount of  $^{238}\text{Pu}$ , which may be a constraint if fuel availability is an issue. On the other hand, the Stirling and Brayton ARPS options require control electronics, which are sensitive to the strong ionizing radiation near Jupiter. Those electronics packages would need to be shielded, with the associated increase in overall mass and engineering expense. The TPV option requires significantly larger heat rejection fins than the other options. The issues associated with launch environment on those large fins were not examined in this study. Currently, the sensitivities of the TPV design to the high-radiation environment are not well understood, but it is likely that additional shielding would be required, reducing the TPV's overall specific power for this mission. Using standard RPS systems such as the MMRTG and SRG could be a viable option, but would result in a heavier lander design that uses more  $^{238}\text{Pu}$  fuel.

Each of the RPS options was compared using a set of standard criteria (Table 2.4.1-5). No single option stands out as a clear favorite. For example, the low mass of the TPV option is more than offset by the issues of radiation sensitivity, power degradation, unknown shielding requirements, and unknown launch dynamics issues. And the Brayton option is edged out by the advanced RTG due to the latter's greater flight heritage and lack of radiation-sensitive control electronics. And while the Stirling option is the heaviest, it provides the most power. For purposes of this study, the advanced RTG was baselined due to its radiation-hard design and heritage.

Table 2.4.1-5. Comparison of ARPS Systems for the Europa Lander Concept

Criteria	Adv RTG	Adv Stirling	TPV	Brayton	Rationale
Power	Green	Yellow	Green	Green	Advanced Stirling outputs ~80 We compared to the unit power of ~110 We for the other options.
Mass	Yellow	Red	Green	Yellow	The advanced Stirling option required 3 units. TPV has the highest specific power, but shielding mass was not included in the analyses.
Volume	Green	Green	Red	Green	TPV requires large radiator panels with good radiant exposure for cooling.
Heritage	Green	Yellow	Red	Red	Advanced RTG has relatively greater design heritage than the others.
Integration	Green	Green	Green	Green	All options are largely comparable here for this mission concept.
Environmental Emissions	Green	Green	Green	Green	Sensitive instruments (magnetometers and seismometers) are protected from power supplies and sources of noise.
Robustness	Green	Yellow	Green	Green	Advanced Stirling is single string requiring multiple units.
RPS Complexity	Green	Yellow	Green	Yellow	Advanced RTG and TPV are fundamentally simpler systems compared with advanced Stirling and Brayton due to their passive operation, lack of moving parts, and lack of active electronics or sophisticated controllers.
Power Degradation	Yellow	Green	Red	Green	TPV has the greatest power degradation rate, which would be further exacerbated due to Jovian trapped radiation.
<sup>238</sup> Pu Usage	Yellow	Yellow	Yellow	Green	Redundant Stirlings somewhat negate their low fuel use per unit. The Brayton required the least (2 GPHS) and the advanced RTG required the most (5 GPHS). This could be a driver were fuel availability an issue.
ARPS Ranking for the Europa Lander Concept	Green	Yellow	Red	Yellow	The advanced RTG is baselined due to its rad-hard design and heritage. Brayton and Stirling use less fuel but are radiation sensitive. TPV is both rad-soft and has a larger physical volume than other ARPS concepts, complicating lander integration.

---

#### **2.4.1.17 Summary and Conclusions**

A Europa lander design concept is described that examines the feasibility of using advanced RPS technologies for long-life surface operation. The technologies compared include advanced RTG, advanced Stirling, TPV, and Brayton systems. Landing on Europa presents unique challenges for RPS technologies due to the high-radiation environment and the need to land without damaging the RPS. Due to the intense radiation environment at and around Europa, the TPV concept was considered unsuited for this mission due to the typical radiation softness of PV arrays. The advanced Stirling and Brayton RPSs may also have issues surviving the high radiation Jovian environment due to the radiation softness of their controller electronics, and their potential susceptibility to SEUs. The advanced RTG was the mission baseline due, in part, to its relative insensitivity to the radiation environment and its stronger design heritage.

RPS technology would enable a 30-day Europa surface mission and allow science data collection over several tidal cycles. The spacecraft design using the advanced RTG option had a launch mass of 825 kg and a landed dry mass of 400 kg. Using a Delta IV-Heavy to launch onto a 2015  $\Delta$ V-EGA trajectory allows a launch mass of 5580 kg. This can accommodate an orbiter of 1500 kg (inserted into Europa orbit) along with the 825 kg lander. An alternate trajectory provides even more capability but with a longer cruise duration.

This study focused on the feasibility of using four advanced RPS options to enable longer surface science operations. The scope of the study did not allow rigorous examination of all design trades. Several areas were identified that warrant further study of this design concept. Heating of the SRM during cruise and EDL may be performed by using waste heat from the lander's ARPS unit, eliminating the need for heater power from the orbiter spacecraft. The use of RHUs, instead of electrical heaters, may reduce the lander power requirements. Potential effects on collected samples and interference with the science instruments would need to be examined. Mass savings may be possible by using a bipropellant system or a low-temperature gel propellant system for the stop-and-drop burn, instead of an SRM. This would increase the landed dry mass and also increase the propellant required for terminal descent. Lastly, future Europa lander studies need to address NASA's Planetary Protection requirements, which were not explicitly considered in this limited concept study.

## 2.5 ROVER MISSIONS

### 2.5.1 Titan Rover Mission

The Solar System Exploration Decadal Survey (Space Studies Board, 2003) identified Titan as one of the top priority science destinations in the large moons category. The exploration of Titan in the form of future orbiter and/or lander missions was also rated high in the Solar System Exploration Strategic Roadmap (NASA, 2005). In fact, Titan ranked second in this list after a projected Europa Geophysical Observer mission. The complexity of a Titan mission could vary from a single element, such as an orbiter (discussed in Section 2.3) or an in situ explorer (discussed here) to multiple elements with the inclusion of both orbiter and in situ elements.

In situ exploration could be achieved in multiple ways, all having their own advantages and disadvantages. These ways include, with increasing complexity, a static lander, a balloon, a surface rover, and an aerobot. A static lander could be similar in functionality to the Huygens probe, but might be a different size. A balloon could cover vast areas, but provide only vertical control for surface access. Furthermore, its mass would be limited, compared to surface-based assets. A surface rover could traverse significant distances, similar to those planned for the Mars Science Laboratory mission. An aerobot would have all axis control and good surface access, but again be limited in mass compared to a surface-based mission. An aerobot concept has been explored in detail under the recent Vision Mission studies (Lunine, 2005).

Consideration should be given to a combined Titan orbiter and in situ mission because, while excluding an orbiter would reduce mission costs, it would also reduce science return on atmospheric remote sensing and could increase mission complexity and introduce landing location limitations due to direct-to-Earth (DTE) communication constraints.

The present study focuses on a surface rover concept without the support of an orbiter. In effect, the chosen configuration would fill the gap between a Huygens probe (JPL, 2005; Fig. 2.5.1-1) derivative static lander platform and the Vision Mission aerobot concept. A key goal of this study was to assess the benefits of advanced RPS systems in powering the Titan rover concept. Newer, more efficient power conversion technology with higher specific power would enable greater amounts of payload and potentially new mission architectures or the use of smaller (less expensive) launch vehicles.

#### 2.5.1.1 Science Goals

Titan and Europa are the premier targets for future in situ exploration of the outer solar system, Europa because of the possible presence of liquid water oceans that might harbor life, and Titan because of the “pre-biotic” organic chemistry that may be taking place on the surface. Future



**Figure 2.5.1-1.** First Color View of Titan's Surface (Cassini-Huygens)

missions to the surface of Europa face a number of daunting challenges: (1) landing on the

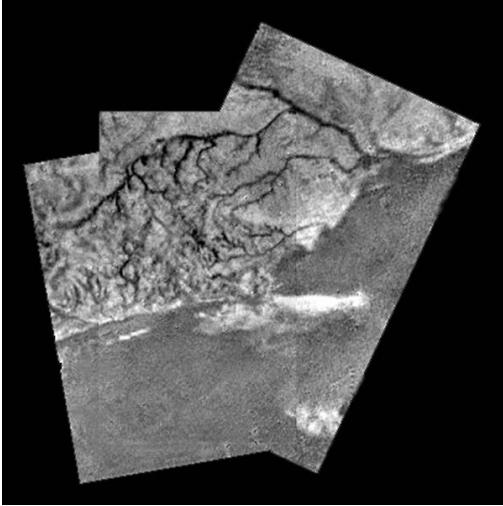


**Figure 2.5.1-2.** Cassini-Huygens Descent Image Mosaic. Drainage channels presumably cut by liquid methane rainfall and runoff dissect the elevated highlands in the upper part of the image.

surface of this airless body is difficult, (2) the severe radiation environment allows mission survival there for very limited times, and (3) it may be extremely difficult to obtain samples of surface materials that have been in contact with the hidden ocean. By contrast, (1) Titan's atmosphere allows for aerobraking descents, (2) the radiation environment is not a mission-critical factor, and (3) the organic materials desirable for sampling should be widely distributed (and easily accessible) over the surface. The recent Titan landing by the Huygens probe (JPL, 2005; Fig. 2.5.1-2) has focused considerable scientific interest on this remarkable body, and future missions to Titan are under consideration.

Titan represents a "natural laboratory" that could illuminate key questions relating to the origins of life. Titan's atmosphere is in some

ways similar to that of early Earth. Many organic compounds are present in Titan's atmosphere; these are produced by photolytic processes driven by solar ultraviolet radiation. These organics condense in Titan's stratosphere and may thereafter be deposited on the surface.

Imaging from the Cassini mission has revealed remarkable surface features on Titan that were previously obscured from view by atmospheric hazes (Fig. 2.5.1-1), although the highest resolution was limited to about 400 m/pixel. From these images and those of the Huygens descent imager, there is clear evidence of the presence of fluids on Titan's surface, and there are many features that are thought to have formed by cryovolcanic eruptions of water-rich ice materials.

The presence of organic compounds and water (in the form of ice) gives rise to speculation that Titan may at present support organic chemical processes that could be direct precursors to life. Some of the most critical science objectives for future missions to Titan can only be addressed from lander or rover platforms. The exact surface composition, the distribution and nature of organics, and the present-day chemical interactions of the surface and atmosphere are among these. The thick, smoggy atmosphere of Titan makes it difficult (if not impossible) to study these phenomena from orbit. Surface observations could also answer questions about the nature of the geological and meteorological processes that are operating to shape the surface. For purposes of this study, five interrelated potential science objectives were identified. Objective 1 is to determine the composition of Titan's surface materials; Objective 2 is to characterize the organic chemistry taking place at Titan's surface; Objective 3 is to describe the interactions between the surface materials and atmosphere; Objective 4 is to characterize the morphology of the surface; and Objective 5 is to describe the surface meteorology (pressure, temperature, and wind speeds). These objectives are further detailed below:

**Objective 1: To determine the composition of Titan's surface materials.** Although theoretical models suggest what materials may be found, scientists are certain to be surprised by ground-truth measurements of what is actually there. The present mission study addresses this objective

by obtaining measurements of Raman-shifted backscattered light, to characterize surface mineralogy; by assessing the elemental composition of surface materials, via laser induced breakdown spectroscopy (LIBS); and by additional mass-spectroscopic measurements obtained using a gas chromatograph-mass spectrometer (GCMS), which allows discrimination of many organic species. Materials identification would be facilitated by imagery obtained using a sampling microscope, which could examine core samples.

**Objective 2: To characterize the organic chemistry taking place at Titan's surface.** Measurements obtained by the suite of composition instruments (GCMS, LIBS, Raman) together with the complementary surface temperature and other environmental measurements would address this objective. By sampling in different locations, at different depths, and at different times we may constrain the nature and rates of ongoing chemical processes.

**Objective 3: To describe the interactions between the surface materials and the atmosphere.** As with Objective 2, this would require multiple observations by multiple instruments, at multiple locations, and with observations spaced in time. Meteorological observations and surface imagery would contribute to this description.

**Objective 4: To describe the morphology of Titan's surface.** Observations by a panoramic camera (Pan Cam) could provide information on surface structures over distance scales from millimeters to hundreds of meters. This information may be difficult to obtain from orbit.

**Objective 5: To describe the surface meteorology of Titan.** Orbiter missions would provide global information on clouds, precipitation, hazes, and atmospheric composition. However, in situ information on temperature, winds, and precipitation is of intrinsic interest, as it constrains key processes taking place at the surface. Among the processes of interest are chemical reaction rates and fluvial and wind-driven erosion rates. The meteorological package included in this mission study would provide measurements that address this objective. An acoustic monitor would provide complementary data.

### 2.5.1.2 Mission Goals

The Titan rover mission concept aims to land a long-lived roving in situ explorer on the surface of Titan. The mission would launch on an Atlas V 501 on a 7.6-yr transit towards Titan. Using an aeroshell and parachutes, the Titan rover would be delivered to the surface, where it could then deploy (Fig. 2.5.1-3) and begin its primary mission. The rover would operate on the surface on a three-yr mission studying the composition and chemistry of the surface material.

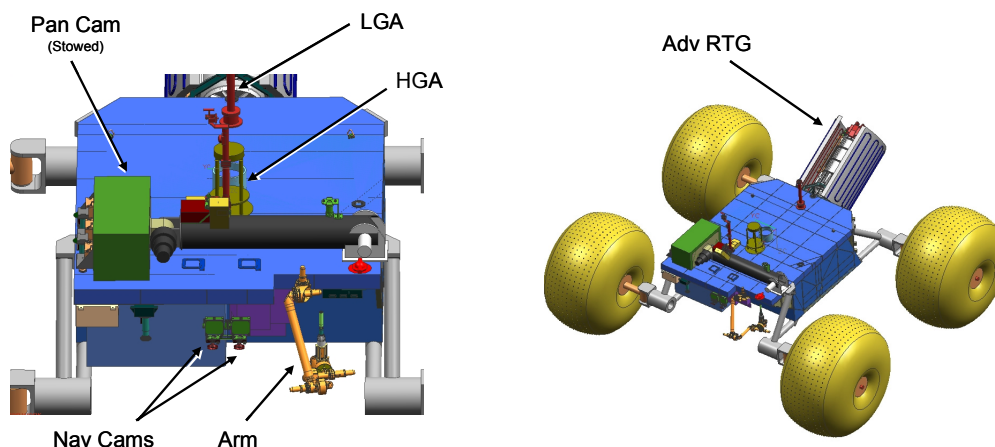


Figure 2.5.1-3. Conceptual Titan Rover WEB (Left) and Fully Deployed Rover (Right).

**2.5.1.3 Mission Architecture Overview and Assumptions**

The Titan rover mission described here has many elements that are common with the Mars Science Laboratory (MSL) mission, which is currently in design phase. In both cases the rover would be launched on a direct entry to its destination. In addition, during the cruise phase, the rover would be in an aeroshell. The rovers would be long lived on the surface, powered by an RPS, an MMRTG for MSL, and an ARPS for the Titan rover.

Table 2.5.1-1 shows six trajectories that were examined for the years between 2012 and 2015 using a Delta IV-Heavy LV. From these six opportunities the 2015 launch—utilizing an Earth-Jupiter (EJ) gravity assist—allowed for a launch mass of 5730 kg and an entry mass of about 4200 kg. For this study, the spacecraft would be launched to a  $C_3$  of  $25.7 \text{ km}^2/\text{s}^2$  and arrive at Titan after a 7.6-yr cruise time. The corresponding aeroshell entry speed at Titan would be 5.9 km/s, which is comparable to the 5.4 km/s entry velocity of the MER rovers. This entry velocity, therefore, does not require dedicated technology development for the thermal protection system of the aeroshell. Instead, it could use the same thermal control system (TCS) materials as used on previous Mars missions or on the Huygens probe to Titan.

The 2015 opportunity allows for the second highest entry mass with a reasonable cruise time. A 2012 launch opportunity with a Venus-Earth-Earth-Jupiter (VEEJ) gravity assist could deliver about 6800 kg at Titan entry, but programmatically it was considered too early (just two yrs following the second New Frontiers mission, and just before the third planed NF mission). Additionally, the trip time would be 8.7 yrs, over a year longer than the selected 2015 trajectory. Therefore, this launch opportunity would not allow time for the development of the advanced RPSs. Furthermore, the entry velocity to Titan’s atmosphere for a 2012 launch would be much higher (8.2 km/s), potentially requiring additional TCS development.

This study assumed the use of a 4.5-m aeroshell for the Titan rover (Fig. 2.5.1-4) and explored a range of different LVs including a Delta IV-Heavy, Delta IV 4040-12, and Atlas V 501. The Delta IV-Heavy had the largest delivered mass capability (~4200 kg), which was significantly more than required for the ~780-kg rover and entry system, 800-kg cruise stage, and 730 kg of propellant needed for the 706-m/s DSM. Both the Delta IV 4040-12 and Atlas V 501 could deliver the spacecraft to Titan with the inclusion of a downsized cruise stage and mass allocation for an adjusted DSM. The launch masses for these LV options are estimated at 1285 kg and 1455 kg, respectively. The mass breakdown for the rover/lander/aeroshell configuration at Titan is given in Section 2.5.1.12.

**Table 2.5.1-1. Representative Trajectory Trade Space**

Launch Date	Gravity Assists	Trip-time (yrs)	$C_3$ ( $\text{km}^2/\text{s}^2$ )	DLA (deg)	Launch Mass (kg)	DSM (m/s)	9.5 au Mass (kg)	Entry Speed (km/s)	Entry Mass (kg)	Payload Mass (kg)
2012	VEEJ	8.7	10.6	15	7730		7600	8.2	~6800	~1600
2013	E	7.0	47.9	-22	3500	650	2800	6.6	~2000	~480
2013	E	8.0	47.7	-22	3500	550	2900	5.5	~2100	~550
2013-14		6.1	105.2	10	500*		480	4.9	~280	~75
2015	EJ	7.6	25.7	-12	5730	706	5000	5.9	~4200	~1050
2016	J	6.9	80.8	15	1200*		1150	4.6	~950	~240

\*Atlas V-551 launch vehicle (Delta IV-Heavy incapable)

Alternatively, the larger delivered mass would allow for the delivery of multiple aeroshells to Titan, or a combination of an in situ explorer and an orbiter. Both of these options would increase the mission cost, moving it towards a large Flagship-class mission. As a baseline, the smaller mission concept was adopted with a lower category launch vehicle combined with a single aeroshell entry.

Throughout the study, the assumed 2015 launch date corresponded to a 2012 technology cut-off date. This class A/B mission warranted full redundancy, although the cost implication of this assumption was not assessed. The full mission duration was assumed at 10.6 yrs, which includes the 7.6-yr cruise phase and the 3-yr surface operations.

After arriving at Titan, the rover would enter the atmosphere stowed inside an aeroshell on a unpowered pallet lander that would include crushable materials to absorb landing shocks. The aeroshell (Fig. 2.5.1-4) would be used to slow down the entry, followed by a Viking-style parachute landing. This aeroshell was not designed in detail. Instead, it was assumed that it would account for 35% of the entry mass (Hall, 2005).

The rover would make a hard landing atop a rectangular lander platform  $\sim 1.5 \text{ m} \times 2.0 \text{ m}$  in size. Based on the aeroshell and parachute configuration the velocity at landing would be 6 m/s. To withstand the impact, the pallet lander would need to be approximately 2 cm thick and of crushable material, allowing the mission to stay within the 40g acceleration/deceleration load tolerance of the ARPS.

The Titan rover uses an MSL-based chassis and electronics layout with a mast-mounted Pan Cam, rear-mounted RPS, and forward-mounted robotic arm with a sample gathering drill. Once landed, the rover would deploy its inflatable wheels and perform initial system checks prior to beginning its 3-yr surface mission. This wheel deployment process is shown in Figure 2.5.1-5. The four 1.5-m diameter inflatable wheels offer the Titan rover advantages in traversing the surface of Titan not available to the smaller, rigid wheels used on MER and MSL. Rather than a sandy surface like Mars, Titan could potentially have a gummy, organic surface that could bog down small wheels. The large inflatable wheels also potentially offer the capability to float on the surface of liquid methane if needed.

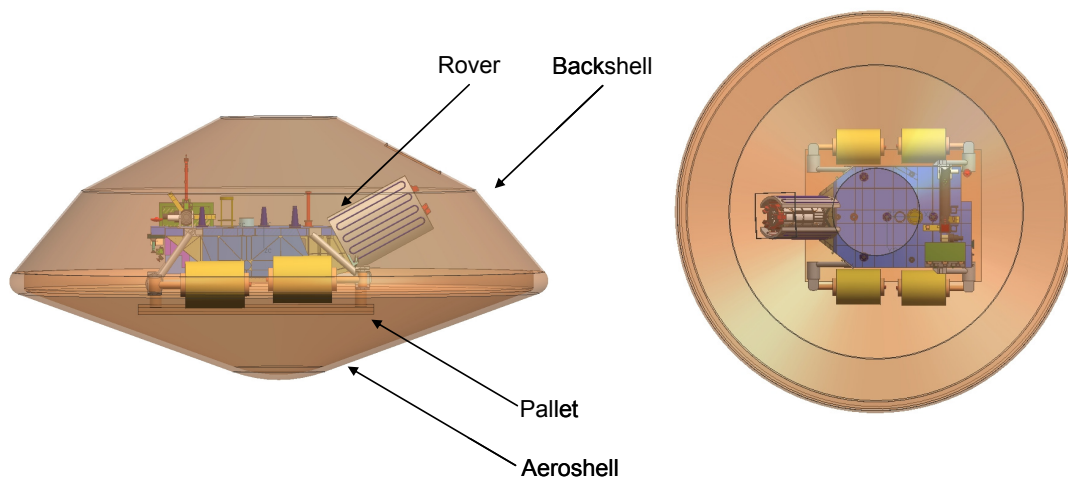


**Figure 2.5.1-4.** Titan Rover Concept Stowed Inside a 4.5-m Viking-Type Aeroshell.

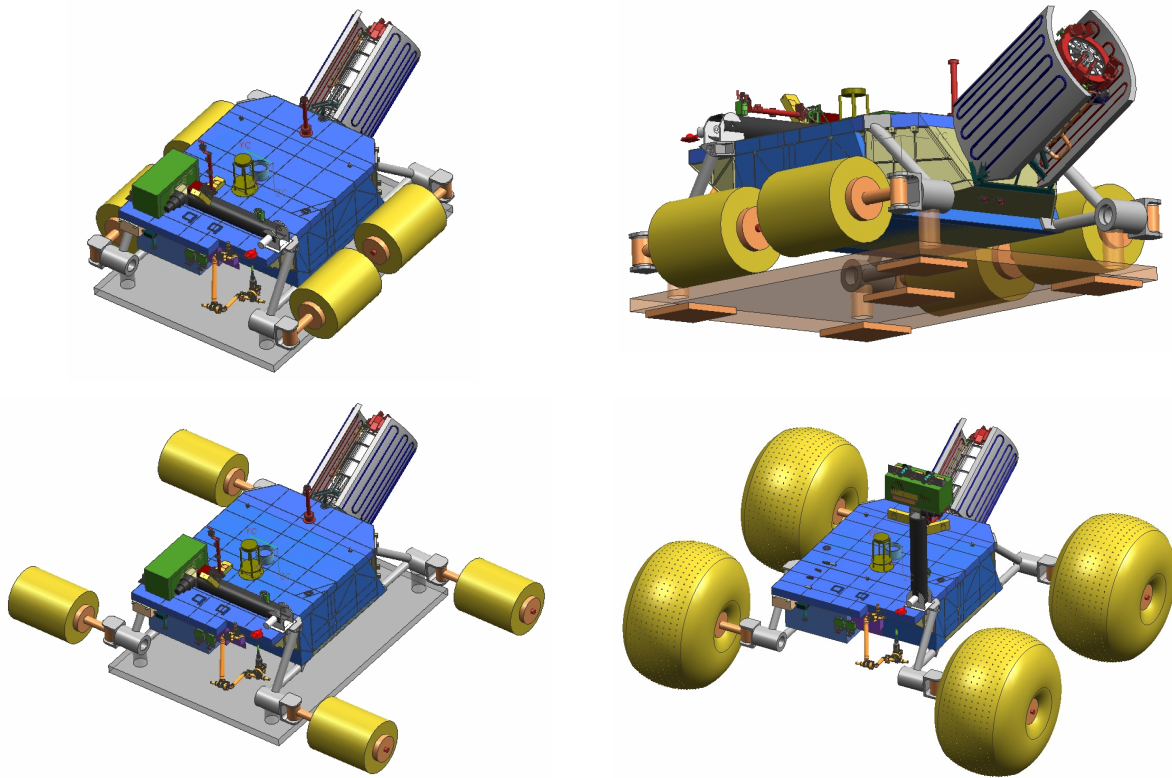


**Figure 2.5.1-5.** Deployment of the Conceptual Titan Rover from Stowed Configuration (Top-Left and Top-Right) through Wheel Deployment (Bottom-Left) to Inflated Wheels and Deployed Mast (Bottom-Right).

The Titan rover would receive electric and thermal power from its ARPS. While the mission baselines the use of an advanced RTG, other ARPS options could potentially be used.

Similar to MSL, the Titan rover would view its world through the use of its MER-styled Navigation Cameras (Nav Cams) and Hazard Cameras (Hazcams). The Nav Cam would be mounted on the Pan Cam mast, providing them 2 DOF allowing them to identify obstacles such as trenches that could trap or hamper the rover on its traverse. Using information gathered from its cameras, the rover would autonomously navigate hazards while driving, greatly enhancing its ability to travel. The Titan rover could travel at a rate of up to 150 m/hr for up to 5 hrs/day under ideal surface conditions. This would allow the rover to cover a considerable amount of ground in search of scientific targets.

The ACS would provide control and knowledge during the traverse. The direction heading would be controlled within  $2^\circ$  of commanded trajectory; the heading knowledge to less than  $1^\circ$ ; knowledge of absolute position on the surface to within 5 km; and knowledge of relative position to within 10 meters. The DTE communication would require HGA-pointing control of the mechanical boresight within  $1^\circ$ , allowing for post-reconstructed position knowledge using Earth resources. The HGA is two-axis articulated with accuracy able to meet the pointing requirement of  $1^\circ$  of control and  $0.5^\circ$  of knowledge to communicate directly back to Earth. Earth's position would be determined from the position of the Sun. The Pan Cam and Skycam would be used to measure the direction of the Sun within  $0.5^\circ$ , allowing the telecom system to meet its pointing requirements.

#### **2.5.1.4 Power Source Trade Study**

Alternative power sources were looked at for powering the Titan rover concept, including solar power generation, batteries, and fuel cells. Due to the length of the surface mission (3 yrs), the use of fuel cells would be impractical due to the mass of the fuel itself. Similarly, an all-battery design could not last long enough on the surface to meet the 3-yr requirement. As the mission concept is to land in the polar regions to allow a nearly constant view of the Sun, solar power may at first seem to be a feasible option; however, at 9.5 AU, the Sun's solar insolation is only ~1% that in Earth orbit, without taking into account any loss due to Titan's clouds and thick obscuring atmosphere. Titan's extremely cold environment would require the use of LILT tolerant photovoltaic arrays. The LILT solar arrays on the European Space Agency's Rosetta spacecraft produce ~395 We for 64 m<sup>2</sup> at 5.25 AU. Assuming the same power efficiency for the Titan rover concept, ~45 m<sup>2</sup> of solar arrays would be required to generate the same power level as just one advanced RTG. In addition, a solar-powered rover would need resistance heaters for its thermal management system, requiring an array much larger than this. Furthermore, to power the spacecraft during cruise, a second solar array almost as large as the first would be needed in addition to the array on the rover. The mass of these two large arrays, combined with the structural support, gimbals, and associated equipment to allow the concept to maneuver with the array without blocking the telecom system would be prohibitively massive and complex compared to the simple and efficient configuration with a single advanced RTG. Consequently, the baseline configuration assumes an advanced RTG.

#### **2.5.1.5 Advanced RPS Characteristics**

The Titan rover concept is based on an MSL-styled chassis with the RPS mounted on the back of the rover, opposite the Pan Cam. The advanced RTG produces 112 We BOM degrading over time at an approximate rate of ~1.6% a yr due to natural decay of the <sup>238</sup>Pu and the degradation of the thermocouples. This reduces the RPS output to ~93 We at EOM after 10.6 yrs. This mission duration is within the 14-yr life span of an MMRTG, and it is assumed that the advanced RTG would have similar longevity. The rover would land on the surface using parachutes, requiring crushable material to lower the deceleration loads down to the 40-g limit for the advanced RTG. The ~9% conversion efficiency results in only a small portion of the 1250 Wth (BOM)/1054 Wth (EOM) being converted to electrical power. A portion of this heat would be routed to the rover to warm its electronics using a heatpipe system. The remainder of the thermal power would be released to the environment through the advanced RTG housing. On Titan, the RTG would benefit from the extremely cold temperatures and convective atmosphere, eliminating the need for radiator fins (the RTG housing has enough surface area in itself to not require fins). However, the advanced RTG would require additional active cooling while in cruise to remove the heat from the advanced RTG within the aeroshell. Assuming an auxiliary coolant loop like that of the MMRTG, the cruise heat rejection system would be connected to the advanced RTG during flight and discarded before the rover lands.

#### **2.5.1.6 Science Instruments**

The Titan rover described in this mission study would carry a suite of instruments for determining surface composition. The environmental and engineering instruments (radiation monitor, acoustic monitor, meteorology package) are relatively simple and are not described here in detail. The meteorology package directly addresses science objectives 3 and 5 (Section 2.5.1.1).

The Pan Cam is becoming a standard instrument on surface-mission designs; its heritage from the MER mission. This instrument directly addresses the fourth science objective of this mission, to describe the morphology of Titan's surface. In addition, Pan Cam imaging would provide

needed context for interpreting all of the compositional measurements obtained. The Pan Cam would stand atop a 1.5-m tall mast that would fold against the deck of the rover. In addition to the stereo cameras, the Pan Cam unit mounts two Navcams and a fisheye camera (Skycam) pointed to the sky. The Skycam would allow the rover to gather detailed information on its position and orientation.

Obtaining samples from the surface and from immediately beneath the surface would add an extra dimension to the compositional measurements. The ultrasonic drill coring system (UDCS) would enhance the measurements addressing science objectives 1, 2, and 3. The corer is mounted on the robotic arm in a retractable pod. The arm would position the corer against targets to be sampled. Samples collected with the corer would be placed in a rotating sample carousel. From the carousel the samples could be transferred to the “composition” instruments for analysis. The mechanism is shown in Figure 2.5.1-6.

The “compositional analysis” instruments obtain complementary information on the samples evaluated. The Raman spectrometer nondestructively determines molecular compositions of ices, minerals, and some organics. The laser induced breakdown spectrometer ablates the surface of a sample, generating short-lived plasma, whose emissions constrain the elemental composition of the sample. The GCMS would characterize organics more precisely than is possible with Raman and LIBS, and is particularly valuable for detecting the most volatile species. These instruments address science objectives 1, 2, and 3 for the mission.

Finally, the addition of a sampling microscope would greatly aid in the categorization of the physical properties of the surface materials selected for analysis. By resolving textures, colors, and crystallinity of samples this instrument would address science objectives 1, 2, 3, and to some extent even 4 and 5. A summary of the science payload and instrument descriptions for the proposed titan lander mission is given in Table 2.5.1-2.

**2.5.1.7 Data**

Information onboard the rover would be handled by a dual-string CDS. Data would be stored in flash memory until downlinked DTE through the HGA during the 2 hrs of daily telecom contact. The data rate and volume information is included in Table 2.5.1-3. Compression of the data to be

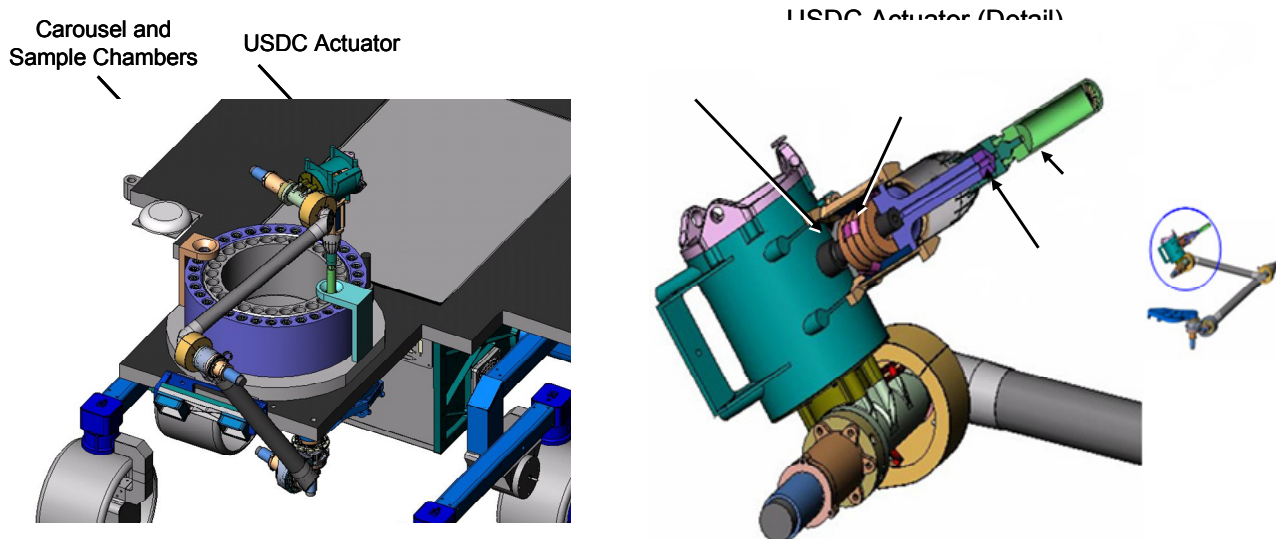


**Figure 2.5.1-6.** Conceptual Titan Rover Arm and Sample Collection Mechanism.

Table 2.5.1-2. Titan Rover Science Payload and Instrument Descriptions

Instrument Name	Purpose	Science Objectives Addressed	Heritage
1. Gas Chromatograph-Mass Spectrometer (GCMS)	Obtain composition of surface materials, particularly organic species, to understand surface chemical processes.	Objectives 1 and 2: To determine the composition of Titan’s surface materials, and to characterize the organic chemistry taking place at Titan’s surface	Huygens
2. Raman Spectrometer (Raman)	Obtain mineralogical composition of inorganic surface materials plus some organics.	Objectives 1 and 2: To determine the composition of Titan’s surface materials, and to characterize the organic chemistry taking place at Titan’s surface	New
3. Laser-Induced Breakdown Spectrometer (LIBS)	Obtain elemental composition of surface materials.	Objectives 1 and 2: To determine the composition of Titan’s surface materials, and to characterize the organic chemistry taking place at Titan’s surface	MSL
4. Panoramic Camera Imaging System (Pan Cam)	Obtain near- and far-field images of Titan’s surface.	Objective 4: To describe the morphology of Titan’s surface; also indispensable for identifying the sources of the samples analyzed by the GCMS, RAMAN, LIBS, UDCS, and microscope.	MER
5. Ultrasonic Drill Coring System (UDCS)	Obtain samples from beneath the uppermost surface layer.	Contributes to Objectives 1 and 2, determining composition of surface materials and characterizing organic chemistry, by adding the “depth dimension” to the datasets.	New
6. Sampling Microscope	Obtain information on texture, color, and crystallinity of materials selected for analysis.	Objectives 1 and 2: To determine the composition of Titan’s surface materials, and to characterize the organic chemistry taking place at Titan’s surface	MSL
7. Meteorology Package	Obtain in situ data on atmospheric pressure, temperature, and winds.	Objective 5: To describe the surface meteorology of Titan; and Objective 3: to describe the interactions between the surface materials and the atmosphere of Titan.	Pathfinder MER
8. Acoustic Monitoring System	Record the distribution of ambient sound waves at Titan’s surface.	Objective 5: To describe the surface meteorology of Titan; and Objective 3: to describe the interactions between the surface materials and the atmosphere of Titan.	New
9. Radiation Monitor	Measure the local radiation environment.	Objective 5: To describe the surface meteorology of Titan; and Objective 3: to describe the interactions between the surface materials and the atmosphere of Titan.	New

transferred would reduce the total data volume that has to be sent to Earth. The scientific instruments would downlink an average of 28.8 Mb/day in total after compression.

Each CDS string contains an advanced power PC computer and 16 Gb of flash memory for storage of mission-critical and scientific information. The electronics used in the CDS have a minimum radiation tolerance of 50 krad with an RDF of 2 to meet the mission’s radiation environment.

Table 2.5.1-3. Titan Rover Concept Data Rates

Instrument	Data Rate/Volume
Gas Chromatograph Mas Spectrometer	1 Mb/analysis
Raman Spectrometer	17 b/spectra (raw), 50 Raman spectra/hr
Laser-Induced Breakdown Spectroscopy	30 kb/spectra
Panoramic Camera	50.4 Mb/frame (raw), 12 frames for full panorama
Sampling Camera/ Microscope	8 Mb/frame
Meteorology Package	57.4 kb/day
Acoustic Monitor	100 kb/day
Radiation Monitor	10 kb/day

2.5.1.8 Communications

The telecom system for the Titan rover concept is shown in Figure 2.5.1-7. The Titan rover would communicate back to Earth using 8.4 GHz X-band with a 0.5-m diameter 2-axis gimballed HGA. The mission assumes that the spacecraft would be communicating to an 180 × 12-m DSN antenna array. During the mission, the rover would communicate with Earth directly using the HGA for 2 hrs/day. The requirement for DTE communications plays a critical driving role in choosing a landing site, as only the poles would allow for daily communication with Earth. From the polar regions on Titan, Earth would stay 20°–25° above the horizon for the entire 8-hr telecom period. The HGA requires control of the mechanical boresight within 1°. Two omnidirectional LGAs are carried as backup to the HGA. The two LGAs are located on opposite sides of the rover’s deck. The LGAs would be pointed 25° above the horizon to ensure that Earth falls within ~10° of the boresight of one LGA (assuming the rover is rotated appropriately). If communication using the HGA is lost during the mission, the rover could rotate itself until Earth falls into the boresight of one of its LGAs. At Saturn, Earth appears very close to the Sun, allowing the rover to use the Sun as a target for orienting itself towards Earth in an emergency scenario.

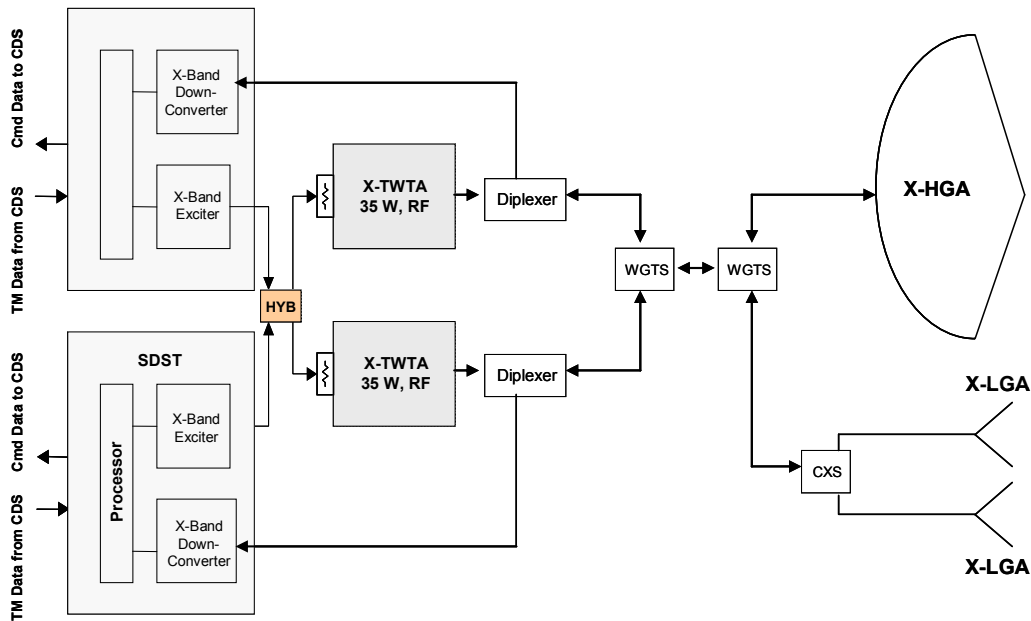


Figure 2.5.1-7. Titan Rover Concept Telecom Block Diagram

### 2.5.1.9 Thermal

To maintain system operating temperatures, the Titan rover would use passive and active TCS throughout its mission. To reduce loads on the electrical power system, no electric heaters are used in the design. The rover would satisfy its thermal needs using a combination of RPS heat, radioisotope heater units, and thermal insulation. The TCS of the Titan rover concept is similar to that used on Cassini. A portion of the heat generated by the RPS would be collected and transferred to electronic components using ammonia heatpipes. A second set of variable conduction heatpipes would be used to closely control the heat flow to specific components in the spacecraft, such as the telecom transmitter. Flight electronics are contained within insulated WEBs to keep in the heat transferred from the RPS.

The advanced RTG used in the baseline design produces 1138 Wth BOM and 1054 Wth EOM of thermal power after electrical conversion. Due to the heat transfer environment, only the TPV option would need radiator fins on Titan; the other ARPS designs could reject the heat through their casings alone. During cruise, the aeroshell would trap in the heat generated by the RPS requiring the TCS to pump out the thermal energy. As the thermal environment on the surface of Titan allows for better heat transfer than deep space, the RPS would require a secondary radiator set to tie into its auxiliary cooling tube to reject the excess heat while in cruise. To protect the spacecraft from the heat generated by the aerocapture maneuver in Titan's atmosphere, the spacecraft would carry a heat-shielded aeroshell. During the aerocapture maneuver, PCM would be carried to store the heat of the RPS. This PCM would be ejected with the aeroshell after entry into Titan's atmosphere.

Thirty RHUs would be carried on the rover to provide spot heating for elements outside the heatpipe loop, such as the drive motors and arm actuators. This would reduce the amount of electrical power (for heaters) that would normally be required to maintain rover operating temperatures.

### 2.5.1.10 Mobility

The Titan rover would travel across the surface on its four large (1.5-m diameter) inflatable wheels. Each wheel would be constructed of PBO (polybenzoxazole)/Xylon and would carry a small electric pump to inflate it by pumping in the ambient atmospheric gas, which is mostly nitrogen. The rover would use a compliant suspension which, when combined with the compliance of the inflated wheels, would allow it to easily adapt to the terrain encountered. As Titan has only 1/7th Earth gravity, each wheel requires only ~5 W of power to operate, totaling ~20 W for the entire rover. During driving periods, the rover would traverse the surface at a maximum speed of 0.15 m/hr, covering up to 750 m each day. Over the course of the 3yr mission, the rover could cover over ~800 km under ideal conditions, although the actual distance would likely be less due to wheel slippage and other factors. To accomplish this rapid traverse, the Titan rover would use automated steering for hazard avoidance along pre-defined paths. After receiving a trajectory from mission controllers giving it the relative direction and distance of the traverse, the rover would progress along the trajectory using its hazard and navigation cameras to identify and avoid obstacles such as boulders and crevices. The rover's orientation could be gained at any moment using two sets of measurements: accelerometers would give the local-nadir measurement, and the Pan Cam or Skycam would measure the Sun angle.

Local landmarks would be located with the navigation cameras and monitored during short pauses taken at regular intervals to gather the rover's relative position. The relative position could also be gained using the IMU and wheel tachometers. After a traverse, the new absolute position would be determined using the Skycam and uploaded to Earth. Pan Cam and Navcam images would be pieced together during post-reconstruction of a traverse to generate a

contiguous pictorial map. Absolute position estimates taken over the course of the mission would be used to determine the map scale and locate the maps created with the rover’s cameras.

Many scientists believe that bodies of liquid methane may exist on Titan. With its large inflatable wheels, the Titan rover concept would be able to float on a liquid methane body if required. The rover’s weight on Titan would be ~527 N, which would displace 0.84 m<sup>3</sup> of liquid methane on Titan using <20% of the internal wheel volume. This could raise the possibility of purposely entering bodies of liquid to collect scientific samples.

**2.5.1.11 Power**

The Titan rover concept uses a hybrid RPS/battery power system to meet its electrical needs in a mass-efficient manner. The baseline configuration carries a single advanced RTG and a 12 A-hr rated Li-Ion battery. The advanced RTG would provide ~94 We of power EOM to the rover’s systems. This allows for charging the rover batteries when the power requirements drop below the level of the advanced RTG. The operational power modes for the rover are outlined in Table 2.5.1-4. The use of high-power/high-data rate science operations, telecom, and moving across the surface would drive the sizing of the battery and RPS requirements, with the high-rate science resulting in the largest power load of 146.7 We. The rover would use DSA/X2000 power electronics designs. Electrical systems on the rover would obtain power from an unregulated 28-V DC power bus.

The duty cycle would be driven by the constant power output of the advanced RTG. Figure 2.5.1-8 shows how that output of the advanced RTG compares to the power modes for the mission. Adding a second RTG unit to the system would enhance the science gathering capabilities of the mission by eliminating the need for long recharge times. It should be noted that even if the rover were capable of operating continuously, operating as such would be a tremendous strain on ground resources and personnel and would drive up cost. And although autonomous navigation using navigation and hazard cameras would improve the ability to operate in between telecom periods, taking more advantage of an extended duty cycle, it would potentially require significant technology investment.

**Table 2.5.1-4. Titan Rover Power Modes**

<b>Subsystem</b>	<b>Science Low (We) (1.55 hrs/day)</b>	<b>Science High (We) (3.1 hrs/day)</b>	<b>Telecom (We) (2 hrs/day)</b>	<b>Drive (We) (5.1 hrs/day)</b>	<b>Recharge (We) (12.25 hrs/day)</b>
ACS	10.6	11.6	7.8	49.8	
C&DH	6.5	6.5	6.5	6.5	6.5
Power	3.1	6.9	6.7	6.5	2.0
Structures & Mechanisms				20.0	
Thermal	18.7	18.7	18.7	18.7	18.7
Telecom	5.0	5.0	69.8	5.0	5.0
Instruments	7.0	64.2			
<b>Total—Current Best Estimate (CBE)</b>	<b>50.8</b>	<b>112.9</b>	<b>109.4</b>	<b>106.5</b>	<b>32.1</b>
Contingency	30%	30%	30%	30%	30%
<b>Total (CBE + Contingency)</b>	<b>66.1</b>	<b>146.7</b>	<b>142.3</b>	<b>138.4</b>	<b>41.8</b>

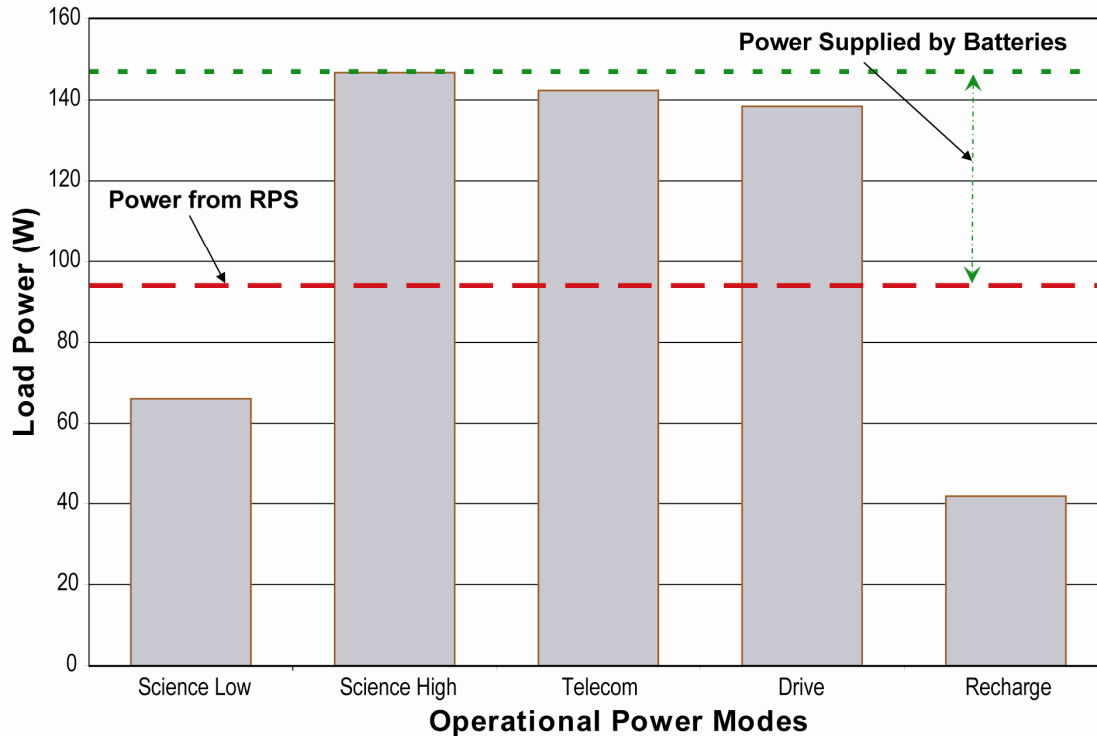


Figure 2.5.1-8. Titan Rover Concept Power Levels

2.5.1.12 Mass

The masses of the Titan rover concept and associated stages are shown in Table 2.5.1-5. The rover in its baseline configuration has a mass of ~376 kg with contingency. It was estimated that a total of 1455 kg could be launched to a  $C_3$  of  $25.7 \text{ km}^2/\text{s}^2$  using an Atlas 501 LV. The original mass for the cruise stage was based on the larger Delta IV-Heavy, and an estimate of 195 kg with contingency was made by scaling down the size for the smaller launch Atlas 501 vehicle. With a launch capability of 1455 kg, the Titan rover’s entry mass would leave ~677 kg available for the cruise stage, DSM, and LV contingency. Such a large launch margin would help accommodate any growth in the rover’s mass during development. Additional unallocated mass for the rover could be used for more science instruments or perhaps an additional advanced RTG unit to reduce charging times and yield more science.

Table 2.5.1-5. Titan Rover Concept Mass Breakdown

Subsystem	Mass, kg	Contingency %	CBE + Contingency, kg
<b>Rover Total</b>	<b>289.1</b>	<b>30%</b>	<b>375.9</b>
Instruments	38.0	30%	49.4
ACS	13.1	21%	15.9
CDS	3.0	30%	3.8
Power	35.2	30%	45.8
Structures	149.4	30%	194.2
Telecom	19.5	12%	21.7
Thermal	31.0	28%	39.7
<b>Landing Pallet</b>	<b>91.0</b>	<b>30%</b>	<b>130.0</b>
<b>Aeroshell</b>	<b>272.4</b>	<b>(35% of total mass)</b>	<b>272.4</b>
<b>Total Entry Mass</b>	<b>652.5</b>	<b>19%</b>	<b>778.3</b>

**2.5.1.13 Radiation**

Saturn’s radiation belts have only a fraction of the intensity of those surrounding Jupiter, and the radiation levels on the surface of Titan are not significant contributors to the TID for the mission. The chosen Earth-Jupiter gravity assist, however, would include a Jupiter flyby with a TID below 20 krad behind 100 mils of aluminum with an RDF of 1. In addition to environmental sources, the rover would accrue dose from its advanced RTG. MSL is expected to receive ~2 krad of TID from one MMRTG with an RDF of 2 over the course of the cruise to Mars and a 1000-sol surface mission (Jun, 2002). The advanced RTG has 63% the <sup>238</sup>Pu as an MMRTG, producing a correspondingly lower dose rate. For the 10.6-yr mission of the Titan rover this adds up to a TID of ~3.6 krad with a RDF of 2, nearly twice that of MSL. The total TID including environmental sources would be less than ~44 krad with an RDF of 2, which would be manageable with current electronics hardness levels. To accommodate the dose, the electronics onboard the rover would be designed to be radiation tolerant to 50 krads with an RDF of 2.

**2.5.1.14 Alternate RPS Power Systems**

The baseline configuration of the Titan rover uses a single advanced RTG as its power source; however, the mission could potentially be accomplished with the advanced Stirling, Brayton, or TPV RPSs with an associated increase in power system mass and/or integration complexity. As shown in Table 2.5.1-6, there is a moderate mass difference between the four advanced RPS options considered for the present mission. Figure 2.5.1-9 shows conceptual illustrations of how the Titan rover would be integrated with the advanced Stirling, Brayton, and TPV generators.

The TPV option is the lightest configuration (not accounting for the cruise-phase radiators), with power output comparable to that of the advanced RTG (110 We BOM) and ~90 We at EOM. On the surface of Titan, the cold, dense atmosphere would reduce the required size of the TPV fins to about 20% (~0.5 m<sup>2</sup>) of that needed during the deep space portion of the mission. The primary disadvantage of TPV for the Titan rover concept is the large fin area required during the cruise phase (~2.5 m<sup>2</sup>), potentially complicating spacecraft and launch vehicle integration. Additionally, the large size of the cruise-phase TPV radiator would increase the mass of the spacecraft, thus decreasing the effective specific power of the TPV.

The advanced Stirling generator is another viable option. A total of three advanced Stirling units would be required to meet the rover’s power needs and the requirement for one spare unit per *JPL Design Principles* (Yarnell, 2003). This would result in a heavier power system compared with those of the advanced RTG, Brayton, and TPV; however, more power would be available to expand the duty cycle of the rover beyond what a single 110-We ARPS system could support.

**Table 2.5.1-6. ARPS System Mass Comparison for the Titan Rover Mission Concept\***

	Advanced RTG (kg) 1 unit	TPV (kg) 1 unit	Advanced Stirling (kg) 3 units	Brayton (kg) 1 unit
Total Advanced RTG System Mass	25.5	15.9	41.1	28.9
Difference from Advanced RTG Baseline		-9.6	15.6	3.5
*Mass values are without contingency and do not reflect system ripple effects.				

Table 2.5.1-7. ARPS Radiator Sizes for the Conceptual Titan Rover

Operating Region	Required Radiator Area (m <sup>2</sup> )			
	Advanced RTG	TPV	Advanced Stirling	Brayton
Deep Space	1.4	2.5	0.21	0.63
Titan Surface	0.4	0.5	0.07	0.22

Another option would be to use a single Brayton RPS. As this unit is assumed to be internally redundant with two turbo-alternators each operating at 50% capacity (see Section 3), a separate spare unit would not be required for the mission. That is, failure of one of the two turbo-alternators would still allow the rover to operate at full capacity, since the functioning turbo-alternator (previously operating at only 50% capacity) would be spun up to full capacity. The possible torque on the system from the unbalanced Brayton would not be expected to create problems for the rover. Conceptual illustrations of the Titan rover using the advanced Stirling, Brayton, and TPV RPSs are shown in Figure 2.5.1-9. Using the advanced RTG for this mission would save ~20 kg of mass compared with the standard MMRTG, and ~43 kg relative to two SRGs (one prime and one redundant). Table 2.5.1-8 shows a comparison on 10 different categories for the four ARPS options for the Titan rover mission concept.

The result of the assessment is that the advanced RTG is the overall choice for the Titan rover mission, though the advanced Stirling, Brayton, and TPV are potentially viable options with an associated increase in mass, size, and/or integration complexity. The Brayton would be the second choice, followed by the advanced Stirling. The TPV would be the least-preferred option due to its lack of heritage and large radiator size.

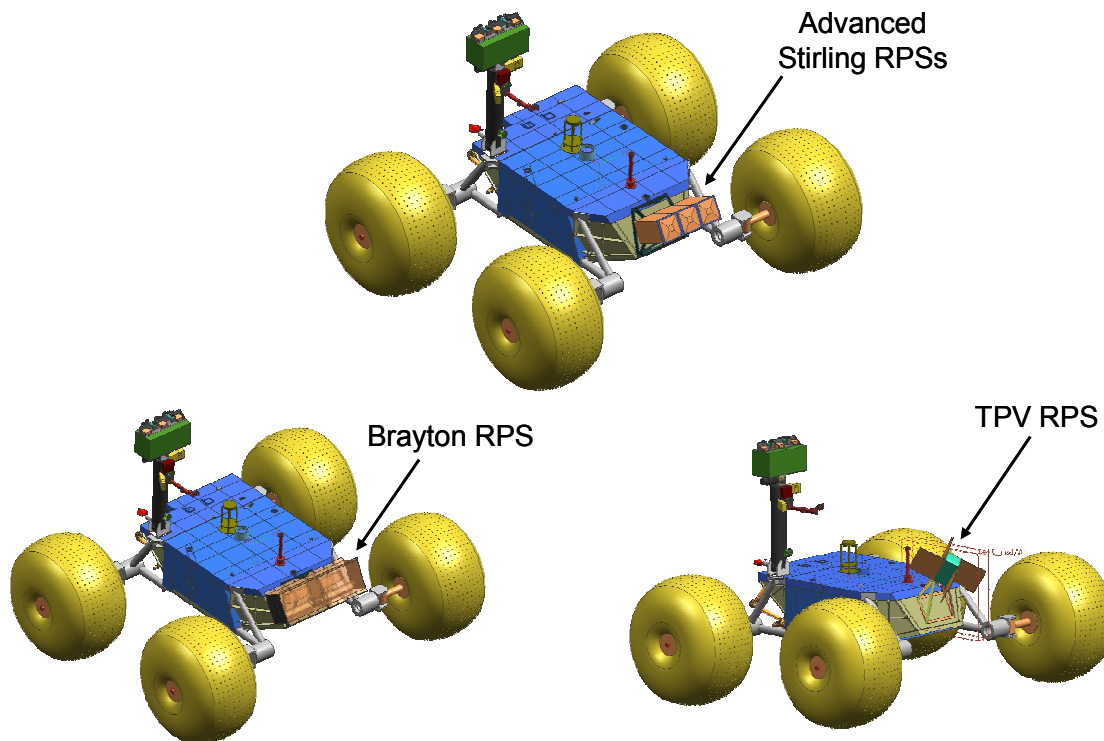


Figure 2.5.1-9. Conceptual Illustrations of the Titan Rover Using Advanced Stirling, Brayton, and TPV RPSs.

Table 2.5.1-8. Comparison of ARPS Systems for the Titan Rover Concept

Criteria	Adv RTG	Adv Stirling	TPV	Brayton	Rationale
Power	Green	Yellow	Green	Green	The lower power output of the advanced Stirling requires two units (plus one spare) to meet the rover's power needs. The advanced RTG, Brayton, and TPV require only one RPS unit.
Mass	Green	Yellow	Green	Yellow	The advanced RTG and TPV have the lowest overall relative mass compared with the Brayton and advanced Stirling, the latter of which is the heaviest configuration due to its need for three RPS units.
Volume	Green	Green	Yellow	Green	Due to the cold, convective Titan atmosphere, only the TPV option would require radiator fins. During cruise phase, a second set of fins would be required to release heat into space. The TPV has the large size fins of all the RPS systems considered in this study.
Heritage	Green	Yellow	Red	Red	The advanced RTG shares significant design heritage with the MMRTG (assumed to have been flight proven by the time of this mission), and would utilize many of its subsystems and components, thus making it the preferred option from a heritage perspective. The advanced Stirling has some heritage with terrestrial-based systems of similar design. The remaining two ARPS systems have little, if any, relevant heritage.
Integration	Green	Green	Yellow	Green	All RPS designs would require two sets of radiators for cruise and for surface operations. The TPV's radiators would be the largest, potentially complicating spacecraft accommodation and integration.
Environmental Emissions	Green	Green	Green	Green	EMI fields and vibration are not expected to be an issue in this design due to lack of fields or wave experiments and the nature of rover mission.
Robustness	Green	Yellow	Green	Green	The advanced RTG and TPV use cross-strapped series/parallel electrical connections such that an individual uncouple or cell failure does not take down the entire system. The Brayton uses a fully redundant architecture to reduce single-point failures. The advanced Stirling is single string, requiring an additional Stirling unit for redundancy.
RPS Complexity	Green	Yellow	Green	Yellow	The advanced RTG and TPV are fundamentally simpler systems compared with the advanced Stirling and Brayton due to their passive operation, lack of moving parts, and lack of active electronics or sophisticated controllers.
Power Degradation Rate	Yellow	Green	Yellow	Green	The advanced RTG and TPV offer higher power degradation rates (1.6%/yr and 2%/yr respectively) compared with dynamic systems (~0.8%/yr).
<sup>238</sup> Pu Usage	Yellow	Green	Yellow	Green	The higher efficiency of dynamic conversion systems allows for the use of less <sup>238</sup> Pu in the advanced Stirling and Brayton RPSs. This could be a driver were fuel availability an issue.
ARPS Ranking for the Titan Rover Concept	Green	Yellow	Yellow	Green	The advanced RTG offers the best option from a robustness, heritage, and inherent reliability standpoint, and thus was chosen as the mission baseline.

**2.5.1.15 Summary and Conclusions**

A concept study was performed to demonstrate the feasibility of Titan rover mission using ARPS power systems. The surface-mission duration would be at least 3 yrs. The rover would be based on the MSL design, and would use four 1.5-m diameter inflatable wheels to enable it to traverse the surface of Titan, providing superior mobility than smaller ridged wheels. The rover concept baselines a single advanced RTG providing ~94 We EOM and a 12 A-hr Li-Ion battery to meet its energy needs. The Titan rover concept could also use three advanced Stirling generators, one Brayton generator, or one TPV generator with an increase in system mass and/or complexity. The rover in its baseline configuration has a mass of 376 kg with a 30% contingency. The design is not optimized; therefore, the mass and power values are only first-order approximation.

Due to the high-level nature of the study, there are several issues that need to be addressed in future studies. Detailed designs for the aeroshell, pallet lander, cruise stage, and DSM stage have not been developed, and better estimates on their masses would be required before a more accurate determination of mass margins could be calculated. Additionally, NASA's Planetary Protection requirements were not explicitly considered in this concept study and need to be addressed in future detailed studies.

## 2.5.2 Venus Rover Mission

This concept study illustrates how a long-lived Venus rover mission could be enabled by a novel application of advanced RPS technology. General Purpose Heat Source (GPHS) modules would be employed to drive an advanced thermoacoustic Stirling heat engine (TASHE), pulse tube cooler, and linear alternator that provides electric power and cooling for the rover. TASHE is a system for converting high-temperature heat into acoustic power, which then drives a pair of flexure-bearing linear alternators to produce electric power. Heat would be provided by GPHS modules and the “cold” side would be furnished by the Venus ambient atmosphere (460°C). For this Venus rover mission, the TASHE would perform two important functions: generating electric power and cooling the rover electronics by removing parasitic heat from the electronics and ambient environment.

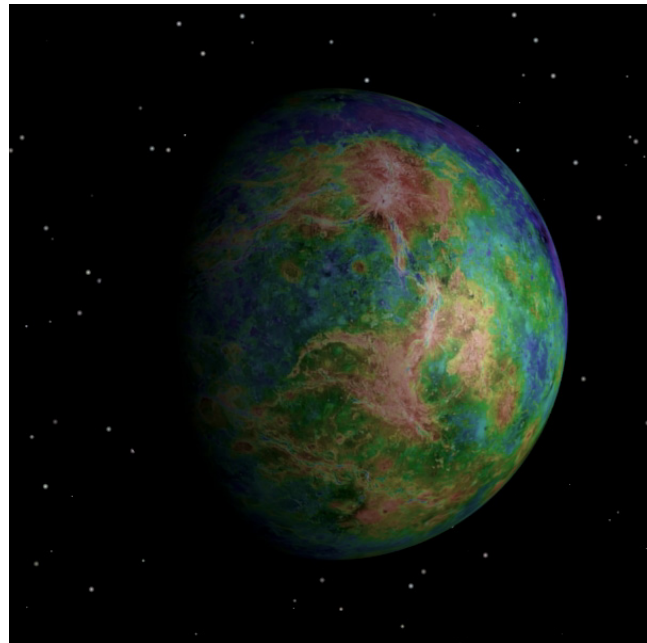


**Figure 2.5.2-1.** Venus with False Coloring to Highlight Surface Features

While working TASHE systems have operated in various laboratories at the kilowatt level, Northrop Grumman Space and Technology (NGST) and Los Alamos National Laboratory (LANL) have performed much work to scale the TASHE down to the 100-We power range (Tward, 2003; Petach, 2004a; Backhaus, 2003).

A small team of specialists worked in a collaborative engineering environment to examine this mission concept, which focused on determining the feasibility of using the TASHE system in the hostile Venus environment. The ~680-kg rover described here would provide a mobile platform for science measurements on the Venus surface. Previous missions to the Venus surface survived only for hours, but this rover concept is designed for a surface lifetime of 60 days, with a potential of operating well beyond that. A suite of science instruments is described that would collect data on atmospheric and surface composition, surface stratigraphy, and subsurface structure. An Earth-Venus-Venus trajectory would be used to deliver the rover to a low entry angle allowing an inflated ballute to provide a low-acceleration and low-heat descent to the surface. All rover systems would be housed in a pressure vessel in vacuum with the internal temperature maintained by the TASHE at under 50°C. No externally deployed or articulated components would be used and penetrations through the pressure vessel would be minimized. S-band communications would minimize atmospheric attenuation for the direct to Earth return of science data.

### 2.5.2.1 Science Goals

Although Venus and Earth are similar in size, and presumably similar in their primordial composition, the evolutionary pathways of the two planets have been strongly divergent. Venus today possesses a dense atmosphere with strong greenhouse warming, producing surface temperatures of approximately 460°C. For this reason, Venus lacks a hydrosphere and biosphere. From Magellan mission radar observations, it is known that global resurfacing has occurred, and thus it has been concluded that the planet likely continues to be geologically active.

Potential science goals for future in situ exploration of Venus' surface would be to characterize the elemental and mineralogical composition of the surface; to understand the interaction of the surface with the atmosphere; to characterize the atmospheric composition, especially isotope ratios of key species; to characterize planetary volcanism, in terms of present activity, emissions to the atmosphere, and composition, including changes in composition with time; to characterize the surface meteorology (winds and pressure variability); and to characterize the surface geology and morphology at the landing site and in surrounding areas. These goals are consistent with those described by the Solar System Exploration Decadal Survey.

The high surface temperatures and caustic atmosphere pose strong challenges for surface missions. The Soviet Union launched a series of orbiters and landers, primarily in the 1970s, to address key science questions. The Venera landers typically survived for less than 1 hr on the surface. The Pioneer Venus mission was flown by the U.S. in 1978 and experienced comparably short lifetimes for its probes. Thus, survival in this harsh environment is one of the most important factors limiting science return.

Although not explored in this mission scenario, the potential for surface operations over an extended period (months to years) could yield uniquely important data that would contribute to a better understanding of the present state and the past evolution of Venus. For example, by landing in a location on the slope of one of Venus' highlands, and traversing to lower elevations, the rover might detect and measure both the unusual heavy-metal frosts that have been predicted to occur at higher levels, and also the compositional variability of the basaltic surface rocks as a function of elevation at a particular locality (Schaefer, 2004).

The goal of determining surface composition is addressed here by the inclusion of a Raman spectrometer system, and also by an X-ray fluorescence instrument. The goals of characterizing the atmospheric composition and the interactions of the surface and atmosphere are addressed by including a neutral mass spectrometer (NMS). The rover's imaging system would aid in characterizing the surface geology, stratigraphy, and geomorphology. Direct information on subsurface layering and structures would be obtained by the ground-penetrating radar system. Lastly the rover would include simple exterior sensors to monitor atmospheric pressure and wind speeds while on the surface.

#### **2.5.2.2 Mission Goals**

The primary goal of this study is to examine the feasibility of using the novel advanced RPS-driven Stirling thermoacoustic system to enable extended science operations in the extremely hostile surface environment of Venus. The mission concept entails landing a rover onto the Venus surface, conducting science measurements in different areas on the surface, and returning the science data to Earth. The study focused on developing a rover design to satisfy the science goals with the capability to operate for 60 days. This mission life influences several design parameters, including Earth elevation angle and the maximum communications range to Earth. No specific odometry requirement was defined for this concept study due to the uncertain surface topography and the likelihood of very rugged terrain. The thermal control system and electrical power systems were tailored to use the TASHE for vehicle power as well as cooling. A top-level mission design, science instrument package, telecommunications, and avionics systems were developed to help characterize the rover systems requirements.

2.5.2.3 Mission Architecture Overview and Assumptions

This mission concept (Table 2.5.2-1) would land a rover on the surface of Venus for conducting surface and atmospheric composition and surface geology studies from a mobile platform. The rover would survive on the surface using an advanced Stirling system for electric power and cooling. A large spherical ballute would be used during atmospheric entry to reduce heating and deceleration loads. The rover would communicate directly to Earth without any orbiting relay segment.

Table 2.5.2-1. Mission Overview for the Venus Rover Concept

Launch Date	November 2, 2013
Launch Vehicle	Delta IV-Heavy (4450-14)
Launch C <sub>3</sub>	13.31 km <sup>2</sup> /s <sup>2</sup>
Venus Flyby	March 29, 2014
Cruise Duration	20 months
Arrival Date	June 20, 2015
Entry & Descent	Direct with ballute
Surface Lifetime	60 days
Power Source	Advanced RPS, TASHE
Communications	Uplink: X-band Downlink: DTE, S-band
Surface Cooling	TASHE integrated cooler

The trajectory design is constrained by several important factors: Earth visibility, the need to land on the sunlit side for imaging and navigation, and the need for a low entry angle for compatibility with the ballute-based atmospheric entry. The landed rover must be able to communicate with Earth. Since this concept relies on DTE communication, this requires that the Earth be in view of the rover during entry and after landing. The Sun must also be in view, in order to perform visual science and navigation imaging, as well as allowing the rover to have improved knowledge of the Earth’s location for communication support. The entry ballute design requires a very shallow entry angle of  $-5^\circ$ . An Earth-Venus-Venus (EVV) trajectory was found that satisfies these requirements (Fig. 2.5.2-2). Extensive trajectory analysis was not performed; therefore, more optimized solutions are likely to be available.

EDL would utilize a large inflated ballute, which would minimize both the entry heating and deceleration loads (Fig. 2.5.2-3). The nominal 64-m diameter ballute would be deployed at an altitude of 140 km and at a speed of 11 km/s. The peak heating would be a very low 3.3 W/cm<sup>2</sup> and the peak deceleration would be  $\sim 34g$ . The ballute would be jettisoned at 94-km altitude,

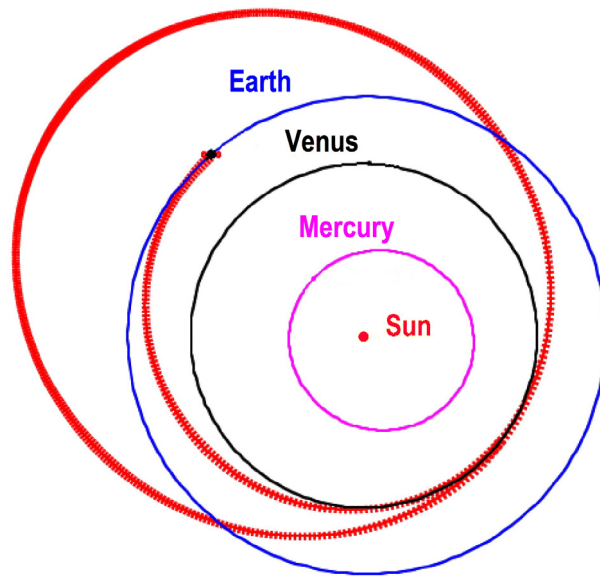


Figure 2.5.2-2. Earth-Venus-Venus Trajectory of the Venus Rover Mission Concept

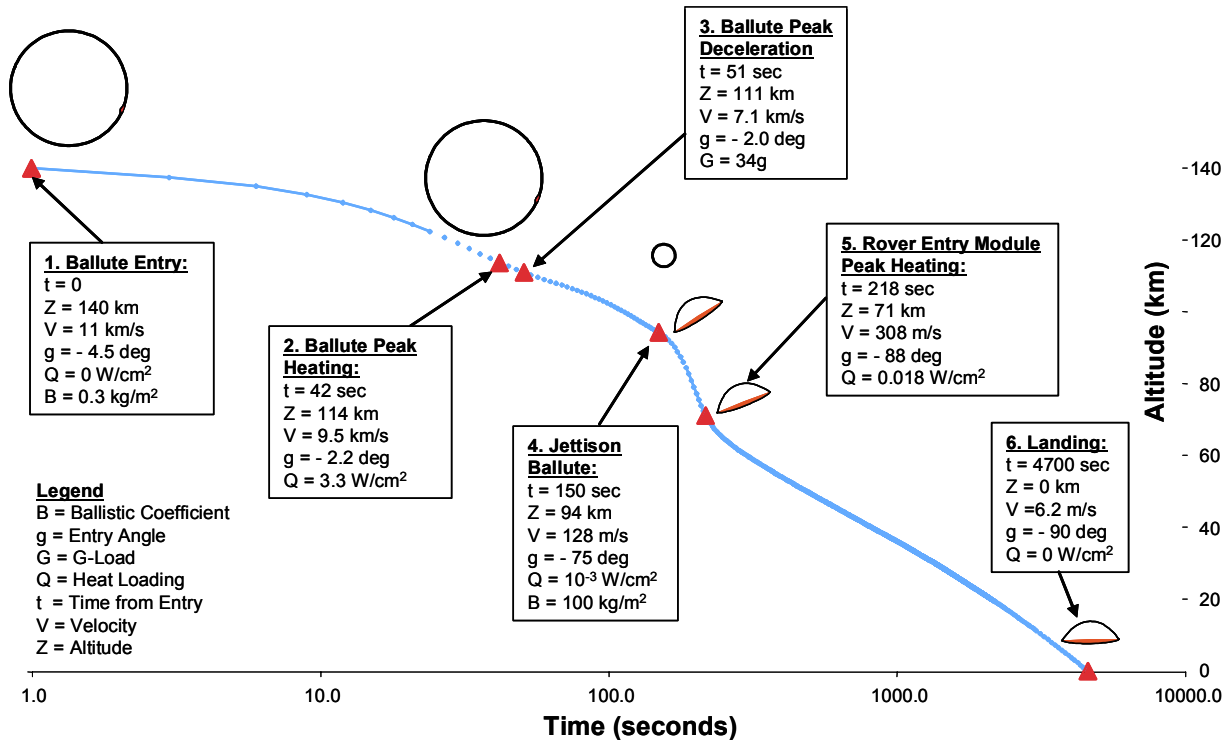


Figure 2.5.2-3. Venus Rover Concept Ballute Entry Sequence

where the rover would be released to drop slowly through the thick Venus atmosphere and land on the surface 76 min later. The rover landing would be cushioned by a platform of crushable material that absorbs the impact energy and reduces the impact acceleration.

After a 20-month cruise, the rover would land just as the Sun was rising, allowing 19 days of sunlit operations before the Sun would set. The Sun would rise again 78 Earth days later. Other trajectories are likely that would increase the initial period of sunlit operations with Earth visibility; however, study scope limitations prevented this optimization.

After landing, the rover would drive off its landing platform and begin in situ operations. The nominal drive scenario for every 24 hrs is to perform two 30-min drives and four 165-min data acquisition periods. During each day the data is returned to Earth using four 60-min communication sessions. The remainder of the time would be spent motionless while the batteries are recharged. Low-power science operations might be performed during this period, such as meteorology measurements.

The rover’s pressure vessel would be designed to minimize the parasitic heat associated with the surface area while providing sufficient wheel base for mobility. A cylindrical pressure vessel with spherical end-caps houses the electronics and instruments. The cylinder measures 1.5 m long and 0.5 m in diameter and would be constructed of 13.5-mm thick titanium.

Even though most of the rover systems include relatively mature technologies, several technology assumptions were made in developing this mission concept (Fig. 2.5.2-4). The following technologies were assumed to be available at TRL 6 by 2009 to support a 2013 launch date: the TASHE system and high-efficiency power alternator, high-temperature secondary batteries, high-temperature data and power cabling, high-temperature S-band antennas and RF

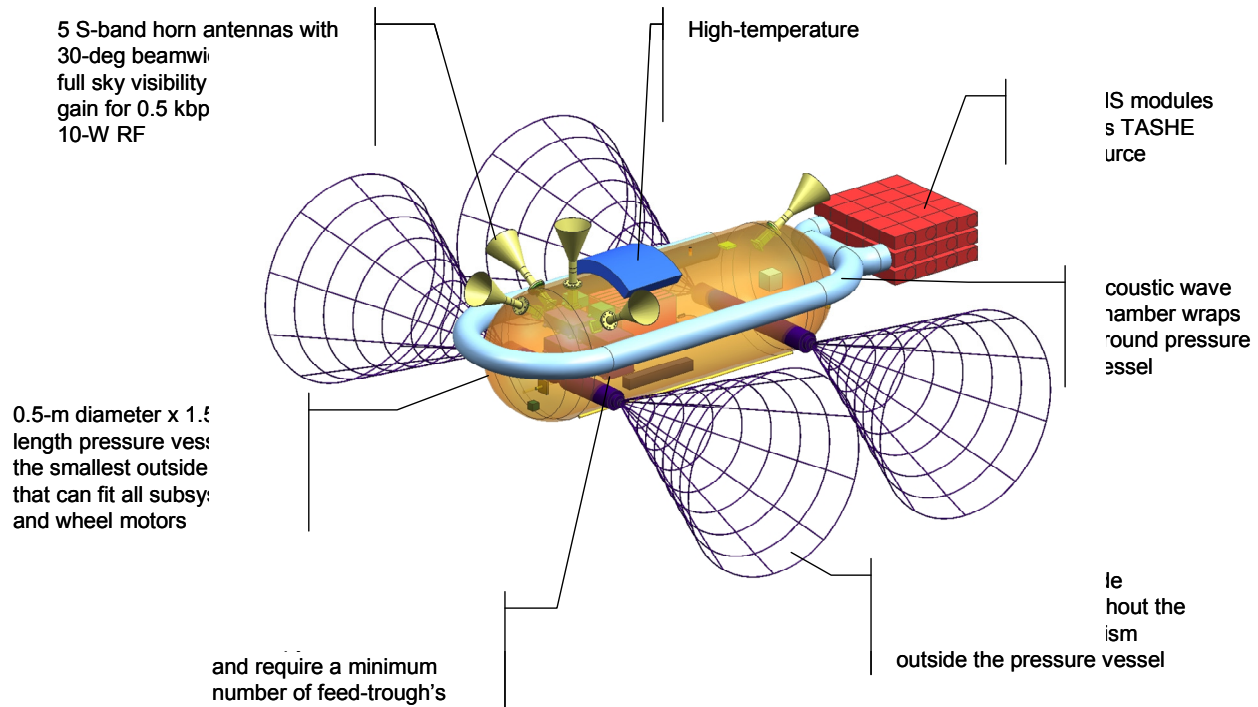


Figure 2.5.2-4. Conceptual Venus Rover Configuration

co-axial cabling, high-efficiency MLI, high-temperature window ports and feed-throughs for the pressure vessel, 1- $\mu\text{m}$  Sun sensor and optical fibers, and a high-temperature mobility system.

#### 2.5.2.4 Power Source Trade Study

The extreme temperature and pressure of Venus and the requirement for a long-duration surface mission limit the type of power system that can be used for this conceptual mission. Previous missions to the Venus surface have been powered by batteries with surface durations on the order of a few hrs. As the present mission duration requirement is 60 days, it is clear that battery power alone is insufficient for this concept. Solar arrays were likewise considered, but the caustic and high-temperature Venus atmosphere would rapidly degrade their performance, making them impractical for this application. Existing and next-generation RPSs such as the MMRTG and SRG are not designed for the intense pressure and temperature of the surface of Venus, and thus are not viable candidates for this mission. As a key mission requirement is the need for active cooling of rover subsystems, mission-specific dynamic RPS systems are a natural choice for such an application. Stirling and Brayton RPSs are two such systems that could be directly coupled to a cryocooler to efficiently generate both electrical power for the rover's subsystems and cooling to maintain steady-state temperatures within the rover pressure vessel. Such advanced RPS systems are considered enabling for this mission concept.

#### 2.5.2.5 Advanced RPS Characteristics

This rover mission concept uses an RPS in a novel way to survive on the surface of Venus. An assembly of GPHSs would be used as the heat source to drive a thermoacoustic Stirling heat engine and integrated PTR to produce both electric power and critical refrigeration. The TASHE provides that novel capability. A mission-specific Brayton RPS with integrated cryocooler was also considered, but had significantly lower conversion efficiency than the TASHE system, and thus was not pursued further in this study.

The TASHE incorporates a Stirling heat engine that produces an acoustic pressure wave to drive a piston in a linear alternator, which produces electricity (Tward, 2003). The thermoacoustic driver employs no moving parts to convert high-temperature heat into acoustic power. The TASHE is coupled with a vibrationally balanced flexure-bearing linear alternator to generate the electric power. NGST has demonstrated a system efficiency of 18% for a 50 We test unit and has developed a 100-We demonstration unit (Petach, 2004a). Additionally, the thermoacoustic power drives the PTR to provide critical cooling for this application. The 100-We TASHE unit in operation at NGST is shown in Figure 2.5.2-5.

The TASHE is composed of a closed-loop flow path filled with high-pressure helium (Petach, 2004a). The loop contains the regenerator, heat exchangers, and other ductwork necessary to force the helium gas in the regenerator to oscillate and execute a Stirling thermodynamic cycle when heat is applied (Petach, 2004b). The GPHS modules are placed in the gas loop and provide a 1200°C hot-end heat source. The cold-end heat exchanger is thermally coupled with the Venus atmosphere to provide a 500°C heat rejection temperature.



**Figure 2.5.2-5.** TASHE and Linear Alternator Operating at NGST (Tward, 2005)

To generate electric power, the oscillating gas flow impinges on an opposed pair of pistons in the linear alternator, which is derived from NGST's low-mass, flight-proven cryocooler compressors. Each half of the alternator contains a piston attached to a voice coil mounted on flexure springs. The flexures maintain a non-contacting, non-wearing, gas seal between the piston and the cylinder. The moving coil and piston are resonant with the thermoacoustic driver. Electrical power is produced by conversion of a fraction of the acoustic power using the piston and voice coil.

The TASHE system is mounted on the outside of the rover pressure vessel with the GPHS modules at the rear of the rover. Rover electronics are housed in the front of the pressure vessel to accommodate weight and balance requirements and gain distance from the ionizing radiation of the GPHS modules. The GPHS modules are packaged in an insulated housing with an integrated channel network for transferring heat from the GPHS modules to the helium gas. Sized for the 120-Hz resonant frequency, the resonator tube is 3.3-m long and is wrapped around the exterior of the rover pressure vessel. The mass of the components of the TASHE and cryocooler system was estimated to be ~133 kg, and was derived as follows: 20 kg for the Stirling engine and PTR, 85 kg for Pu fuel, 3 kg for the linear alternator, 20 kg for structure; and 5 kg for waste heat radiation panels and heat pipes.

### **2.5.2.6 Science Instruments**

The pressure vessel rover design presents challenges for science instrument selection and design. The optical designs must collect all imaging through small ports (there can be no external mast for a conventional panoramic camera). The navigation camera fields of view may be limited by these ports. Atmospheric sampling is proposed using a tiny inlet port that uses the high ambient

pressure to draw small samples into several collection containers. Surface materials sampling is even more difficult, and therefore was not included in this concept. Mineralogical composition measurements would be taken at a short distance through ports using a fiber optics Raman spectrometer. Significant new technology development would be required for any instrument operating outside the pressure vessel. Table 2.5.2-2 outlines mass and power estimates for the science instruments.

**Table 2.5.2-2. Baseline Science Instrument Summary for the Venus Rover Concept**

Science Instruments	Science Objective	Mass (kg)	Power (We)
Raman Spectrometer	Surface Composition	2.5	18
Neutral Mass Spectrometer	Atmospheric Composition	7	8
Navigation Cameras (4)	Surface Geology, Roving	10	10
IR Sun Sensor	Engineering	1	3
Ground Penetrating Radar	Surface Geology	1.1	5
X-Ray Fluorescence	Surface Composition	1	0.5
Meteorology Station	Atmospheric Temperature & Pressure	1	0.5

Surface and atmospheric composition analyses would be performed with the Raman spectrometer and NMS, respectively. The Raman spectrometer and X-ray fluorescence (XRF) instruments would perform remote analysis of the outside surface materials while keeping the instrument systems inside the rover’s pressure vessel. The XRF would examine the elemental composition of the targeted surface materials from alpha scattering, and the Raman spectrometer would examine the mineralogy.

The Venus atmosphere would be sampled for NMS measurements. That sampling device is envisioned to collect samples through a small aperture using the 90-bar outside pressure to fill a small collection tube. A mechanism would then move that sample away for analysis, while a new collection chamber is positioned for receiving a sample. In this way, the rover would be able to make many atmospheric measurements over the mission.

Four Navcams would be used for navigation, hazard avoidance, and surface imaging. Two are mounted facing forward and two facing rearward to provide stereo images each way. Panoramic imagery would be obtained by taking multiple stereo image pairs while rotating the rover. The camera data rate is computed using a 240 × 240 pixel charge coupled device (CCD) at 10 b/pixel and 5:1 compression. This results in each stereo image pair requiring 230 kb of storage. The nominal operations scenario includes two 30-min drives during each 24 hrs of operation. During those drives, navigation stereo images are taken every 2 min. The 15 stereo image pairs from each drive require 3.46 Mb of storage per drive and 6.9 Mb/day.

The IR Sun sensor is primarily an engineering instrument and would be used for crudely finding the Sun line. This is used in the ephemeris and navigation calculations to estimate the rover’s location and predict Earth’s location for selecting the downlink antenna (see description in Section 2.5.2.8).

The ground-penetrating radar (GPR) would take measurements during drive sequences to resolve subsurface layering along the traverse performed. These measurements would be performed periodically when the rover stops. The GPR data rate is 65 kb/s and each brief measurement collects approximately 65 kb.

The meteorology station would measure atmospheric pressure, temperature, and wind speed. This instrument would employ custom sensors that would be designed to survive the high temperature and pressure environment.

**2.5.2.7 Data**

The avionics equipment would provide central processing functions as well as data storage, power distribution, and mobility controller electronics, along with interfaces for the instruments, communications, and navigation equipment. The central processing functions include science data processing and compression, Navcam image processing and compression, ephemeris and navigation functions for tracking rover position and relative Earth location, rover mobility sequence control, and power management. Processing is performed with a 3U format RAD750 processor board that supports speeds as high as 240 MIPS. On board storage is provided by 2 Gb of solid-state nonvolatile memory. Temperatures inside the pressure vessel would be less than 50°C, allowing the internal electronics to use Class-B components.

Data collection rates and volumes are outlined in Table 2.5.2-3. During a nominal 30-min drive sequence, the rover would stop 15 times for taking navigation images and for taking GPR data. The Navcams would generate 230 kb of compressed image data for each stereo image pair, yielding approximately 3.46 Mb of compressed images for a 30-min drive. If GPR data is taken at each stop, then each 30-min drive yields 975 kb of GPR data, bringing the total data volume for a drive to about 4.5 Mb. The compositional science instruments operate during periods when the rover is stationary. These data collection periods are estimated to generate about 720 kb of data each.

**Table 2.5.2-3. Data Rates and Data Volumes for the Venus Rover Instruments**

Science Instruments	Data Rate or kb/sample	Data Volume for a 30-min Drive (kb)	Data Volume for Stationary Data Collection (kb)
Raman Spectrometer	1 kb/s		10
Neutral Mass Spectrometer	5 kb/s		50
Nav Cameras (4)	100 kb/s	3460	460
IR Sun Sensor	10 kb/s		150
Ground Penetrating Radar	65 kb	975	
X-Ray Fluorescence	2 kb/s		20
Meteorology Station	1 kb/s	30	30
<b>Total Data Volume per Drive/Stationary Data Collection Period</b>		<b>4465</b>	<b>720</b>

**2.5.2.8 Communications**

The rover telecommunications system is designed to provide communications during both cruise and surface operations. The dual-frequency design would use X-band for commanding and for cruise operations and would use S-band for downlink from the Venusian surface. Using S-Band on the surface minimizes the RF and DC power requirements for downlink. Atmospheric attenuation at X-band would be approximately 10 dB, while at S-Band it would be only about 1 dB. The DSN 70-meter stations are expected to provide S-band service for a 2013–2015 mission time frame; however, the planned DSN 12-meter arrays will not support S-band.

A key design driver for this system is to avoid any moving parts exposed to the Venus atmosphere. This prevents having to use a gimballed HGA. Five fixed MGAs are mounted to the

upper side of the pressure vessel. For communication sessions, one of these MGAs is selected to maximize performance based on the rover’s knowledge of Earth’s location in the sky.

The dual-string design would use 10-W (RF) S-band SSPAs to achieve 500-b/s downlink at the maximum Earth range of 0.6 AU with a 4 dB link margin. Commanding is performed using X-band and an LGA on the rover’s upper side. Uplink performance when using a 70-m DSN station is estimated to be 31 b/s at 0.6 AU with an 8-dB margin. The maximum Earth range of 0.6 AU occurs at the date of landing and drops below 0.6 AU for more than 100 days.

Technology development is required to produce the RF feed-throughs that are required to connect the amplifiers with the MGAs on the exterior of the pressure vessel. These would effectively be solid RF transparent waveguides that seal small ports in the pressure vessel wall. For this study, these are estimated to contribute 6 Wth of parasitic heat each.

The nominal roving scenario includes four 60-min communication sessions every 24 hrs. This allows a total of 6.9 Mb of data to be returned to Earth during each day of roving. Each stereo image pair requires approximately 8 min to relay to Earth. A nominal 30-min drive includes a maximum of 15 GPR datasets and 15 stereo image pairs that dominate the total data volume. The total science data collected during a 30-min drive is approximately 4.5 Mb (Table 2.5.2-3). Approximately 149 min are required to transmit this data to Earth.

**2.5.2.9 Thermal**

While thermal control systems are critical to all missions, thermal issues are highlighted here due to the very hot surface temperatures. The Venus surface atmosphere is comprised of about 96.5% CO<sub>2</sub>, 3.5% N<sub>2</sub>, and other trace elements with a pressure of ~90 bar and a temperature of about 460°C. Using the TASHE enables surface operations for a much longer duration than previous missions, and thereby enables new science investigations that have not previously been possible.

The thermal control system must reject the large parasitic heat loads from the pressure vessel hull and from all its penetrations, totaling 300 Wth (Table 2.5.2-4). In addition, it must manage the thermal environment in the vacuum interior of the pressure vessel where all electronics are housed. The pressure vessel maintains a vacuum at 10<sup>-6</sup> torr. A vacuum environment contributes to minimizing the overall thermal loads by eliminating any convective heat transfer from the vessel walls. Getter material is employed to help maintain this vacuum by absorbing outgassing products from the components inside the vessel. The interior of the vessel is lined with MLI fabricated with high temperature, gold-plated titanium using metal salt crystal separators. Component heat in the interior is managed by radiative and conductive exchange with the cooler.

**Table 2.5.2-4. Parasitic Heat Loads for the Venus Rover Concept**

<b>Heat Source</b>	<b>Description</b>	<b>Thermal Load (Wth)</b>
Pressure Vessel Hull	Venus atmosphere adds 42.3 Wth/m <sup>2</sup> over the surface area (3.14 m <sup>2</sup> )	133
Drive Motors	32.5 Wth each × 4 motors	130
Optical Penetrations	6 holes @ 0.5 cm and 0.5 Wth each	3
NMS Instrument	Atmospheric sampling assembly	2
Cable Penetrations	8 feed-throughs (Manganin wire) @ 0.25 Wth each	2
RF Waveguide	5 waveguide conduits @ 6 Wth each	30
Instruments	Heat dissipation from science instruments (80 We)	80
Alternator	Heat dissipation from linear alternator	34
<b>Total Thermal Load</b>		<b>414 Wth</b>

The thermal control system relies on a pulse tube cooler that is integrated with the TASHE system, as was described in Section 2.5.2.5, to keep the rover’s electronics below 50°C. Approximately 3 kW of acoustic power is provided to the cooler for managing the ~414 Wth of parasitic heat loads. A capillary-pumped loop system is employed within the rover pressure vessel to move heat from the warm electronics to the cold heat exchanger. For this study, the cooler efficiency was estimated at 14%.

Beyond the extreme environment on Venus, the thermal control system must also do its job during cruise, and entry/descent phases. The large number of GPHS modules generates over 13 kWth of heat that is transferred using passive high-temperature heat pipes to small carbon-carbon radiator panels. Approximately 4 m<sup>2</sup> of radiator surface area is required to radiate this heat to the Venus atmosphere. These radiators could be mounted on the outside of the pressure vessel or outboard of the GPHS module assembly. The same method would be used to accommodate this heat dissipation requirement during cruise operations, although additional design work would be needed to properly address those modes.

**2.5.2.10 Mobility**

Four large conical wheels would provide mobility for the rover. The wheel design is similar to those employed by Lavochkin’s Marsokhod rover designs (The Planetary Society, 2005). These large wheels use an open design conical wire frame to minimize mass and allow elastic motion for shock absorption. Each wheel is driven by an independent electric motor that it designed to operate in a high-temperature and -pressure environment. The motors are mounted inside the rover pressure vessel and are isolated from the atmospheric pressure using labyrinth seals (Fig. 2.5.2-6). The wheels are non-articulated, and steering is achieved by skid-steering.

Rover control would be performed with preprogrammed sequences sent from Earth. The rugged terrain of some Venus regions may result in slow progress and very low odometry. This situation would be somewhat mitigated by the rover’s power and thermal control systems’ not being severely life limited as those of previous Venus missions have been. The current design concept would have limited rover operations during periods when Earth is not in view or when the Sun

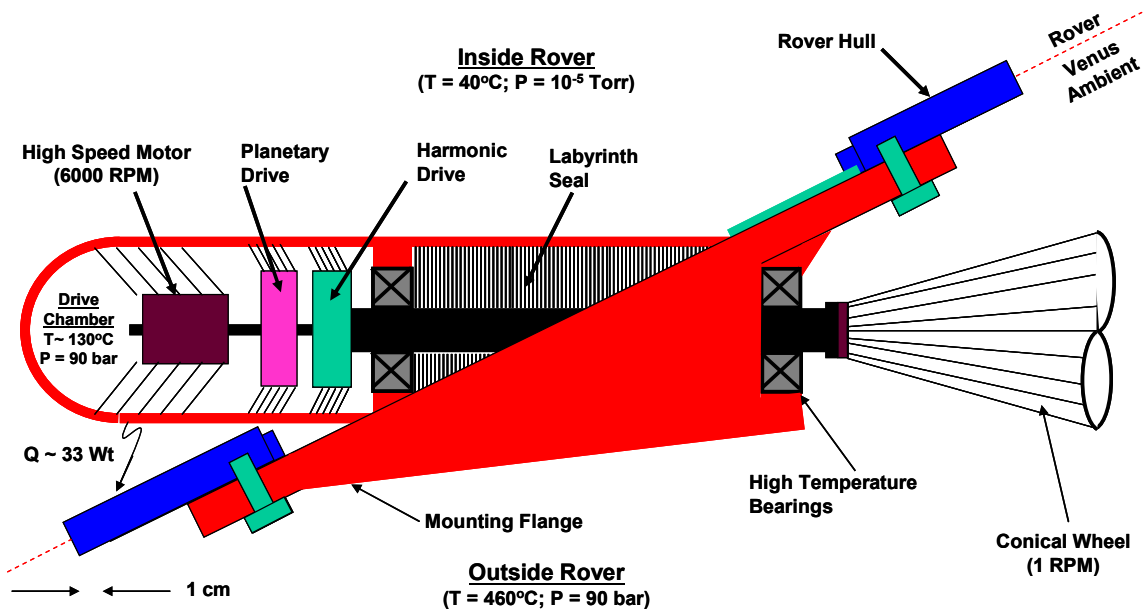


Figure 2.5.2-6. Venus Rover Drive-Train Concept

has set. Without Earth contact, rover movement sequences cannot be sent to the rover and science data cannot be returned. Also, rover travel is impaired by darkness without any rover-based illumination source to assist in navigation imaging.

Mobility would consume the most power and generate the most internal heat in comparison to all other surface operational modes. To manage the heat load, roving would be limited to 2 half-hour drives during a 24-hr period. Using the peak wheel speed of 1 rpm, the rover would travel a maximum of 2.5-m/min (assuming contact on the rim of the conical wheels). This would result in a maximum range of 150-m/day from two 30-min drives. This maximum odometry would not include wheel slipping from traction loss and from skid steering, which is likely to occur. Also, the conical wheels will not always make contact with the surface at their greatest diameter.

Drive sequences would be planned on a daily basis and uploaded to the rover from Earth. To minimize the power and heat load, the rover would employ limited semi-autonomous control when driving, using its stereo navigation images to avoid obstacles or stop. This would reduce the number of images that could be transmitted to Earth for controllers, significantly reducing the power and thermal loads.

#### **2.5.2.11 Propulsion**

The rover vehicle has no in-space propulsion capability. The details of the cruise phase propulsion requirements were not included in this concept study. The mission design includes selection of the Delta IV-Heavy (4450-14) LV. That was the smallest LV with a 5-m fairing, required for stowing the entry ballute. The EVV trajectory requires correction maneuvers totaling approximately 60 m/s to be performed by a cruise-stage propulsion system. In order to focus the study on the feasibility of the Venus rover system the details of that propulsion system were not examined.

#### **2.5.2.12 Power**

Electric power would be produced by the TASHE linear alternator during all mission phases, including: launch, cruise, entry/landing, and surface operations. The alternator's steady 80-We (BOM) is supplemented by high-temperature secondary batteries to accommodate the high-load power modes. Five significant power modes were defined in order to size the electric power subsystem for surface operations: *Roving*, *Telecom*, *Science*, *Recharge*, and *Wake* (Table 2.5.2-5). *Roving* mode is the peak power mode due to the power consumption by the four wheels and requires 260 We. *Telecom* mode refers to the time when the rover is sending or receiving communication signals from Earth and requires 123 We. The 84-We power required in the *Science* mode is an average value for several instruments' operation. This power includes the instruments as well as the required data processing and storage loads. *Recharge* mode requires 39 We and is the lowest power mode. The rover would be asleep during this mode which would allow it to recharge its batteries for another operations cycle. A 5-min transition period before and after each recharge period is called *Wake*. The 65 We required during this period covers the typical system checks and activities needed just before and just after the rover sleeps. A *Cruise* mode was defined to roughly estimate the demands on the power system during cruise (Table 2.5.2-5).

A 10-Ahr Na-NiCl<sub>2</sub> "Zebra" battery was chosen for this application. This battery was selected in a trade with Na-S and LiAl-FeS<sub>2</sub> batteries. While all of these batteries are designed for high-temperature operation, the Na-NiCl<sub>2</sub> provides a high specific energy (approximately 110 Whr/kg) with a high technology readiness level. The battery is mounted on the top surface of the rover (colored blue in Fig. 2.5.2-4). Additional packaging development would be required for this application.

Table 2.5.2-5. Power Modes and Levels for the Venus Rover Concept

Subsystem	Mode 1 Roving (We)	Mode 2 Telecom (We)	Mode 3 Science (We)	Mode 4 Recharge (We)	Mode 5 Wake (We)	Mode 6 Cruise (We)
Science Payload	5.0	0.5	13.0			
Attitude Control	25.3					12.0
CDS	33.8	35.1	27.8	10.0	27.8	
Power Control	18.9	8.9	6.0	2.9	4.7	3.4
Structural and Mechanisms	100.0					
Telecommunications	13.0	46.0	13.0	13.0	13.0	16.0
Thermal	4.4	4.4	4.4	4.4	4.4	4.4
<b>Rover Total (CBE)</b>	<b>200.4</b>	<b>94.9</b>	<b>64.2</b>	<b>30.3</b>	<b>49.9</b>	<b>35.8</b>
Contingency (30%)	60.1	28.5	19.3	9.1	15.0	10.7
<b>Rover Total + Contingency</b>	<b>260.5</b>	<b>123.4</b>	<b>83.5</b>	<b>39.4</b>	<b>64.9</b>	<b>46.5</b>

The power and energy profile for a nominal day of roving (Fig. 2.5.2-7) illustrates the two 30-min drive sequences, the four 60-min communications sessions, and the four data collection periods.

2.5.2.13 Mass

For this concept, the Delta IV-Heavy LV would inject 1560 kg of launch mass onto the EVV trajectory with a  $C_3$  of  $13.31 \text{ km}^2/\text{s}^2$ . Since the launch vehicle was chosen for its large fairing, the launch mass is much lower than the LV’s capability of 3410 kg to that trajectory. The entry mass of 1040 kg includes the ballute system, rover vehicle, and rover entry/landing pad. The rover vehicle mass is ~680 kg and includes 30% contingency on all elements.

A breakdown of the mass is shown in Table 2.5.2-6 with details for the payload instrumentation as well as the rover subsystems. The excess launch capability allows generous room for mass growth or a communications relay orbiter.

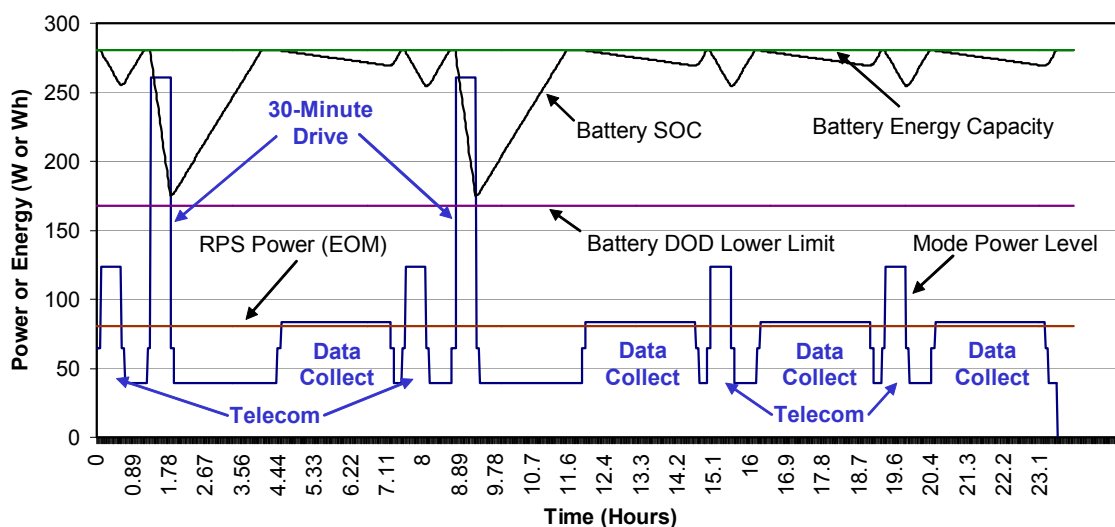


Figure 2.5.2-7. Power and Energy Profile for Nominal Daily Operations for the Venus Rover Concept

Table 2.5.2-6. Venus Rover Concept Mass Budget

Venus Rover	Mass (kg)	Margin	Mass + Margin (kg)
<b>Science Instruments</b>	<b>24</b>	<b>30%</b>	<b>31.2</b>
Raman Spectrometer	3	30%	3.9
Neutral Mass Spectrometer	7	30%	9.1
Navigation Cameras (4)	10	30%	13.0
IR Sun Sensor	1	30%	1.3
Ground Penetrating Radar	1	30%	1.3
X-Ray Fluorescence	1	30%	1.3
Meteorology Station	1	30%	1.3
<b>Rover Subsystems</b>	<b>473</b>	<b>30%</b>	<b>614.9</b>
TASHE and PTR Systems	133	30%	172.9
Power Control and Distribution	11	30%	14.3
Command & Data	15	30%	19.5
Thermal	32	30%	41.6
Telecom	18	30%	23.4
Attitude Control	4	30%	5.2
Structures & Mechanisms	246	30%	319.8
Cabling	28	30%	36.4
Spacecraft Adapter	11	30%	14.3
<b>Rover Vehicle Total</b>	<b>522</b>	<b>30%</b>	<b>678.6</b>
Rover Entry/Landing Pad	32	30%	41.6
Ballute System	246	30%	319.8
<b>Entry System Mass</b>	<b>800</b>	<b>30%</b>	<b>1040.0</b>
Cruise Stage Allocation	400	30%	520.0
<b>Launch Mass</b>	<b>1200</b>	<b>30%</b>	<b>1560.0</b>

#### 2.5.2.14 Radiation

The ionizing radiation dose for this mission is not expected to be a stressing factor for the electronic systems. The number of GPHS modules would be roughly the same as were flown on the Cassini spacecraft, where the RTGs were mounted against the spacecraft bus chassis. Solar radiation was estimated to contribute 5.3 krad (Si) TID over the 20-month cruise period and another 0.6 krad/month for surface operations. The 53 GPHS modules would contribute another 1.2 krad (Si) TID during cruise and 0.06 krad/month for surface operations. This was estimated by scaling MSL RTG data (Kang, 2005) from 8 GPHS modules to 53 GPHS modules, without considering true attenuation of the 53-GPHS module assembly or the Ti pressure vessel or other factors. These estimates total 6.5 krad for cruise and 0.66 krad/month for surface operation.

#### 2.5.2.15 Alternate RPS Power Systems

An alternate to the Stirling cycle-based TASHE design might be a modified high-temperature Brayton power converter. Craere has begun developing a Brayton converter for use with GPHS modules that would achieve greater than 20% system efficiency (Zagarola, 2005). As for the Stirling engine, an alternator is required to generate DC power and a cooler is needed for system refrigeration. In this application, the Brayton system would have more moving parts and potentially an associated impact on reliability. Previous analysis by Craere has employed a cold-side heat rejection temperature of 250 K to 350 K (Zagarola, 2005). This Venus rover concept

requires a much higher cold-side temperature of approximately 773 K, which would reduce the system efficiency of the Brayton converter. Creare engineers have estimated that this application would require approximately 160 GPHS modules (personal communication with Zagarola, 2004), compared with 53 modules using the TASHE system. As a result, the more efficient thermoacoustic Stirling heat engine was baselined for this mission.

#### **2.5.2.16 Summary and Conclusions**

This Venus rover concept study demonstrates the feasibility of using an advanced RPS-driven Stirling thermoacoustic heat engine to enable a mobile science platform on the surface of Venus with an operational lifetime far surpassing that of previous missions. The extreme heat and pressure of the surface atmosphere drive the rover design and configuration, as well as science instrument selection. Minimizing parasitic heat sources drives the design to have the smallest possible surface area, using a vacuum pressure vessel for electronics, and minimizing the number of penetrations through the pressure vessel. This is necessary to reduce the cooling load and thereby reduce the required number of GPHS modules. A stationary lander would not have any wheels and so would certainly benefit from fewer penetrations and a minimal surface area. However, mobility could add tremendous value to the science return for any Venus surface mission.

The rover carries a suite of science instruments for performing surface and atmospheric composition analysis, as well as surface geology and meteorology. Mobility allows science measurements to be made in different locations. The rover design avoids using articulated antennas, camera masts, or other mechanisms exposed to the Venesian atmosphere. All rover electronics and instruments are housed in a pressure vessel in vacuum at below 50°C. Four independently-driven wheels would provide mobility, which is also the highest power mode of operation. For this concept, 53 GPHS modules would be required to provide sufficient thermal energy to drive the TASHE and pulse-tube cooler. These GPHS modules are mounted on the rear of the vehicle and waste heat would be removed using high-temperature heat pipes and approximately 4 m<sup>2</sup> of radiator panels.

A nominal operational scenario was developed to balance the power demands from the drive and navigation systems, science instruments, and communications. High-temperature batteries would be mounted on the exterior of the rover and supplement the steady 80 We provided by the TASHE. Without adding an orbiter for communications relay, downlink direct to Earth would be significantly aided by using S-band. Static MGAs would also be mounted on the rover's exterior to provide DTE downlink communications. Commanding would be transmitted using X-band, while downlink would use S-band to minimize the DC power requirements. Atmospheric attenuation at X-band is roughly 10 dB, while at S-band it is only about 1 dB.

Several technical challenges remain unaddressed, including the mobility system design and performance details, the possibility of driving in darkness based on navigation autonomy or illumination for navigation imagery, the design of the required pressure vessel pass-throughs, and the design for GPHS heat rejection during cruise and descent phases. Additionally, Planetary Protection requirements were not explicitly addresses due to the limited scope of this concept study.



3. POWER TECHNOLOGY FOR ADVANCED RPS SYSTEMS

3.1 INTRODUCTION

Four basic power-conversion technologies are considered in the advanced RPS mission studies presented in this report. These include (1) advanced thermoelectrics, (2) advanced Stirling, (3) Brayton, and (4) TPV. RPSs based on these power-converter technologies operate similarly in that they would convert the heat produced by a nuclear heat source (via radioisotope decay of <sup>238</sup>Pu) into electrical power that can be used to power a spacecraft (Fig. 3-1). The power-conversion process and efficiency, however, are significantly different in each case as described below. None of the advanced RPS systems described herein have been built in a flight-like configuration, nor have they been flown in space; however, research and development have been performed to various degrees for all four technologies. To facilitate mission- and system-level trade studies, preliminary performance characteristics have been estimated for conceptual advanced RPS generators based on each of the conversion technologies mentioned above. The basic operation and conversion efficiency of each conceptual generator are based on the analyses and/or subsystem test results performed by NASA, its contractors, and/or industry. The balance of each system is, where appropriate, based on the multi-mission RPS generators (MMRTG and SRG) currently in development by NASA and DOE (Abelson, 2005a).

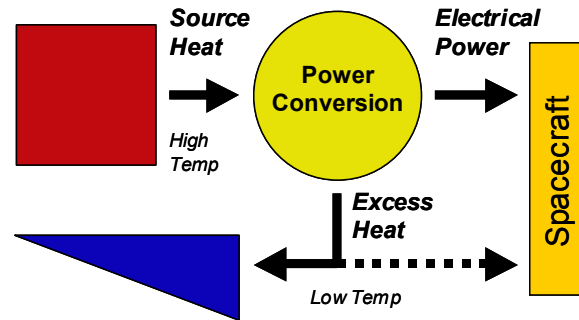


Figure 3-1. Key Components of a Space-Based Nuclear Power System

3.2 HEAT SOURCES

The GPHS module is the current nuclear heat source used on NASA space missions (Fig. 3-2). Each GPHS module contains approximately 0.6 kg of <sup>238</sup>PuO<sub>2</sub> fuel in four equally sized fuel pellets encapsulated within 0.5-mm thick iridium-alloy clads. The nominal thermal output of each GPHS module is ~250 Wth at beginning of life (BOL) (Hyder, 2000). There are three variants of the GPHS module: (1) the original version used on Galileo, Ulysses, and Cassini (1.435 kg, 5.31 × 9.72 × 9.32 cm), (2) the Step-1 Enhanced GPHS to be used on the proposed New Horizons Pluto–Kuiper Belt mission (1.514 kg, 5.31 × 9.96 × 9.32 cm), and (3) the Step-2 Enhanced GPHS to be used in the MMRTG and SRG RPSs (1.606 kg, 5.82 × 9.96 × 9.32 cm; Wiley, 2004). The conceptual advanced RPS systems assessed in this report are assumed to use the Step-2 Enhanced GPHS module.

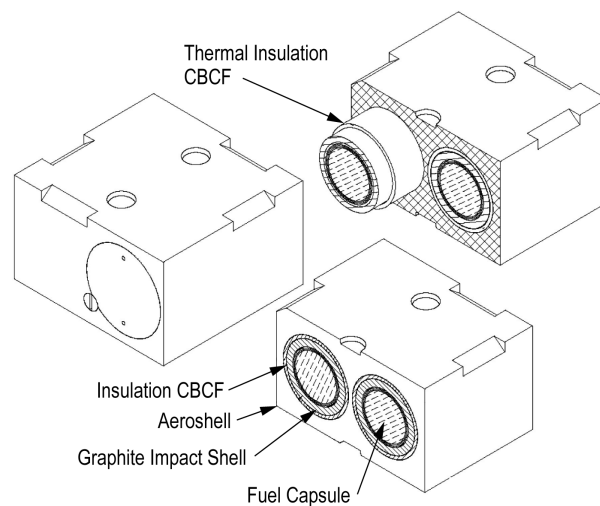
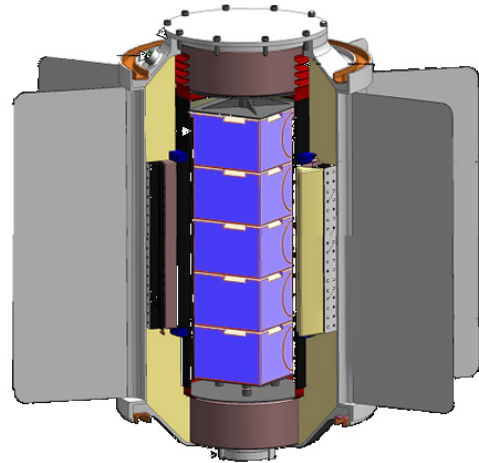


Figure 3-2. General-Purpose Heat Source Module (DOE)

**3.3 ADVANCED RADIOISOTOPE THERMOELECTRIC GENERATOR**

RTGs have been used for space-based applications since 1961, when the Transit 4A Earth-orbiting spacecraft first employed the 2.7-We (BOM) SNAP-3B7 RTG for power generation. Since then, a total of 22 space missions have successfully used RTGs for electrical power production. The fundamental physical process involved in thermoelectric (TE) power conversion is the Seebeck effect, which is the electromotive force that arises between two dissimilar materials (i.e., metals or semiconductors) when their junctions are subjected to a temperature difference. The electromotive force generated by the thermocouple can be used to drive an electric circuit, or if large enough, a spacecraft power system. The key advantages of RTGs are their long life, robustness, compact size, and high reliability. RTGs are able to operate continuously, independent of solar insolation, and are relatively insensitive to radiation and other environmental effects. TE converters are easily scalable, and possess a linear current-voltage curve, making power generation easy to control via a shunt regulator and shunt radiator. They produce no noise, vibration, or torque during operation. These properties have made RTGs ideally suitable for missions in the extreme environments of outer space and on planetary surfaces.



**Figure 3-3.** Conceptual Advanced 112-We Radioisotope Thermoelectric Generator.

RTGs used to date have employed thermoelectrics made from lead telluride (PbTe), tellurides of antimony, germanium and silver (TAGS), or silicon germanium (SiGe). Advanced RTGs (Fig. 3-3) would potentially use new thermoelectric materials called Skutterudites that potentially offer higher efficiency and performance than RTG materials. Skutterudite thermoelectrics are comprised of  $CeFe_4Sb_{12}$ -based (P-type) and  $CoSb_3$ -based (N-type) alloys (Fig. 3-4). Low-temperature Skutterudite thermoelectrics could act as “drop-in” replacements for the PbTe/TAGS

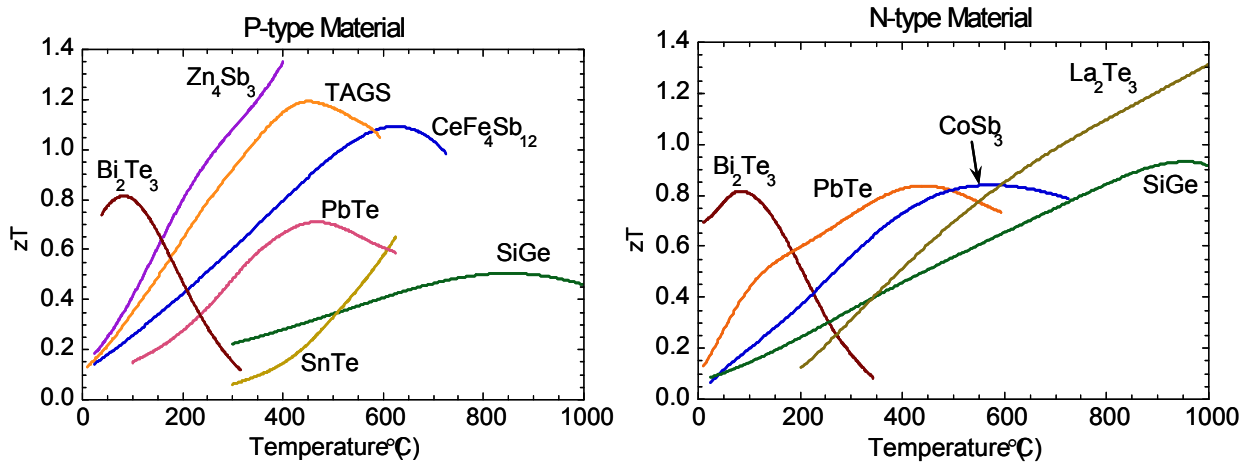


**Figure 3-4.** Thermoelectric Figure of Merit (ZT) for P-type and N-type Materials (Snyder, 2004) as a Function of Temperature.

thermoelectrics currently being used in the MMRTG being developed by DOE and NASA, potentially increasing the generator’s specific power by over 30% (Ewell, 2005a). Intermediate- and high-temperature Skutterudites are being considered for more advanced RTGs that would have conversion efficiencies between 9% and 15% and specific powers >6 We/kg<sup>1</sup> (Ewell, 2005a).

Two upgraded MMRTG concepts were considered in this study, including an 8-GPHS-module RPS that could produce upwards of 160 We (BOM) and share a similarly sized outer housing with the MMRTG. The second option considered a smaller, 5-GPHS-module variant that could produce a similar amount of power as the standard MMRTG (~112 We at BOM) but using three less GPHS modules due to the more efficient Skutterudite thermoelectrics. The mission studies considered in this report assume the later 5-GPHS module-based RTG variant, which permits a more direct comparison with the Brayton and TPV advanced RPSs described herein.

Performance values were estimated for the 5-GPHS module version of the advanced RTG over a range of relevant operating environments including deep space, the surface of Titan (i.e., for a lander or rover mission), and in Venus atmosphere at 60 km altitude (i.e., for a Venus aerobot mission). The results of this preliminary analysis are presented in Table 3-1. The overall generator conversion efficiency was estimated at 9% for a hot-shoe temperature of 700°C, and fin temperature of 130°C. The thermal power would be 1250 Wth (BOM) for 5-GPHS modules, and would produce ~112 We of electrical power (BOM). The specific power of the advanced RTG was estimated at ~4.3 We/kg for deep space and Venus (at 60 km altitude), and ~4.4 We/kg for the surface of Titan. The deep space performance parameters are also generally applicable to the surface of solar-system bodies without an atmosphere and where the heat-sink temperature is much less than the RPS fin temperature (e.g., Europa, shadowed portions of the Moon, etc.) The

**Table 3-1. Performance Estimates for a Conceptual Skutterudite-Based Advanced RTG\***

Parameter	Deep Space	Titan Surface	Venus at 60 km Altitude
Power (BOM), We	112	112	112
Mass, kg	26.2	25.5	25.9
# GPHS Modules	5	5	5
Thermal Power, Wth	1250	1250	1250
Specific Power, We/kg	4.3	4.4	4.3
Conversion Efficiency, %	9.0	9.0	9.0
T <sub>hot</sub> , °C	700	700	700
Fin Temperature, °C	130	130	130
Heat-Transfer Environment	Radiative Only	Convective (P) and Radiative (S)	Radiative (P) and Convective (S)
Radiative Sink Temperature, K	4	94	240
Ambient Temperature, K	N/A	94	240
Ambient Pressure, bar	Vacuum	1.5	0.2
Ambient Composition	Vacuum	N <sub>2</sub> (P)	CO <sub>2</sub> (P)
Required Radiator Surface Area, m <sup>2</sup>	1.36	0.40	1.00

\*Notes: (P) indicates a primary contributor or constituent, and (S) indicates a secondary contributor or constituent.

<sup>1</sup> Analysis will begin in 2006 on a deep-space only version of a higher power (≥200 We) advanced RTG with the goal of achieving a specific power of ≥6 We/kg using advanced high temperature thermoelectrics.

radiator fin sizes were calculated for each operating environment considered in the study, and determined to have a minimal impact on RTG mass and specific power, as demonstrated above. A key result of the study, however, is that no RTG fins are expected to be required on the surface of Titan due to its cold, convective atmosphere. That is, the generator housing provides sufficient surface area to reject all heat while on the Titan surface. However, supplemental radiator area (external to the generator) would be required during the cruise phase to reject the heat while operating in deep space.

The power level of RTGs decreases with time due primarily to three different physical processes: (1) radioactive decay of the  $^{238}\text{Pu}$  fuel, causing less heat to be produced over time; (2) reduced Carnot efficiency of the thermoelectrics caused by a smaller temperature differential across the TE element due to  $^{238}\text{Pu}$  decay; and (3) changes in thermoelectric properties (thermal conductivity, electrical conductivity, and Seebeck coefficient), sublimation, and changes in insulation effectiveness (either thermal or electrical) as a result of the deposition of the sublimation products on the insulation (Ewell, 2005b). The decay of  $^{238}\text{Pu}$  is a well-understood process, and corresponds to a thermal (and electrical) power degradation of  $\sim 0.8\%/yr$ . The degradation modes of Skutterudite thermoelectrics is not yet fully characterized; however, life tests are currently underway to assess the thermoelectric degradation rates, and multiple strategies (including the use of special coatings, and aerogel insulation) are being studied that would reduce Skutterudite sublimation rates. For the purposes of this study, it has been assumed that the TE degradation of Skutterudites is the similar as for PbTe-TAGs (as used in the MMRTG) and equivalent to a power degradation rate of  $\sim 0.8\%/yr$ . The total power degradation rate of the advanced RTG is the sum of the degradation rates of the  $^{238}\text{Pu}$  fuel and the Skutterudite thermoelectrics, and corresponds to  $\sim 1.6\%/yr$  (Section 3.8).

### 3.4 ADVANCED STIRLING GENERATOR

The Stirling generator is a dynamic power-conversion system based on the thermodynamic cycle invented by Robert Stirling in the 19<sup>th</sup> century. The typical Stirling generator involves a double-piston system comprised of a displacer and a power piston (Fig. 3-5). The displacer piston moves

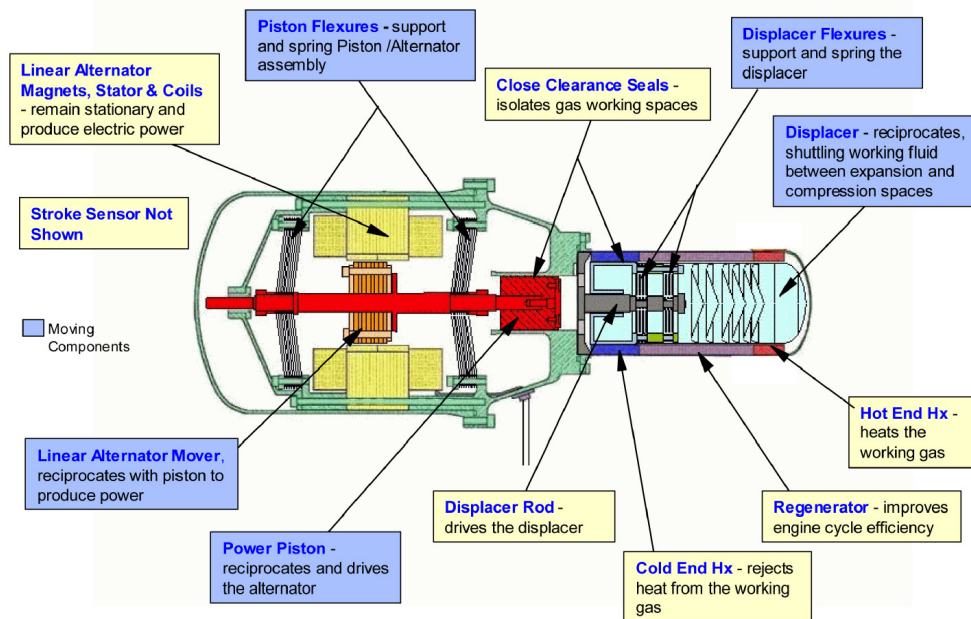


**Figure 3-5.** Cutaway of a Stirling Converter Integrated with a Linear Alternator in a Hermetically Sealed Pressure Vessel.

the working fluid (typically helium) between the hot side and cold side of the Stirling engine through a regenerator. The power piston performs the thermodynamic work of compression and delivers the mechanical work to a linear alternator. The alternator, in turn, produces AC power at a controlled frequency and voltage depending on the load. A rectifier converts the AC power to DC power for use by the spacecraft bus.

A radioisotope heat source provides the heat to the hot-end heat exchanger (or heater head) of the Stirling convertor (Fig. 3-5), and radiator fins reject heat from the cold end. An electronic controller is used to perform active stroke-control to maintain the prescribed heater-head operating temperature (necessary to maximize conversion efficiency) while compensating for the gradual decrease in thermal power from the radioisotope heat source (i.e., due to  $^{238}\text{Pu}$  decay). The commonly considered Stirling engine type for space power applications is the Free Piston Stirling Engine (FPSE), coupled with a linear alternator, which can be configured within a hermetically sealed vessel to prevent helium loss. The FPSE requires no lubricants because there is nominally no contact between any moving parts in this design (Hyder, 2000).

Key features of the Stirling-based RPS include its relatively high power-conversion efficiency, compact size, and scalability. Higher conversion efficiencies mean that a Stirling-based RPS generally requires less  $^{238}\text{Pu}$  fuel than do static power-conversion systems (RTG and TPV), potentially translating into lower cost and greater availability. The primary disadvantage of the Stirling generator is its lack of space qualification. No Stirling generator has flown in space for power production; however, ground testing of several models of Stirling generators is currently in process, and Stirling-based cryocoolers have been used for space applications for many decades. DOE and NASA are currently developing the SRG, which is planned to be the first space-qualified RPS, and potentially available for space applications early in the next decade (Abelson, 2005).

The Stirling generator considered in the mission studies herein is based on an advanced design being researched and tested by SunPower (Wood, 2005), and represents a next-generation capability beyond the SRG. This advanced Stirling unit is currently undergoing subsystem-level testing and does not yet exist as an integrated RPS system. However, preliminary test results indicate that the power-conversion efficiency is significantly higher than that of the SRG, with values as high as 34% possible (thermal to DC electrical). Key features of the SunPower Stirling responsible for its greater performance include its higher hot-side operating temperature ( $850^{\circ}\text{C}$ ), which increases its Carnot efficiency, and a smaller, lightweight linear alternator, which significantly reduces the generator size and mass, thus increasing generator specific power.

Preliminary system-level performance estimates were made for a conceptual 80-We advanced



**Figure 3-6.** Laboratory Prototype of an Advanced 80 We SunPower Stirling Engine and Linear Alternator (Wood, 2005).

Stirling generator based on the SunPower Stirling engine and linear alternator. The balance of this conceptual system (i.e., controller, structure, thermal insulation, etc.) was based upon the design of the SRG system (Lockheed Martin, 2004), which is the closest and most mature relative to the advanced Stirling system. The specific power of the advanced Stirling generator was estimated at 5.9 We/kg<sup>2</sup>, with a generator mass of 13.7 kg. Each conceptual generator would use one GPHS module and one Stirling convertor assembly, and include an active vibration-cancellation device (i.e., electrically oscillated spring-mass) to reduce vibration induced by the generator. Each Stirling unit is assumed to be block-redundant; thus, missions using this technology would likely require that at least one additional generator be flown to maintain the single-fault tolerance of such a mission-critical system, consistent with JPL design principles (Yarnell, 2003). The conversion efficiency of the conceptual advanced Stirling generator is assumed to be 34% (thermal to DC electrical), and is based on SunPower Stirling test results for T<sub>hot</sub>=850°C, and T<sub>fin</sub>~100°C. Due to the high conversion efficiency, it is estimated that an advanced Stirling generator could dissipate all its heat using just the generator housing without requiring any additional radiator fins, thus decreasing overall generator size.

Performance estimates are presented in Table 3-2 for the conceptual 80-We advanced Stirling generator. The power degradation rate of this generator is assumed to be 0.8%/yr (Wong, 2004), and due solely to the decay of the <sup>238</sup>Pu fuel (Section 3-8). Other power-degradation modes may exist, but they have not been quantified, nor are they included in the above value.

**Table 3-2. Performance Estimates for a Conceptual Advanced Stirling Generator\***

Parameter	Deep Space	Titan Surface	Venus at 60 km Altitude.
Power (BOM), We	80	80	80
Mass, kg	13.7	13.7	13.7
# GPHS Modules	1	1	1
Thermal Power, Wth	250	250	250
Specific Power, We/kg	5.9	5.9	5.9
Conversion Efficiency, %	32	32	32
T <sub>hot</sub> , °C	850	850	850
Fin Temperature, °C	100	100	100
Heat-Transfer Environment	Radiative Only	Convective (P) and Radiative (S)	Radiative (P) and Convective (S)
Radiative Sink Temperature, K	4	94	240
Ambient Temperature, K	N/A	94	240
Ambient Pressure, bar	Vacuum	1.5	0.2
Ambient Composition	Vacuum	N <sub>2</sub> (P)	CO <sub>2</sub> (P)
Required Radiator Surface Area, m <sup>2</sup>	0.21	0.07	0.18
*Notes: (P) indicates a primary contributor or constituent, and (S) indicates a secondary contributor or constituent.			

<sup>2</sup> Recent analysis by the Orbital Science Corporation (OSC) suggests that a specific power of up to 8 We/kg may be possible for a higher power (~150 We) SunPower-based advanced Stirling generator.

3.5 THERMOACOUSTIC STIRLING HEAT ENGINE AND CRYOCOOLER

The TASHE (Fig. 3-7) is an advanced derivative of the Stirling engine concept described in Section 3.4, and is currently being researched by NGST and LANL (Backhaus, 2000, 2002; Tward, 2003; Backhaus, 2004; Petach, 2004b). The TASHE produces acoustic power directly from a heat source without using any moving parts. Electrical power is produced by the conversion of a portion of the acoustic power using a piston and voice coil suspended on flexures. A PTR is directly coupled to the TASHE to convert the acoustic power into thermal power, providing refrigeration with no moving mechanical parts. This results in more efficient cooling relative to conventional thermoacoustic Stirling systems that convert thermal power to acoustic power, then to mechanical power via moving pistons. The mechanical simplicity of the TASHE/Cryocooler system is expected to increase its reliability relative to Stirling engines with moving parts.



Figure 3-7. 1-kWe Engine and Resonator Developed by NGST and LANL (Petach, 2004b).

The working fluid inside the closed system is gaseous helium. The TASHE converts thermal energy from a heat source (i.e., GPHS module) into acoustic energy which, in turn, drives an oscillating flow of helium gas at a specified frequency, flow rate, and pressure amplitude that is required by the pulse tube. The acoustic energy developed by the TASHE is used to perform refrigeration at the first and second stages of the pulse tube. The pulse tube and TASHE both use regenerators or porous media to transfer heat with the oscillating helium gas. The purpose of the resonator is to control the operating frequency of the system and to transfer the acoustic energy from the TASHE to the pulse tube (Fig. 3-8).

An integrated thermoacoustic Stirling engine and cryocooler system would potentially be enabling for space missions requiring large amounts of cooling and operating in extreme environments with little or no insolation. The surface of Venus is one such location where cooling is absolutely essential for any long-duration mission, including the Venus Surface Explorer mission specified in the Solar System Exploration Strategic Roadmap, and the Venus rover mission concept study described in Section 2.5.2. NGST sized a conceptual RPS system for the Venus rover mission described

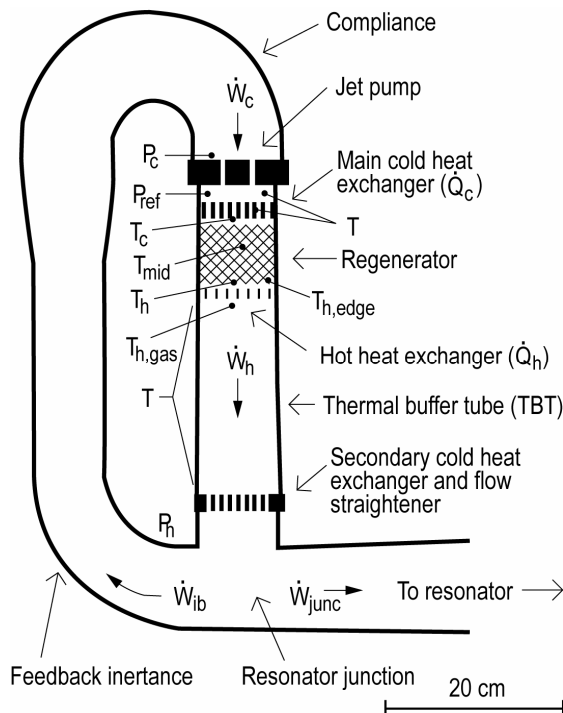


Figure 3-8. Cutaway Illustration of a Conceptual Thermoacoustic Stirling Engine (Petach, 2004b).

in this report based on their TASHE/Cryocooler technology. This system uses 53 GPHS modules as the heat source for the converter, produces 414 Wth of cooling to maintain internal rover operating temperatures at  $\leq 50^{\circ}\text{C}$ , and 80 We of electrical power to operate the rover's subsystems (Fig. 3-9). While not studied in detail for this report, the efficiency of the TASHE can potentially be much higher in environments that afford a lower heat-sink temperature (i.e., deep space, surface of Mars, etc.).

The power-degradation rate of the conceptual TASHE-based RPS is assumed to be approximately 0.8%/yr due solely to  $^{238}\text{Pu}$  decay (consistent with the advanced Stirling and Brayton generators discussed elsewhere in this section). Though other power-degradation mechanisms may exist, they were not addressed in this study.

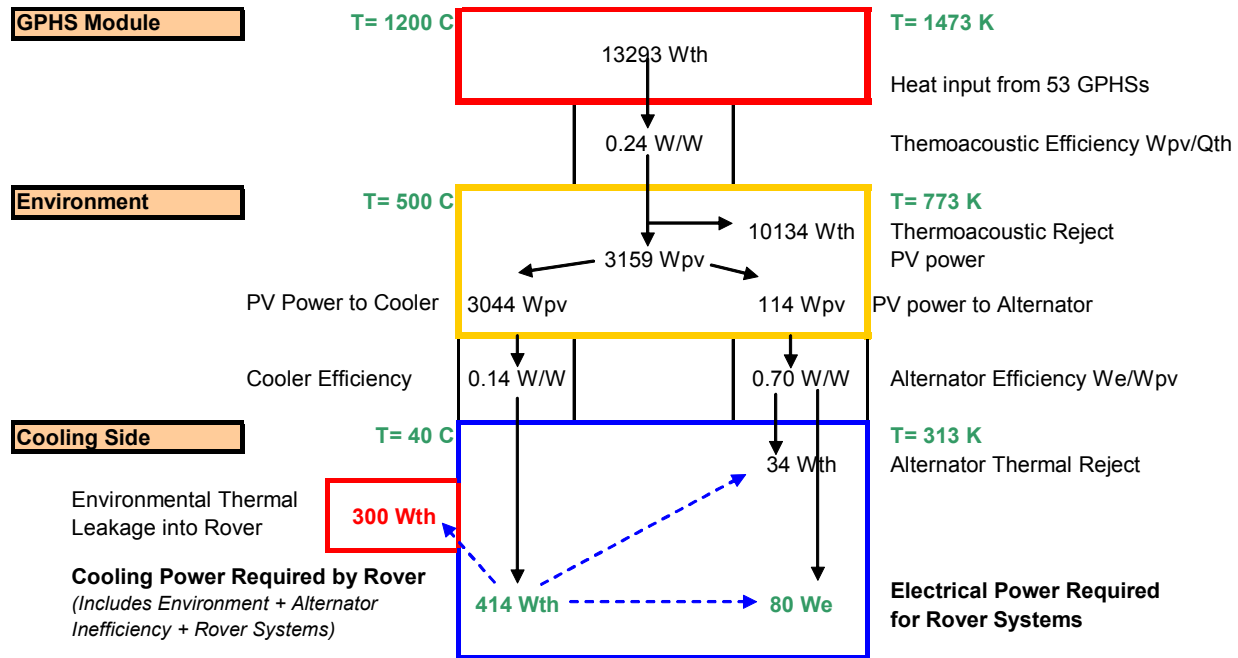


Figure 3-9. Performance and Operating Parameters of a Conceptual Thermoacoustic Stirling Heat Engine and Cryocooler in a Venus Surface Environment.

### 3.6 BRAYTON GENERATOR

The Closed Brayton Cycle (CBC), illustrated in Figure 3-10, has been considered for space applications since the early 1960s (Hyder, 2000) using nuclear or solar heat sources. Early development of the Brayton power system was focused on a wide range of power levels from 500 We to 100 kWe, with a significant amount of work performed by Rockwell in the 1970s through 1990s (Rockwell, 1988, 1989, 1990, 1992). The Brayton cycle, in the form of the Brayton Rotating Unit (BRU), was considered by NASA for the International Space Station as part of a Solar Dynamic Power Module, and a testbed was built in the 1980s to develop this concept (Hyder, 2000). The Mini-BRU was developed as a part of the Brayton Isotope Power System (BIPS) program and produced 1.3 kWe with an overall efficiency of 28%. The most recent nuclear-based CBC system was the Dynamic Isotope Power System (DIPS) designed in the 1980s and based significantly on the Mini-BRU technology. A 6-kWe (EOL) DIPS system was designed during this period. At the time, the BRU and Mini-BRU represented the state of the art for TAC technology for space applications (Hyder, 2000). To this day, however, no nuclear-powered Brayton systems have flown in space.

The Brayton-based RPS system would generally have an electrical output in the range of hundreds of watts to a few kilowatts. Such a system would typically use a radial compressor and power turbine, with the turbo-alternator and compressor mounted on a single shaft. This configuration has the advantage of greater reliability since the alternator is housed within the gas system such that no external mechanical drive or associated seals are required. The TAC is the only rotating component in this type of CBC design. For space power systems, a mixture of helium and xenon is typically used as the working fluid. The use of purified inert gases adds to the lifetime and overall reliability of the system by greatly reducing the potential for corrosion. The precise combinations of inert gases and their relative proportions are selected to optimize heat-transfer and turbomachinery efficiency.

Until recently, NASA had funded the research and development of a ~100-We Brayton system as part of its drive towards higher-efficiency and higher-specific-power radioisotope power systems. One concept developed by Creare (Zagarola, 2003) used a combination of micromachined parts, high-speed (hundreds of thousands of RPMs), precision non-contacting gas bearings, and compact heat exchangers. This system has one moving part (the TAC as shown in Fig. 3-11), and is expected to have low EMI/EMC emissions, and produce minimal vibration. Fully-redundant Brayton converters would be used with two GPHS modules and dual-string electronics to increase reliability. Each converter would nominally be run at half power. In case of the failure of a single converter, the functioning converter would be spun up to 100% to continue generating the full amount of electrical power to the spacecraft (Fig. 3-12).

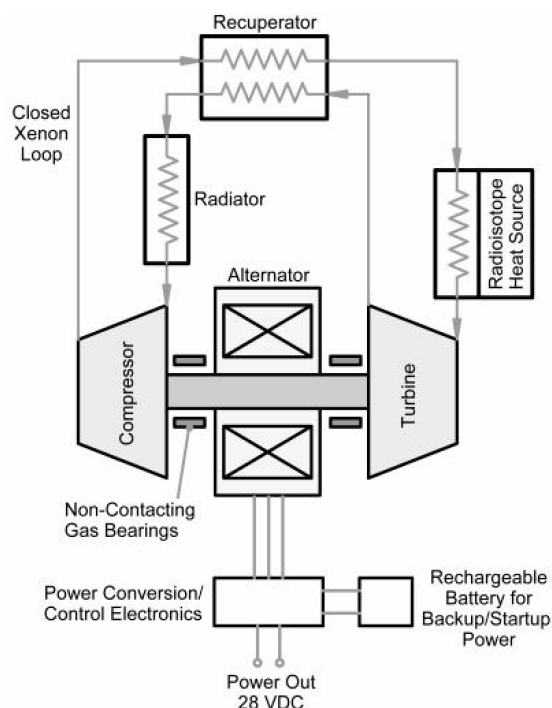


**Figure 3-10.** Thermodynamic Cycle of the Brayton Radioisotope Power System (Zagarola, 2003).

Preliminary analyses were performed on a conceptual Brayton RPS generator to estimate the mass, specific power, and volume of a 110-We fully redundant RPS system. Conversion efficiency values were extrapolated from the Creare literature, as were the mass and basic dimensions of the TAC, controllers, and heat sources. The balance of the system was estimated based on subsystem mass values extrapolated and scaled from the SRG. The result was a conceptual power system with a specific power of 3.8 We/kg, mass of ~29 kg, and a conversion efficiency of 22%. Performance estimates are provided in Table 3-3 for operations in deep space, the surface of Titan, and in the Venus atmosphere at 60 km altitude (where ambient conditions are close to those on Earth). The power-degradation rate for the conceptual Brayton generator was estimated at 0.8%/yr (Wong, 2004) based solely on the decay of the  $^{238}\text{Pu}$  fuel (Section 3.8). Other power-degradation mechanisms may exist with the Brayton generator; however, these have yet to be characterized and were not included in the above value.

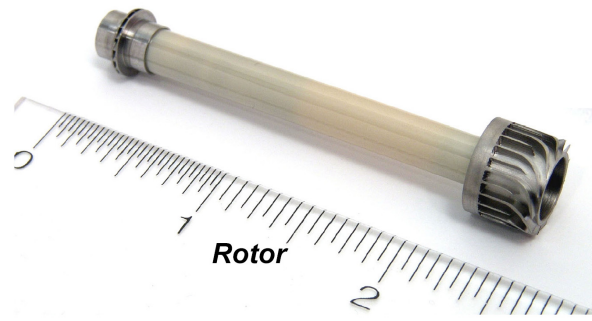


**Figure 3-11.** Turbo-Alternator-Compressor Used in the Creare Brayton Generator Design (Zagarola, 2005).

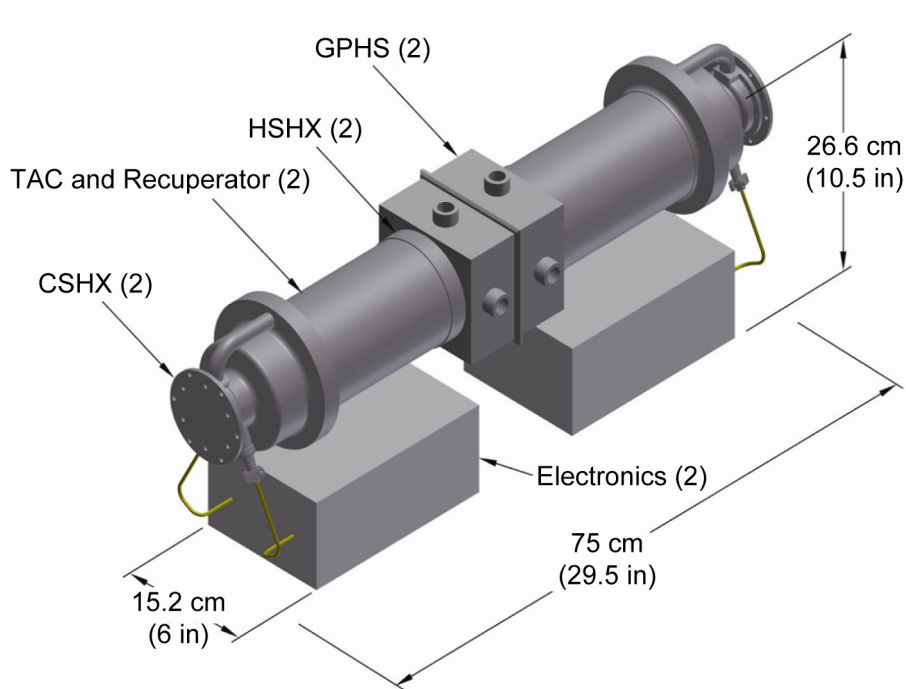


**Figure 3-12.** Conceptual 110-We Brayton RPS System by Creare Using Two Redundant Converters and two GPHS Modules (Zagarola, 2005).

Table 3-3. Performance Estimates for a Conceptual Brayton Generator\*

Parameter	Deep Space	Titan Surface	Venus at 60 km Altitude.
Power (BOM), We	110	110	110
Mass, kg	29.2	28.9	29.2
# GPHS Modules	2	2	2
Thermal Power, Wth	500	500	500
Specific Power, We/kg	3.8	3.8	3.8
Conversion Efficiency, %	22	22	22
T <sub>hot</sub> , °C	777	777	777
Fin Temperature, °C	77	77	77
Heat-Transfer Environment	Radiative Only	Convective (P) and Radiative (S)	Radiative (P) and Convective (S)
Radiative Sink Temperature, K	4	94	240
Ambient Temperature, K	N/A	94	240
Ambient Pressure, bar	Vacuum	1.5	0.2
Ambient Composition	Vacuum	N <sub>2</sub> (P)	CO <sub>2</sub> (P)
Required Radiator Surface Area, m <sup>2</sup>	0.63	0.59	0.22

\*Notes: (P) indicates a primary contributor or constituent, and (S) indicates a secondary contributor or constituent.

### 3.7 THERMOPHOTOVOLTAIC GENERATOR

The TPV generator is a power-generation device that operates by converting the infrared heat produced by a high-temperature heat source into electricity via photovoltaic (PV) cells. TPV research and development began in the early 1960s, and continues to this day (Hyder, 2000). TPV has been considered an attractive concept for space missions due to its higher conversion efficiencies, with NASA and DOE funding research and development of a TPV-based advanced RPS system as recently as 2005 by EdTek, Creare, and Essential Research.

Key components of a TPV generator include a high-temperature heat source (typically operating at 1000 K to 2000 K), IR emitter, IR-bandpass filter, PV array, and radiator (Fig. 3-13). The heat source is used to produce photons with energies primarily in the infrared spectrum. For space power applications, the heat source would likely be the GPHS module described in Section 3-2 with an operating temperature of  $\geq 1100^{\circ}\text{C}$ . The energy spectra of the photons emitted from the heat source is generally quite broad and, thus, an IR emitter and bandpass filter are used to maximize the emission and

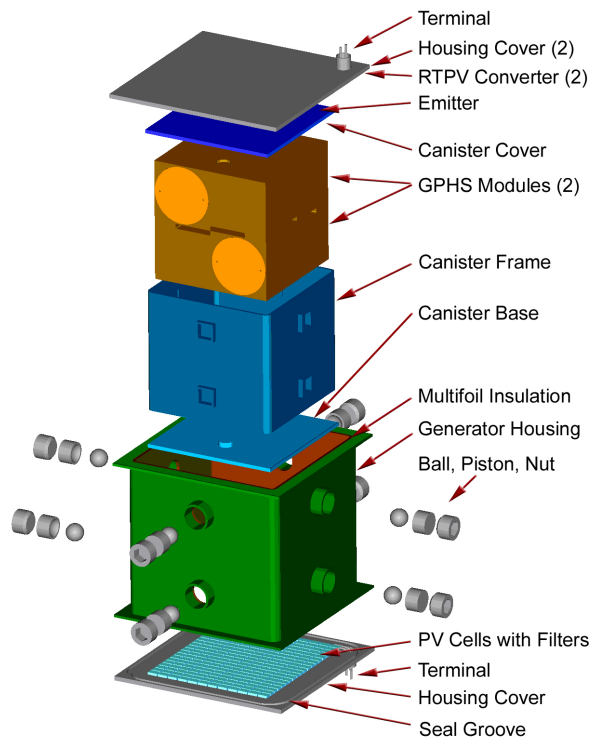


Figure 3-13. Conceptual Illustration of a TPV Generator, Shown without Radiator Fins (Courtesy of OSC).

transmission of photons with energies matched to the bandgap of the PV cells (Fig. 3-14). All other photons are reflected back to the heat source, which acts to maintain the optimal heat-source operating temperature. The PV cells are used for the actual power-conversion process and can be made from a variety of materials. Recent research has focused on gallium antimony (GaSb); however, other PV cell materials under investigation include low-bandgap tertiary (particularly,  $\text{In}_x\text{Ga}_{1-x}\text{As}$ ) and quaternary compounds that can be tailored to better match the heat source wavelength near peak energy (Hyder, 2000). PV cell performance depends strongly on temperature and generally requires operating between  $20^\circ\text{C}$  and  $60^\circ\text{C}$  for optimal conversion efficiencies. This can be a significant drawback for deep space missions where radiation is the only heat-transfer mechanism, resulting in the need for large radiator fins (i.e., on the order of several square meters for a 100-We device), which complicates spacecraft accommodation and integration. Research performed in the 1990s investigated different configurations of TPV radiator fins for space-based applications; two of these concepts are illustrated in Figure 3-15.

As with other photovoltaic cells, TPV cells are susceptible to degradation when exposed to radiation. Potential sources of radiation for a deep space version of a TPV system include the  $^{238}\text{Pu}$  fuel within the GPHS heat sources, galactic cosmic radiation, solar-particle events, charged particles trapped in planetary magnetospheres, etc. As no space-based TPV units have been fully designed or built, it remains uncertain how radiation would impact TPV performance, especially in a high-radiation environment such as the Jupiter system.

To understand the trades associated with using a TPV RPS for space applications, preliminary TPV RPS performance estimates were made for a conceptual 110-We system based on a JPL TPV design using a conversion efficiency and specific power derived from (Ewell, 1993) and extrapolated to a multi-mission design that could operate in the vacuum of space and in planetary atmospheres. The power level for this conceptual TPV system was selected to be consistent with that of the MMRTG and SRG. Fins sizes were computed based on a cell temperature of  $34^\circ\text{C}$ , an average fin temperature of  $14^\circ\text{C}$ , and using a range of heat-rejection temperatures associated with different

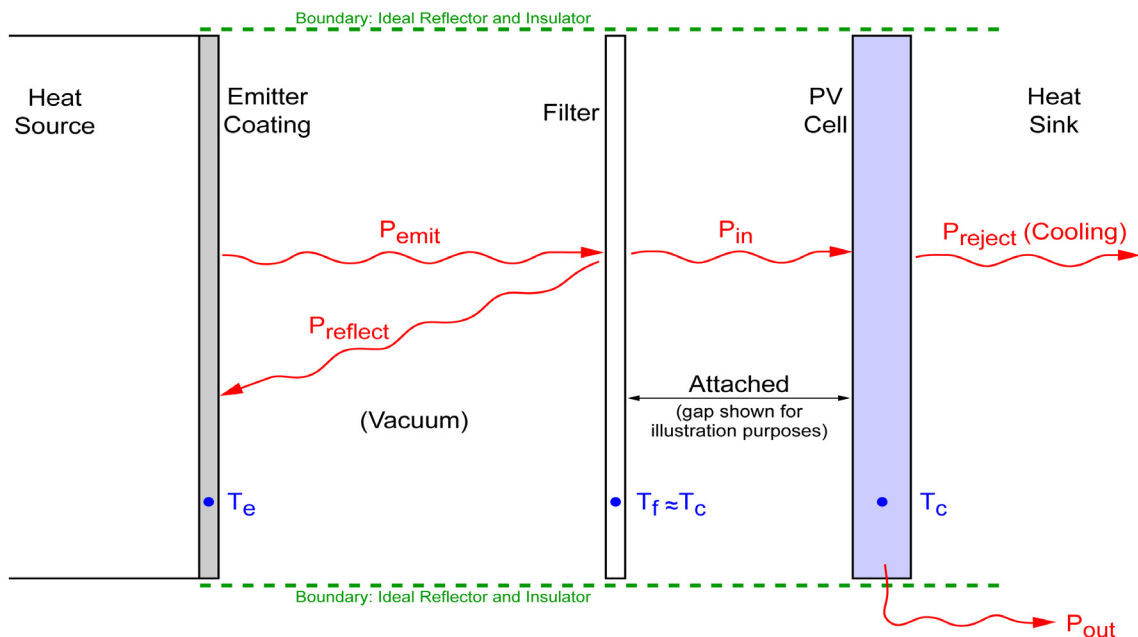
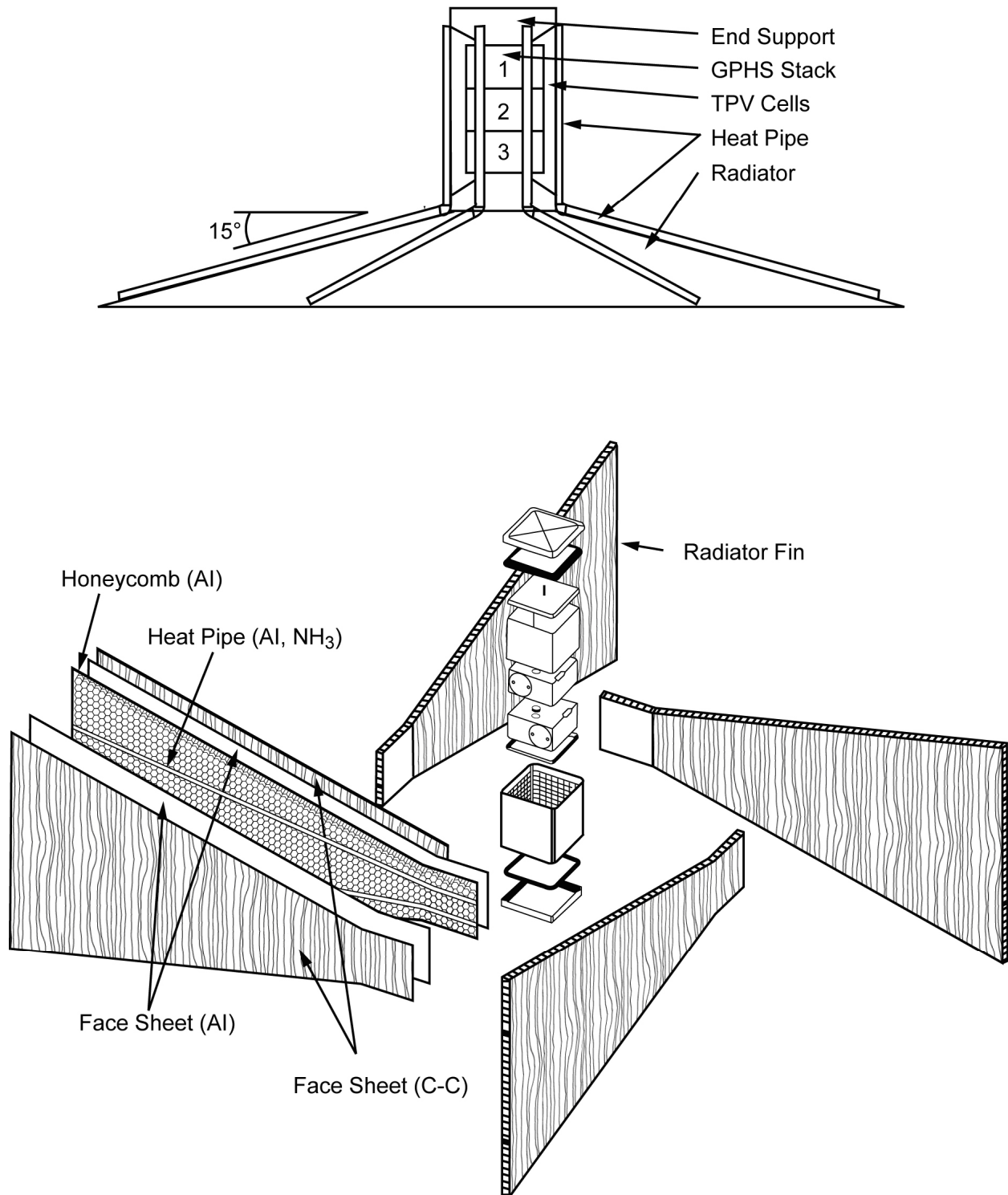


Figure 3-14. Fundamental Operating Concept of a TPV Generator (Crowley, 2003).



**Figure 3-15.** Two Conceptual TPV RPS Systems Studied by JPL (Ewell, 1993) (Top), and Fairchild Space (Schock, 1994) (Bottom). Note the different radiator fin configurations.

operating locations. Due to the large sensitivity of TPV fin size to environment, the specific power of the TPV generator varied significantly and was estimated at 6.3 We/kg for deep space ( $T_{\text{sink}} = 4 \text{ K}$ ), 6.9 We/kg for the surface of Titan ( $T_{\text{sink}} = 94 \text{ K}$ ), and 5.9 We/kg for Venus at 60 km altitude ( $T_{\text{sink}} = 240 \text{ K}$ ). The generator masses were estimated at 17.5 kg, 15.9 kg, and 18.8 kg for the above environments, respectively. Performance estimates for the TPV RPS used in the advanced RPS mission studies herein are presented in Table 3-4.

The power degradation rate of the TPV RPS was assumed to be  $\sim 2\%/yr$  (Wong, 2004), Section 3-8, due to the combined effects of  $^{238}\text{Pu}$  decay (0.8%/yr) and degradation of the PV cells and balance of the system ( $\sim 1.2\%/yr$ ), assuming a relatively benign radiation environment. Though the TPV RPS was considered for the Titan and Europa mission studies considered in this report, it was deemed unlikely that the TPV concept would be practical for an actual Europa mission due to the intense radiation environment (Mrads of total dose behind 100 mils of aluminum) that would significantly degrade the performance of the TPV system (Mardesich, Mueller, Stella and Timmerman, 2005; Ewell, 2005b). However, the Jovian system is a special case in this regard—the radiation levels elsewhere in the solar system are significantly lower than at Jupiter and, thus, could be a better fit for TPV technology.

**Table 3-4. Performance Estimates for a Conceptual TPV Generator\***

Parameter	Deep Space	Titan Surface	Venus at 60 km Altitude.
Power (BOM), We	110	110	110
Mass, kg	17.5	15.9	18.8
# GPHS Modules	3	3	3
Thermal Power, Wth	750	750	750
Specific Power, We/kg	6.3	6.9	5.9
Conversion Efficiency, %	15	15	15
$T_{\text{cell}}$ °C	34	34	34
Fin Temperature, °C	14	14	14
Heat-Transfer Environment	Radiative Only	Convective (P) and Radiative (S)	Radiative (P) and Convective (S)
Radiative Sink Temperature, K	4	94	240
Ambient Temperature, K	N/A	94	240
Ambient Pressure, bar	Vacuum	1.5	0.2
Ambient Composition	Vacuum	$\text{N}_2$ (P)	$\text{CO}_2$ (P)
Required Radiator Surface Area, $\text{m}^2$	2.5	0.48	3.2

\*Notes: (P) indicates a primary contributor or constituent, and (S) indicates a secondary contributor or constituent.

**3.8 SUMMARY**

Several advanced RPS power-conversion technologies were considered in this report, including advanced thermoelectrics, advanced Stirling, Brayton, and thermophotovoltaics. None of these technologies currently exist as an integrated system for space applications; however, NASA has funded research and development of these technologies with the intention of maturing them towards potential use in an advanced RPS system. To understand the relative trades of each technology for space missions, preliminary performance estimates were made for conceptual advanced RPS systems based on the above technologies. The power level of each unit was selected to be ~110 We (excluding the advanced Stirling, which is based on an 80-We convertor), and is intended to be consistent with that of the MMRTG and SRG currently being developed by NASA and DOE. Key performance parameters for the four concepts are shown in Table 3-5 for operation in a deep space environment. Illustrations of each conceptual advanced RPS are shown in relative scale in Figure 3-16. Estimates of each generator’s efficiency and specific power are illustrated in Figure 3-17, and their respective mass and power output (at beginning of mission) are shown in Figure 3-18. The estimated time-dependent power output of each conceptual advanced RPSs shown in Figure 3-19, along with their yearly power degradation rate.

In addition, performance estimates were provided by Northrop Grumman for an 80-We conceptual thermoacoustic Stirling heat engine and integrated cryocooler. This type of system could be enabling for long duration exploration of the surface of Venus.

The performance estimates presented here are believed to be conservative relative to what could be possible by the 2015 time frame were sufficient R&D funding provided to each program. Detailed system-level analyses has not been performed on any of the advanced RPS concepts discussed here; thus, the configuration and performance of an actual advanced RPS could, and likely would vary significantly from the design presented here. However, this work represents a first step in assessing the performance of four advanced RPS technologies and in understanding the relative benefits of each advanced RPS system from a mission perspective.

**Table 3-5. Overall Performance Estimates of the Conceptual Advanced RPS Systems Considered in this Report (within a Deep Space Environment)\***

Parameter	Adv RTG	Adv Stirling	Brayton	TPV
Power (BOM), We	112	80	110	110
Mass, kg	26.2	13.7	29.2	17.5
# GPHS Modules	5	1	2	3
Thermal Power, Wth	1250	250	500	750
Specific Power, We/kg	4.3	5.9	3.8	6.3
Conversion Efficiency, %	9	32	22	15
T <sub>hot</sub> °C, (T <sub>cell</sub> for TPV)	700	850	777	34
Fin Temperature, °C	130	100	77	14
Radiative Sink Temperature, K	4	4	4	4
Required Radiator Surface Area, m <sup>2</sup>	1.36	0.21	0.63	2.5
Redundancy	Built-In	Require Multiple Units	Built-In	Built-In

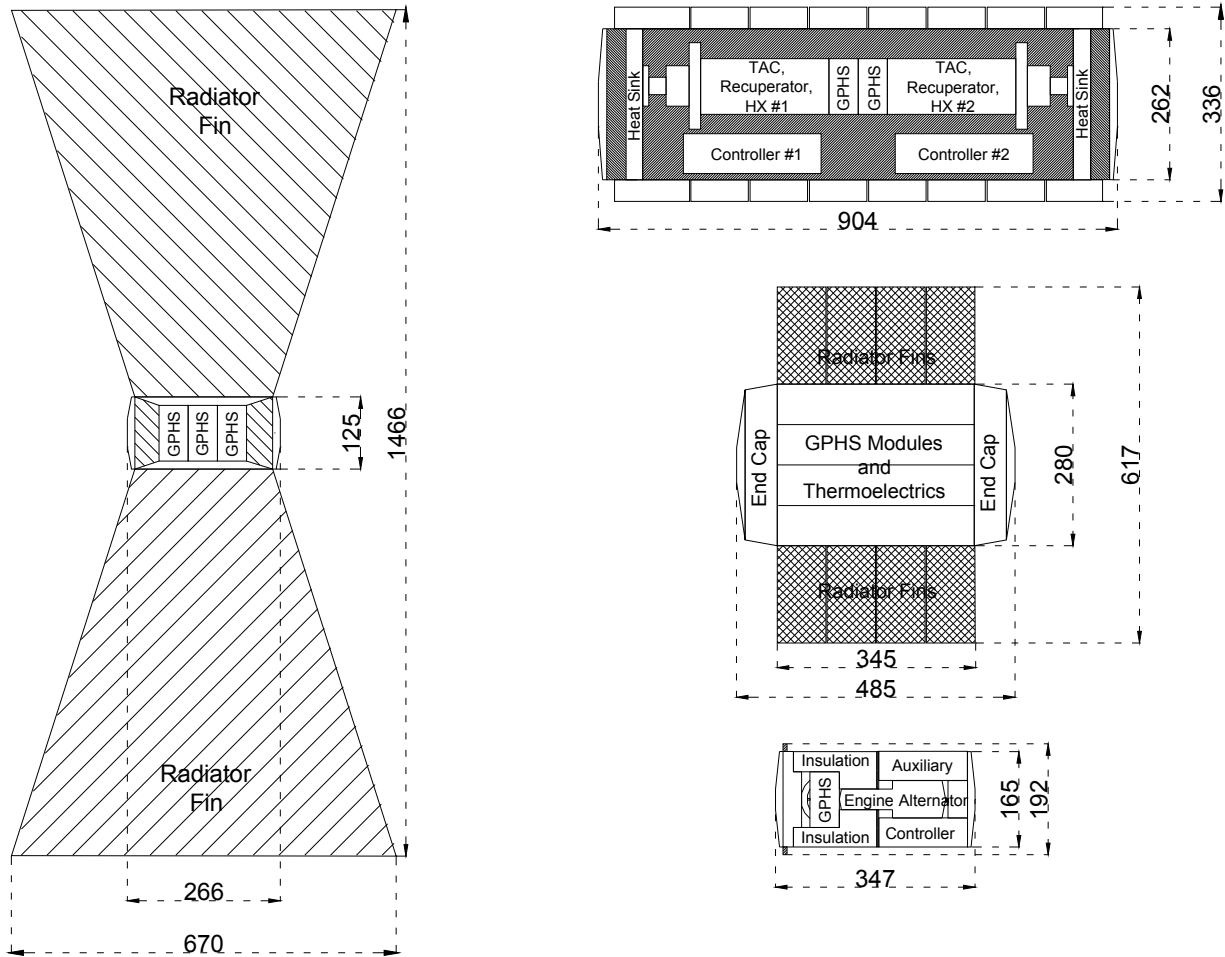


**Figure 3-16.** Relative Sizes of Four Conceptual Advanced RPS Systems Configured for Operation in a Deep Space Environment (Clockwise from Left): TPV Generator (110 We), Brayton Generator (110 We), Advanced RTG (112 We), and Advanced Stirling Generator (80 We). Radiator Fins are All Sized for Deep Space. All Dimensional Units are in Millimeters.

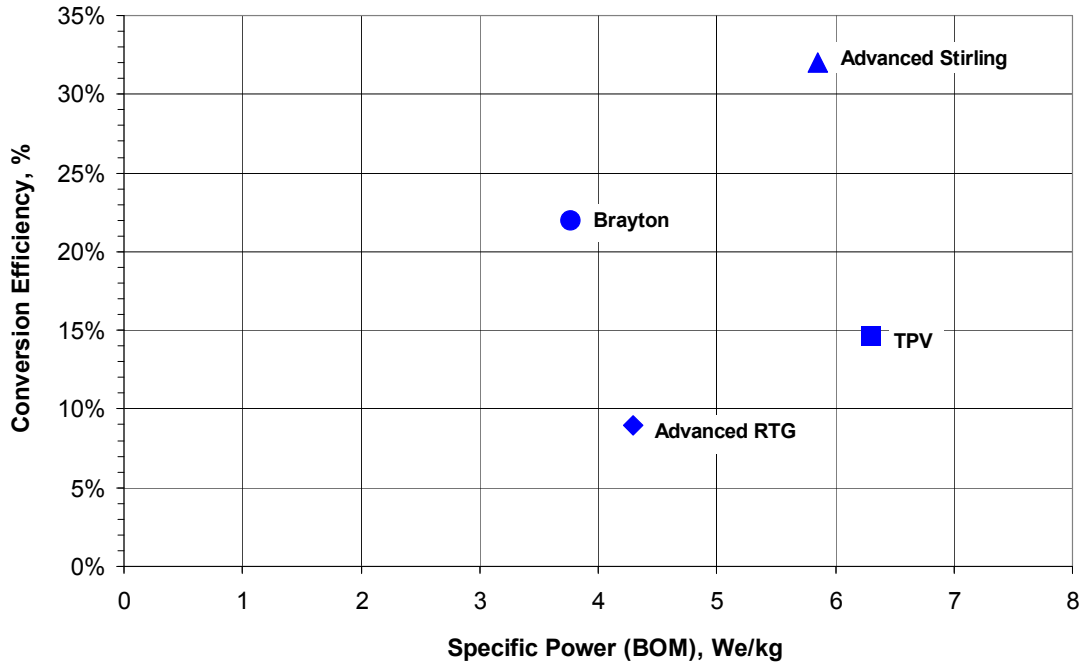


**Figure 3-17.** Conversion Efficiency versus Specific Power for the Four Conceptual Advanced RPS Systems Used in the Mission Studies. Assumes Radiator Fins are Sized for Deep Space.

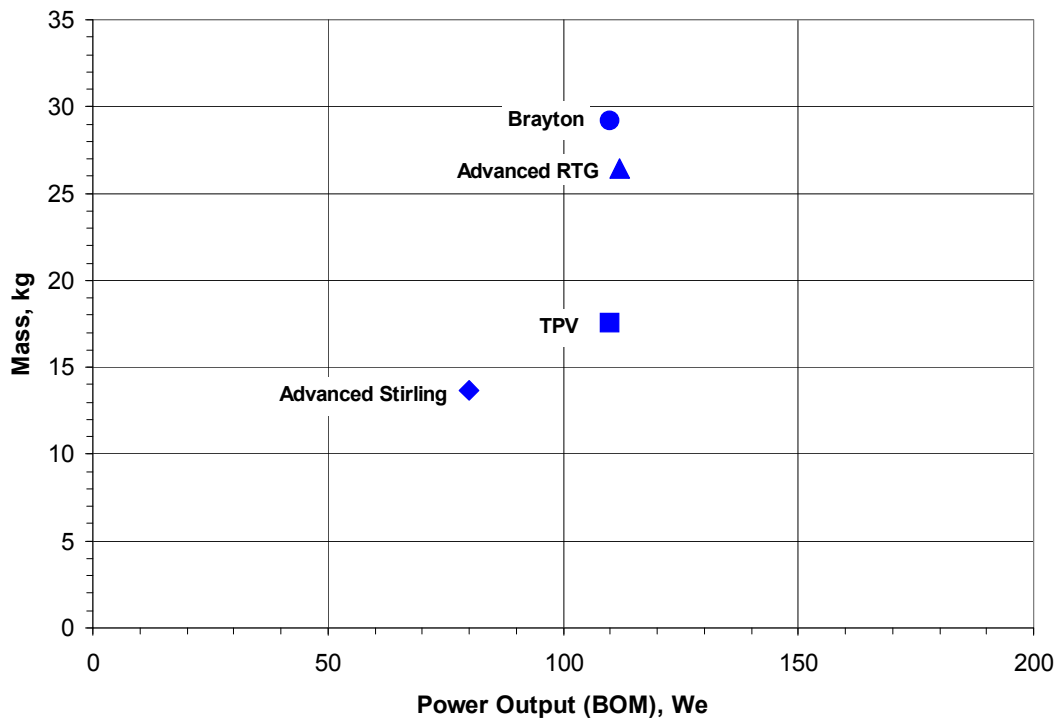


**Figure 3-18.** Generator Mass versus Electrical Power Output for the Four Conceptual Advanced RPS Systems Used in the Mission Studies. Assumes Radiator Fins are Sized for Deep Space.

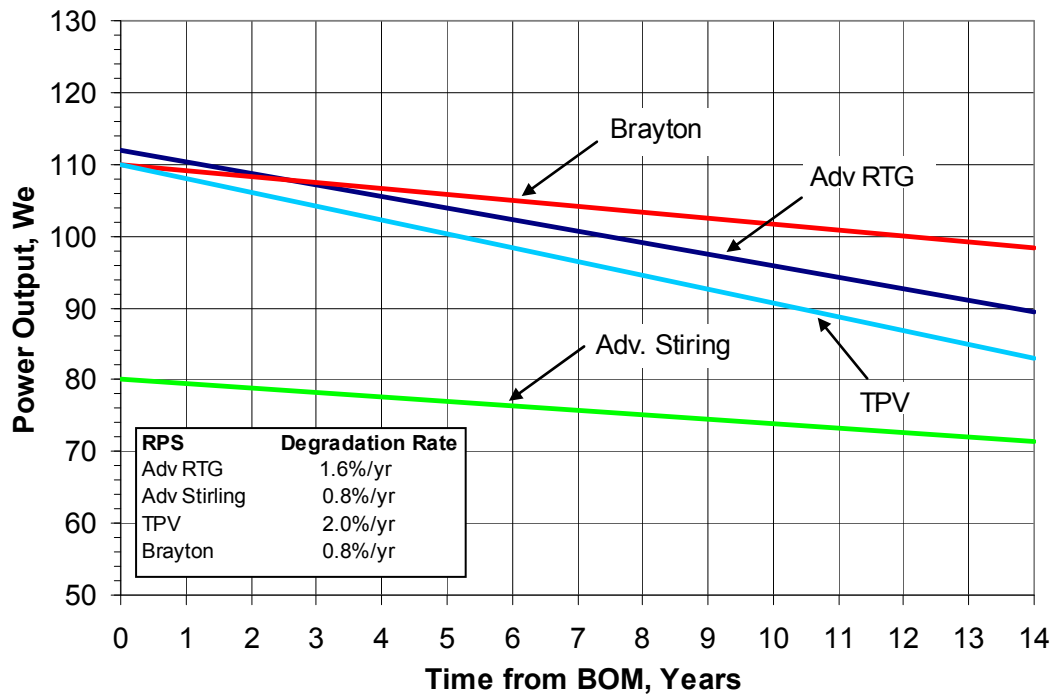


Figure 3-19. Estimated Power Degradation Rates for Each of the Four Conceptual Advanced RPS Systems Used in the Mission Studies.

---

## 4. ACKNOWLEDGEMENTS

The authors of this report gratefully acknowledge the follow individuals who contributed to or supported the development of this document. All personnel are from JPL except where otherwise specified.

### **Section 1 to 2.2 Executive Summary and Mission Studies Introduction**

Robert D. Abelson (Author)

Tibor S. Balint

Michael Evans

James H. Shirley

Thomas R. Spilker

### **Section 2.3.1 Titan Orbiter with Probe**

Robert D. Abelson (Study Lead, Author)

James H. Shirley (Science Co-Lead, Co-Author)

Thomas R. Spilker (Mission Architect, Science Co-Lead, Co-Author)

Stephen Durden (Instrument Support)

Eastwood Im (Instrument Support)

Team-A Design Team

### **Section 2.4.1 Europa Lander**

Michael Evans (Study Lead, Author)

James H. Shirley (Science Lead and Co-Author)

Wayne Zimmerman (Jupiter Icy Moons Lander Support)

Tom Rivellini (Jupiter Icy Moons Lander Support)

Team-P Design Team

### **Section 2.5.1 Titan Rover**

Tibor S. Balint (Study Lead, Author)

Timothy Schriener (Mission Architect, Co-Author)

James H. Shirley (Science Lead, Co-Author)

Jack Jones (Inflatable Wheels)

Team-P Design Team

### **Section 2.6.2 Venus Rover**

Michael Evans (Study Lead, Author)

James Randolph (Mission Architect)

James H. Shirley (Science Lead, Co-Author)

Emanuel Tward, NGST

Michael Petach, NGST

Team-P Design Team

---

**Section 3 Power Technologies for Advanced RPS Systems**

Robert D. Abelson (Author)

Richard Ewell

Bill Nesmith

Michael Petach (NGST)

Virgil Shields

Emanuel Tward (NGST)

Gary Woods (SunPower)

Mark Zagarola (Create)

**Team-A and Team-P Design Teams**

Wayne Zimmerman (Team-P Facilitator, Mobility)

Bob Kinsey (Team-A Facilitator, ACS)

Enrique Baez, Jr. (Configuration Graphics)

Ray Baker (Propulsion)

Rob Carnright (Mission Design)

Joe Cutting (Mission Design)

Ed Danielson (Instruments)

Luke Dubord (Deputy Systems)

Andy Ethers (Configuration Graphics)

Wai-Chi Fang (Avionics)

Tony Ganino (Mobility)

Rob Hall (Mission Design)

David Hansen (Telecom)

Mike Henry (Instruments)

Gerhard Klose (Structures)

Elisabeth Lamassoure (Systems)

Tracy Leavens (Systems)

Bob Miyake (Thermal)

David Morabito (Telecom)

Frank Picha (Propulsion)

Vincent Randolph (CDS)

John Rohr (CDS)

Abhijit Sengupta (CDS)

Partha Shakkottai (Thermal)

Chad Smith (Mission Design)

Kyle Smith (Telecom)

Farinaz Tehrani (Telecom)

Paul Timmerman (Power)

Thomas Valdez (Power)

Keith Warfield (Systems)

Jim Weiss (Science)

Richard Whatley (Telecom)

Jay Whitacre (Power)

**RPS Program Management**

Jackie Green

Erik Nilsen

Gary Burdick

Rao Surampudi

Ajay Misra (NASA HQ)

Dave Anderson (GRC)

Wayne Wong (GRC)

Richard Shaltens (GRC)

**Risk Communication**

Mary Beth Murrill

Sandy Dawson

**Document Services**

Jeanné Washington

John Kovacic

Claire Marie-Peterson

Diana Meyers

Joseph Spahr

Mary Young



---

## 5. REFERENCES

Abelson, R. D., T. S. Balint, K. Coste, J. O. Elliott, J. E. Randolph, G. R. Schmidt, T. Schriener, J. H. Shirley, and T. R. Spilker, 2005a, "Expanding Frontiers with Standard Radioisotope Power Systems," JPL D-28902 / PP-266 0332, Jet Propulsion Laboratory, Pasadena, CA.

Backhaus, S., and G. W. Swift, 2000, "A Thermoacoustic-Stirling Heat Engine: Detailed Study," *J. Acoust. Soc. Am.* 107(6):3148–3166.

Backhaus, S., E. Tward, and M. Petach, 2002, "Thermoacoustic Power Systems for Space Applications," CP608, in *Proc. Space Technology and Applications International Forum–STAIF 2002*, 939-944, edited by M. S. El-Genk, American Institute of Physics.

Backhaus, S., 2003, "Initial Tests of a Thermoacoustic Space Power Engine," CP654, in *Proc. Space Technology and Applications International Forum–STAIF 2003*, 641–647, edited by M. S. El-Genk, American Institute of Physics.

Backhaus, S., E. Tward, and M. Petach, 2004, "Traveling-Wave Thermoacoustic Electric Generator," *Applied Physics Letters* 85(6):1085–1087.

Baines, K. H., P. Drossart, T. W. Momary, V. Formisano, C. Griffith, G. Bellucci, J. P. Bibring, et al., 2005, figure from "The Atmospheres of Saturn and Titan in the Near-Infrared: First Results of Cassini/VIMS," submitted to *Earth, Moon, and Planets*.

Bennett, G. L., J. J. Lombardo, and B. J. Rock, 1983, "U.S. Radioisotope Thermoelectric Generator Space Operating Experience (June 1961-December 1982)," 839171, in *Proc. 18<sup>th</sup> Intersociety Energy Conversion Eng. Conf.* 3:1044–1055, American Inst. of Chemical Engineers, New York, NY. Reprinted, 1984, as "U.S. Radioisotope Thermoelectric Generators in Space," *The Nuclear Engineer* 25(2): 49–58.

Bennett, G. L., 1989, "Historical Overview of the U.S. Use of Space Nuclear Power," *Space Power* 8:259.

Bennett, G. L., 1995, "Space Applications," Chap. 41 in *CRC Handbook of Thermoelectrics*, ed. D. M. Rowe, CRC Press, Inc., Boca Raton, FL.

Boeing Corporation, 2005, "MMRTG Radiation Capability," Canoga Park, CA.

Bush, G.W., 2004, "A Renewed Spirit of Discovery," [Online] Available: [http://www.whitehouse.gov/space/renewed\\_spirit.html](http://www.whitehouse.gov/space/renewed_spirit.html)

Crowley, C. J., N. A. Elkouh, and C. Murray, 2003, "A Brief Introduction to Thermophotovoltaics (TPV)" (Presentation), Creare, Hanover, NH.

Ewell, R., 1993, "Thermophotovoltaic Power System (RTPV)," Jet Propulsion Laboratory, Pasadena, CA.

Ewell, R., and T. Caillat, 2005a, personal communication.

Ewell, R., 2005b, personal communication.

- 
- Furlong, R. P., and E. J. Wahlquist, 1999, "U.S. Space Missions Using Radioisotope Power Systems," *Nuclear News*, 26–34.
- Gilmore, D. G., 2002, *Spacecraft Thermal Control Handbook, Volume 1: Fundamental Technologies*, 373–403, El Segundo, CA: The Aerospace Press.
- Hall, J., 2005, personal communication.
- Hoffman, P., 2005, personal communication.
- Hoffmann, A., 2004, personal communication.
- Hyder, A. K., R. L. Wiley, G. Halpert, D. J. Flood, and S. Sabripour, 2000, *Spacecraft Power Technologies*, 242–250, London: Imperial College Press.
- Im, E., S. L. Durden, and R. Lorenz, 2003, "Titan's Cloud/Precipitation Radar and Altimeter (TCPRA)," NRA 03-OSS-01, Jet Propulsion Laboratory, Pasadena, CA.
- Jet Propulsion Laboratory, 2005, "Cassini-Huygens, Mission to Saturn and Titan," [Online] Available: <http://www.jpl.nasa.gov/cassini/>
- Jones, J., 2005, personal communication, subject: Sorption refrigeration systems.
- Jones, J., 2005, personal communication, subject: inflatable wheels.
- Jun, I., 2002, "Design Cycle Two Review: Preliminary Radiation Environment" (Presentation), Mars Science Laboratory, Jet Propulsion Laboratory, Pasadena, CA.
- Kang, S., and I. Jun, 2005, "Updated RTG Radiation Environments from a Single RTG with Russian Fuel, Rev. C" (Presentation), Mars Science Laboratory, Jet Propulsion Laboratory, Pasadena, CA.
- Langley, T. M., 1993, "Cassini Radiation Control Plan," PD 699-229/JPL D-8813, Jet Propulsion Laboratory, Pasadena, CA.
- Lockheed Martin, 2004, "SRG Engineering Unit (EU) Final Design Review (FDR)", Valley Forge, PA.
- Lunine, J., R. Lorenz, W. Zimmerman, J.L Hall, T. Sweetser, and A. Sengupta, 2005, "Titan Organics Explorer Study (TOES)", University of Arizona, Jet Propulsion Laboratory, NASA Vision Missions.
- Mardesich, N., R. P. Mueller, P. Stella, and P. Timmerman, 2005, personal communication.
- National Aeronautics and Space Administration (NASA), 2005, "SRM 3–The Solar System Exploration Strategic Roadmap," [Online] Available: <http://www.spaceref.com/news/viewsr.html?pid=16756>.
- Petach, M., E. Tward, and S. Backhaus, 2004a, "Design of a High Efficiency Power Source (HEPS) Based on Thermoacoustic Technology," CDRL 3f (NAS3-01103), National Aeronautics and Space Administration, Glenn Research Center, Cleveland, OH.

- 
- Petach, M., E. Tward, J. Randolph, and B. Miyake, 2004b, "Venus Cooling and Power Generation via Thermoacoustics" (Presentation), Northrop Grumman Space Technologies.
- Rivellini, T., 2004, "Jupiter Icy Moons Lander (JIML) R&TD Concept Study Progress Report," Jet Propulsion Laboratory, Pasadena, CA.
- Rockwell International, 1988, "DIPS Technology for NASA Applications," BP 88-3, Rockwell International, Rocketdyne Division, Canoga Park, CA.
- Rockwell International, 1989, "Low Power DIPS Study for Interplanetary Missions – Presentation to Jet Propulsion Laboratory," BD 89-104, Rockwell International, Rocketdyne Division, Canoga Park, CA.
- Rockwell International, 1990, "DIPS Mobile Lunar Power Concepts," BD 90-8, Rockwell International, Rocketdyne Division, Canoga Park, CA.
- Rockwell International, 1991, "Dynamic Isotope Power System Presentation to JPL," Rockwell International, Rocketdyne Division, Canoga Park, CA.
- Rockwell International, 1992, "Dynamic Isotope Power Systems (DIPS) for Space Exploration – Technical Information," BC92-68, Rockwell International, Rocketdyne Division, Canoga Park, CA.
- Schaefer, L., and B. Fegley, Jr., 2004, "Heavy Metal Frost on Venus," *Icarus*, 168:215–219.
- Schock, A., M. Mukunda, C. Or, V. Kumar, and G. Summers, 1994, "Design, Analysis and Optimization of a Radioisotope Thermophotovoltaic (RTPV) Generator, and Its Applicability to an Illustrative Space Mission," International Astronautical Federation, Paris, France.
- Snyder, G. J., 2004, "Application of the Compatibility Factor to the Design of Segmented and Cascaded Thermoelectric Generators," *Appl. Phys. Lett.* 84:2436.
- Space Studies Board, National Research Council of the National Academies, 2003, *New Frontiers in the Solar System: An Integrated Exploration Strategy*, Washington, D.C.: National Academy Press. [Also Online]. Available: <http://www.nap.edu/books/0309084954/html>
- The Planetary Society, 2005, [Online] Available: <http://www.planetary.org/mars/images-rovers.html>
- Tward, E., M. Petach, and S. Backhaus, 2003, "Thermoacoustic Space Power Converter," CP654, in *Proc. Space Technology and Applications International Forum–STAIF 2003*, 656-661, edited by M. S. El-Genk, American Institute of Physics.
- U.S. Department of Energy (DOE), 1987, "Atomic Power in Space – A History," DOE/NE/32117-H1, Washington, DC.
- Wiley, R., and R. Carpenter, 2004, "Small Radioisotope Power Source Concepts" (Presentation), U.S. Department of Energy, Washington, DC.
- Wong, W., 2004, "Development Contracts Phase 1 Accomplishments," NASA Glenn Research Center, Cleveland, OH, p.3.

Wood, J. G., C. Carroll, and B. Penswick, 2005, “Advanced 80 We Stirling Converter Development Progress,” in *Space Technology and Applications International Forum–STAIF 2005*, 688–698, edited by M. S. El-Genk, American Institute of Physics.

Yarnell, N., 2003, “Design, Verification/Validation and Ops Principles for Flight Systems (Design Principles),” D-17868, Rev. 2, Jet Propulsion Laboratory, Pasadena, CA.

Zagarola, M. V., 2003, “Turbo-Brayton Power Converter,” Creare, Hanover, NH.

Zagarola, M., and J. Randolph, 2004, personal communication.

Zagarola, M. V., M. G. Izenon, J. J. Breedlove, G. M. O’Connor, A. C. Ketchum, R. L. Jetley, and J. K. Simons, 2005, “An Advanced Turbo-Brayton Converter for Radioisotope Power Systems,” presentation at the *Space Technology and Applications International Forum–STAIF 2005*, 632–640, edited by M. S. El-Genk, American Institute of Physics.

---

## 6. ACRONYMS AND ABBREVIATIONS

ACS	Attitude Control System
ARPS	Advanced Radioisotope Power Systems
ASAT	Aerocapture Systems Analysis Team
ASIC	Application Specific Integrated-Circuit
AU	Astronomical Unit
BIPS	Brayton Isotope Power System
BOL	Beginning of Life
BOM	Beginning of Mission
BRU	Brayton Rotating Unit
CBC	Closed Brayton Cycle
CBE	Current Best Estimate
CCD	Charge Coupled Device
CDS	Command and Data System
CE	Capillary Electrophoresis
CG	Center of Gravity
CRISM	Compact Reconnaissance Imaging Spectrometers for Mars
DIMES	Descent Image Motion Estimation System
DIPS	Dynamic Isotope Power System
DoD	Department of Defense
DOE	Department of Energy
DOF	Degrees of Freedom
DSM	Deep Space Maneuver
DSN	Deep Space Network
DTE	Direct to Earth
EDL	Entry, Descent and Landing
EJ	Earth-Jupiter
EJGA	Earth-Jupiter Gravity Assist
EM	Electromagnetic
EMC	Electromagnetic Compatibility
EMI	Electromagnetic Interference
EOM	End of Mission
ES-IMS	Electrospray Ionization Mass Spectrometer
EVV	Earth-Venus-Venus
FPGA	Field Programmable Gate Array
FPSE	Free Piston Stirling Engine
GA	Gravity Assist
GCMS	Gas Chromatograph Mass Spectrometer
GPHS	General Purpose Heat Source
GPR	Ground Penetrating Radar

---

HGA	High Gain Antenna
I/O	Input/Output
INMS	Ion and Neutral Mass Spectrometer
IRS	Infrared Spectrometer
Isp	Specific Impulse
JIML	Jupiter Icy Moons Lander
JOI	Jupiter Orbit Insertion
JPL	Jet Propulsion Laboratory
L/D	Lift to Drag
LANL	Los Alamos National Laboratory
LGA	Low-Gain Antenna
LIBS	Laser Induced Breakdown Spectroscopy
LILT	Low-Intensity Low-Temperature
LV	Launch Vehicle
MER	Mars Exploration Rover
MGA	Medium Gain Antenna
MIPS	Millions of Instructions per Second
MIT	Minimum Impulse Thruster
MLI	Multi-Layer Insulation
MMH	Monomethyl Hydrazine
MMRTG	Multi-Mission Radioisotope Thermoelectric Generator
MRO	Mars Reconnaissance Orbiter
MSL	Mars Science Laboratory
NASA	National Aeronautics and Space Administration
Navcam	Navigation Camera
NF	New Frontiers
NGST	Northrop Grumman Space Technologies
NIMS	Near-Infrared Mapping Spectrometer
NMS	Neutral Mass Spectrometer
NRC	National Research Council
NTO	Nitrogen Tetroxide
Op/Nav	Optical Navigation
Pan Cam	Panoramic Camera
PCM	Phase Change Material
PICA	Phenolic Impregnated Carbon Ablator
PJR	Perijove Raise Maneuver
PTR	Pulse Tube Refrigerator
PV	Photovoltaic
RDF	Radiation Dose Factor
RF	Radio Frequency
RHU	Radioisotope Heater Unit

---

RPCT	RPS Power Conversion Technology
RPM	Revolutions per Minute
RPS	Radioisotope Power System
RSS	Root Sum Square
RTG	Radioisotope Thermoelectric Generator
SA	Solar Array
SAR	Synthetic Aperture Radar
SCA	Stirling Converter Assembly
SEU	Single Event Upsets
SDST	Small Deep Space Transponder
SiGe	Silicon Germanium
SNAP	Systems for Nuclear Auxiliary Power
SOC	State of Charge
SRAM	Static Read Only Memory
SRG	Stirling Radioisotope Generator
SRM	Solid Rocket Motor
SSEDS	Solar System Exploration Decadal Survey
SSESR	Solar System Exploration Strategic Roadmap
SSPA	Solid State Power Amplifier
STE	Segmented Thermoelectric
TAC	Turbo-Alternator-Compressor
TAGS	Tellurides of Antimony, Germanium and Silver
TASHE	Thermoacoustic Stirling Heat Engine
TCM	Trajectory Correction Maneuver
TCPRA	Titan Cloud/Precipitation Radar and Altimeter
TCS	Thermal Control Systems
TE	Thermoelectric
TID	Total Ionizing Dose
TPV	Thermophotovoltaics
TRL	Technology Readiness Level
TWTA	Traveling Wave Tube Amplifier
UHF	Ultra High Frequency
USDC	Ultrasonic Sonic Driller Corer
VEEJGA	Venus-Earth-Earth-Jupiter Gravity Assist
We	Watts of Electric Power
Wth	Watts of Thermal Power
WEB	Warm Electronics Box
XRF	X-Ray fluorescence